

Molecular Analysis of the Histamine H₃-Receptor

Dissertation

zur Erlangung des Doktorgrades der Naturwissenschaften (Dr. rer. nat.)
der Naturwissenschaftlichen Fakultät IV – Chemie und Pharmazie –
der Universität Regensburg



vorgelegt von
David Schnell
aus Neuburg a. d. Donau

2009

Der experimentelle Teil dieser Arbeit entstand in der Zeit von August 2005 bis Juli 2009 unter Leitung von Herrn Prof. Dr. R. Seifert am Institut für Pharmakologie und Toxikologie der Naturwissenschaftlichen Fakultät IV – Chemie und Pharmazie – der Universität Regensburg.

Das Promotionsgesuch wurde eingereicht im Dezember 2009.

Tag der mündlichen Prüfung: 22. Januar 2010

Prüfungsausschuss:

Prof. Dr. J. Wegener	(Vorsitzender)
Prof. Dr. R. Seifert	(Erstgutachter)
Prof. Dr. A. Buschauer	(Zweitgutachter)
Prof. Dr. S. Elz	(Drittprüfer)

Für Sabine

Danksagungen

An dieser Stelle möchte ich mich bedanken bei:

Herrn Prof. Dr. Roland Seifert für die Möglichkeit, so ein interessantes Thema bearbeiten zu dürfen, seine wissenschaftlichen Anregungen, stete Motivation und intensive Betreuung, sowie seine konstruktive Kritik bei der Durchsicht dieser Arbeit,

Herrn Prof. Dr. Armin Buschauer für die Aufnahme in das interdisziplinäre und internationale Graduiertenkolleg (GRK 760) „Medicinal Chemistry: Molecular Recognition – Ligand-Receptor Interactions“, sowie für die Erstellung des Zweitgutachtens,

Herrn Prof. Dr. Sigurd Elz für die Bereitstellung der Substanz Imoproxifan und die Übernahme der Funktion des Drittprüfers,

Herrn Dr. Erich Schneider für unzählige anregende Diskussionen, viele gemeinsame Projekte, lange unterhaltsame Laborabende, seinen Enthusiasmus und die ungebrochene Begeisterung für die Wissenschaft,

Frau Dr. Andrea Strasser für die Bereitstellung ihrer Expertise und das Molecular Modelling zum H₃-Rezeptor, was wesentlich zum Gelingen dieser Arbeit beigetragen hat,

Herrn Dr. Patrick Igel für seine Hilfe bei medizinisch-chemischen Fragestellungen und die Synthese zahlreicher Histamin-Rezeptorliganden, sowie für seine Kollegialität und die fruchtbaren Kooperationen,

Herrn Dr. Timothy W. Lovenberg (Johnson & Johnson PRD, San Diego, CA, USA) für die Bereitstellung der H₃-Rezeptor cDNAs, ohne welche diese Arbeit gar nicht möglich gewesen wäre,

Herrn Dr. Pascal Bonaventure (Johnson & Johnson PRD, San Diego, CA, USA) für den selektiven H₃-Rezeptorantagonisten JNJ-7753707 / [³H]JNJ-7753707 und die schnelle Beantwortung meiner Fragen,

allen, die mich bei verwandten Projekten zum H₄R unterstützt haben: Herrn Dr. Robin Thurmond (Johnson & Johnson PRD, San Diego, CA, USA) für die Bereitstellung der cDNAs vieler H₄-Rezeptor-Spezieshomologe und für den selektiven H₄-Rezeptorantagonisten JNJ-7777120 / [³H]JNJ-7777120, Herrn Dr. Max Keller für die Analyse von [³H]JNJ-7777120 per HPLC, Herrn Prof. Dr. Stefan Dove für seine fachliche Unterstützung hinsichtlich der zielgerichteten Mutagenese des H₄R,

den DAAD-Austauschstudenten Katrina Burleigh (USA) und Jonathan Trick (Kanada), sowie meinen Forschungspraktikanten Katrin Domes und Stefanie Reeh, und allen Wahlpflichtpraktikanten für ihre Beiträge zu dieser Arbeit und ihren Einsatz,

meinen Bürokollegen Dr. Corinna Matzdorf, Heidrun Appl, Miriam Erdorf und Dr. Hesham Taha für zahlreiche wissenschaftliche und nicht-wissenschaftliche Diskussionen und das gemütliche Klima,

Frau Gertraud Wilberg für ihre Unterstützung bei vielen Western-Blots und für die Sf9-Zellkultur, sowie bei Frau Astrid Seefeld für die Durchführung von zahlreichen GTPase-Assays,

meinen Laborkollegen Dr. Hendrik Preuss, Dr. Kathrin Nickl und Sarah Geiger für die freundliche Arbeitsatmosphäre,

der Regensburger „Histamin-Truppe“ für die gute Zusammenarbeit und auf das es so weitergeht,

den Kollegen Dr. Martin Göttle, Irena Brunscole, Matthias Desch, Bernhard Hieke, Melanie Hübner, Mirosław Lopuch, Dr. Johannes Mosandl, Dr. Louay Jouma, Nathalie Pop, Daniela Erdmann, Katharina Salb, Elisabeth Schinner, Dr. Dietmar Groß, Dr. Katharina Wenzel-Seifert, Dr. Walter Fuchs, sowie bei Prof. Dr. Frieder Kees, PD Dr. Klaus Höcherl, Prof. Dr. Michael Bucher, Prof. Dr. Jens Schlossmann und allen anderen Mitgliedern des Lehrstuhls für ihre Kollegialität, Hilfsbereitschaft und das gute Arbeitsklima,

dem Graduiertenkolleg 760 der DFG für die finanzielle Unterstützung und wissenschaftliche Förderung,

meinen Kajak-Kumpanen, die mich auf wilden Wassern durch viele tiefe Schluchten in fremden Ländern begleitet haben und mir immer wieder klarmachen, dass es auch noch Herausforderungen außerhalb des Labors gibt,

meinen Eltern, meiner Schwester Alexandra für die Übernachtungsmöglichkeit auf ihrem Sofa während der ersten Zeit in Regensburg, und allen weiteren Familienmitgliedern für ihre Unterstützung und Hilfe,

vor allem aber bei meiner lieben Freundin Sabine.

*Ich kann nicht zu anderen Ufern aufbrechen,
wenn ich nicht den Mut habe, das alte zu verlassen.*

André Gide

Contents

1	General Introduction	1
1.1	G protein-coupled receptors	2
1.2	GPCR signal transduction	4
1.3	Constitutive activity, models of GPCR activation and ligand classification	6
1.4	Histamine and the histamine receptor family	7
1.4.1	Historical perspective	7
1.4.2	Histamine	8
1.4.3	Histamine receptors	10
1.4.4	The histamine H ₃ receptor	13
1.4.4.1	<i>Molecular and biochemical pharmacology</i>	13
1.4.4.2	<i>H₃R ligands</i>	17
1.5	The baculovirus/Sf9 cell system	20
1.6	Scope and Objectives	22
1.7	References	24

2	No evidence for functional selectivity of proxyfan at the human histamine H₃-receptor coupled to defined G_i/G_o protein heterotrimers	34
2.1	Abstract	35
2.2	Introduction	35
2.3	Materials and methods	37
2.3.1	Materials	37
2.3.2	Construction of FLAG epitope- and hexahistidine-tagged cDNA for hH ₃ R	39
2.3.3	Construction of the cDNAs for hH ₃ R-Gα _{i2} and hH ₃ R-Gα _{o1}	39
2.3.4	Generation of recombinant baculoviruses, cell culture and membrane preparation	40
2.3.5	SDS-PAGE and immunoblot analysis	41
2.3.6	[³ H]JNJ-7753707 binding assay	41
2.3.7	[³⁵ S]GTPγS binding assay	42
2.3.8	Steady-state GTPase activity assay	42
2.3.9	Miscellaneous	43
2.4	Results	43
2.4.1	Immunological detection of recombinant proteins expressed in Sf9 cell membranes	43

2.4.2	[³H]JNJ-7753707 and [³⁵S]GTP_γS binding: Quantitative analysis of receptor-to-G protein stoichiometries	45
2.4.3	Steady-state GTPase assay: hH₃R coupling to different Gα-subunits	47
2.4.4	Ligand potencies and efficacies in the steady-state GTPase assay at hH₃R co-expressed with different Gα-subunits	49
2.4.5	Studies with hH₃R-Gα_{i2} and hH₃R-Gα_{o1} fusion proteins	54
2.5	Discussion	55
2.6	References	60
3	Comparison of the pharmacological properties of human and rat histamine H₃-receptors	63
3.1	Abstract	64
3.2	Introduction	64
3.3	Materials and methods	66
3.3.1	Materials	66
3.3.2	Construction of FLAG epitope- and hexahistidine-tagged cDNAs for hH₃R and rH₃R	66
3.3.3	Generation of recombinant baculoviruses, cell culture and membrane preparation, SDS-PAGE and immunoblot analysis	67
3.3.4	[³⁵S]GTP_γS saturation binding assay	69
3.3.5	Steady-state GTPase activity assay	70

3.3.6	Radioligand binding assays	71
3.3.7	Construction of inactive and active models of hH ₃ R and rH ₃ R	71
3.3.8	Miscellaneous	72
3.4	Results	72
3.4.1	Western blot analysis of hH ₃ R and rH ₃ R expressed in Sf9 insect cell membranes	72
3.4.2	Quantitative analysis of receptor-to-G protein stoichiometries	75
3.4.3	hH ₃ R and rH ₃ R coupling to different G α -subunits	75
3.4.4	Ligand potencies and efficacies in the steady-state GTPase assay at rH ₃ R compared to hH ₃ R co-expressed with different G α -subunits	78
3.4.5	[³ H]NAMH binding studies at hH ₃ R and rH ₃ R	83
3.4.6	Binding mode of imoproxifan at hH ₃ R and rH ₃ R	87
3.5	Discussion	90
3.6	References	93
4	Modulation of histamine H ₃ -receptor function by monovalent ions	96
4.1	Abstract	97
4.2	Introduction	97
4.3	Materials and methods	99

4.4	Results	101
4.5	Discussion	107
4.6	References	109
5	Summary/Zusammenfassung	111
A	Appendix	116
A.1	Abstracts and Publications	117
A.1.1	Publications	117
A.1.2	Short Lectures	118
A.1.3	Poster Presentations	118
A.2	Lebenslauf	120
A.3	Ausgewählte Zusatzqualifikationen/Fortbildungen	121
A.4	Teilnahme an Austauschprogrammen	121
A.5	Eidesstattliche Erklärung	122

List of Tables

1	General Introduction	1
	Table 1.1: Overview on histamine receptors.	11
2	No evidence for functional selectivity of proxyfan at the human histamine H₃-receptor coupled to defined G_i/G_o protein heterotrimers	34
	Table 2.1: Quantification of hH ₃ R-to-G protein ratios <i>via</i> [³ H]JNJ-7753707- and [³⁵ S]GTP _γ S-saturation binding.	46
	Table 2.2: GTPase activities in Sf9 membranes expressing hH ₃ R and different G _{α_{i/o}} -proteins.	48
	Table 2.3: Ligand potencies and efficacies in the GTPase assay.	50
	Table 2.4: Potencies and efficacies of selected ligands in the GTPase assay at fusion proteins.	55
3	Comparison of the pharmacological properties of human and rat histamine H₃-receptors	63
	Table 3.1: Quantification of rH ₃ R-to-G protein ratios via western blot, [³ H]JNJ-7753707- and [³⁵ S]GTP _γ S-saturation binding.	76
	Table 3.2: Analysis of rH ₃ R/G protein coupling - GTPase activities in Sf9 membranes expressing rH ₃ R and different G _{α_{i/o}} -proteins.	77
	Table 3.3: Ligand potencies and efficacies in the GTPase assay at Sf9 cell membranes expressing the rH ₃ R and different G proteins.	80
	Table 3.4: [³ H]NAMH competition bindings in Sf9 membranes expressing hH ₃ R or rH ₃ R in combination with G _{α_{i2}} and β ₁ γ ₂ .	85

List of Figures

1	General Introduction	1
	Fig. 1.1: $G\alpha$ protein activation/deactivation cycle after GPCR stimulation by an agonist.	5
	Fig. 1.2: The two state model of GPCR activation.	6
	Fig. 1.3: Differential responses in an effector system upon binding of full agonists, partial agonists, antagonists, partial inverse agonists and full inverse agonists.	7
	Fig. 1.4: Biosynthesis and metabolism of histamine.	9
	Fig. 1.5: Tautomerism of histamine in the monocationic form.	10
	Fig. 1.6: H_3R auto- and heteroreceptor function in the nervous system.	14
	Fig. 1.7: Snake representation of the human H_3R .	15
	Fig. 1.8: H_3R -mediated signal transduction – HA synthesis and release.	16
	Fig. 1.9: Imidazole-containing H_3R -ligands.	18
	Fig. 1.10: Non-imidazole H_3R -antagonists/inverse agonists.	19
	Fig. 1.11: Generation of recombinant H_3R -baculoviruses, protein expression and membrane preparation.	21

2	No evidence for functional selectivity of proxyfan at the human histamine H₃-receptor coupled to defined G_i/G_o protein heterotrimers	34
	Fig. 2.1: Structures of imidazole-containing H ₃ R ligands.	38
	Fig. 2.2: Immunological detection of recombinant proteins expressed in Sf9 cells.	45
	Fig. 2.3: Comparison of the effects of histamine, proxyfan and thioperamide in membranes expressing the hH ₃ R, different G $\alpha_{i/o}$ subunits and $\beta_1\gamma_2$ dimers.	51
	Fig. 2.4: Correlation of potency and efficacy of ligands at the hH ₃ R in the presence of different co-expressed G $\alpha_{i/o}$ -proteins.	53
3	Comparison of the pharmacological properties of human and rat histamine H₃-receptors	63
	Fig. 3.1: Comparison of the amino acid sequences of hH ₃ R (GeneBank Accession No. AF140538) and rH ₃ R (GeneBank Accession No. AF237919).	68
	Fig. 3.2: Structures of imidazole-containing H ₃ R-ligands.	70
	Fig. 3.3: Immunological detection of hH ₃ R and rH ₃ R expressed in Sf9 cells.	74
	Fig. 3.4: Comparison of the effects of histamine, imoproxifan and thioperamide in membranes co-expressing the hH ₃ R or rH ₃ R, G α_{i2} subunits and $\beta_1\gamma_2$ dimers.	78
	Fig. 3.5: Correlation of potency and efficacy of ligands at the rH ₃ R in the presence of different co-expressed G $\alpha_{i/o}$ -proteins.	82
	Fig. 3.6: [³ H]NAMH saturation bindings in Sf9 cell membranes expressing hH ₃ R or rH ₃ R in combination with G α_{i2} and $\beta_1\gamma_2$.	84

	Fig. 3.7: Competition of [³ H]NAMH binding by histamine, imoproxyfan and thioperamide in Sf9 membranes expressing hH ₃ R and rH ₃ R in combination with G α_{i2} and $\beta_1\gamma_2$.	84
	Fig. 3.8: Correlation of affinity and potency of ligands at the hH ₃ R and rH ₃ R.	86
	Fig. 3.9: Binding mode of imoproxifan at the active hH ₃ R and inactive rH ₃ R.	88
4	Modulation of histamine H₃-receptor function by monovalent ions	96
	Fig. 4.1: Na ⁺ - ions act as universal allosteric modulators at many GPCRs, stabilizing the inactive state (R).	98
	Fig. 4.2: Snake representation of the human H ₃ R, focus on Asp80 ^{2.50} .	99
	Fig. 4.3: The effect of NaCl on high-affinity agonist binding and steady-state GTP hydrolysis in Sf9 cell membranes expressing hH ₃ R in combination with G α_{i2} and $\beta_1\gamma_2$.	101
	Fig. 4.4: Regulation of HA-, basal and THIO-regulated GTPase activity by different salts of monovalent ions.	103
	Fig. 4.5: Regulation of HA-, basal and THIO-regulated GTPase activity by NaCl in the presence of different G _i /G _o -proteins.	104
	Fig. 4.6: The effect of Asp80 ^{2.50} →Asn80 ^{2.50} mutation (D2.50N-hH ₃ R) on high-affinity agonist binding and steady-state GTP hydrolysis in Sf9 cell membranes expressing the mutant in combination with G α_{i2} and $\beta_1\gamma_2$.	105
	Fig. 4.7: The G-protein coupling profile of D2.50N-hH ₃ R.	106

Abbreviations

α_2 AR	α_2 -adrenoceptor
aa	amino acid
AA-GTP	guanosine 5`-triphosphate azidoanilide
AC	adenylyl cyclase
Ach	acetylcholine
AcNPV	<i>Autographa californica</i> nuclear polyhedrosis virus
ANOVA	analysis of variance
GPCR	G protein-coupled receptor
ATP	adenosine 5`-triphosphate
β_1 AR	β_1 -adrenoceptor
β_2 AR	β_2 -adrenoceptor
bp	base pair(s)
BSA	bovine serum albumin
CaMKII	calmodulin kinase type II
cAMP	cyclic 3`:5`-adenosine monophosphate
CB ₁ R	cannabinoid receptor subtype 1
CB ₂ R	cannabinoid receptor subtype 2
cDNA	copy DNA
CIP	ciproxyfan
CLOB	clobenpropit
CNS	central nervous system
C-term	intracellular carboxyl terminus of a G protein-coupled receptor
D ₁ R	dopamine receptor subtype 1
D ₂ R	dopamine receptor subtype 2
DA	dopamine
DAG	1,2-diacylglycerol
DHA	dihydroalprenolol
DTT	dithiothreitol
e1, e2, e3	1 st , 2 nd , and 3 rd extracellular loops of a G protein-coupled receptor

EC ₅₀	agonist concentration which induces 50% of the maximum effect
ECL	enterochromaffin-like
EDTA	ethylenediaminetetraacetic acid (Ca ²⁺ - chelator)
E _{max}	efficacy (maximal response)
ERK	extracellular signal-regulated kinase
EST	expressed sequence tag
FLAG	octapeptide epitope for the labeling of proteins
fMLP	<i>N</i> -formyl- <i>L</i> -methionyl- <i>L</i> -leucyl- <i>L</i> -phenylalanine
FPR	formyl peptide receptor
G $\alpha_{12/13}$	α -subunits of G proteins that act as guanine-nucleotide exchange factors
G α_{16}	α -subunit of a G protein that stimulates phospholipase C
G α_{i1} , G α_{i2} , G α_{i3} , G α_{o1}	α -subunits of the G proteins that inhibit adenylyl cyclase
G $\alpha_{q/11}$	α -subunit of a G protein that stimulates phospholipase C
G α_{qi5}	chimeric α -subunit of G $\alpha_{q/11}$ and the carboxyl terminus of G α_i to redirect the signalling of G α_i -coupled receptors towards calcium release
G α_s	α -subunit of a G protein that stimulates adenylyl cyclase
G α_{ss} , G α_{sl}	short and long splice variant of the G protein G α_s
GABA	γ -amino butyric acid
GAP	GTPase-activating protein
G $\beta\gamma$	$\beta\gamma$ -subunits of a heterotrimeric G protein
GDP	guanosine 5'-diphosphate
GEF	guanine-nucleotide exchange factor
GIP	G protein-coupled receptor interacting protein
GROMACS	Groningen Machine for Chemical Simulations
GSK3 β	glycogen synthase kinase 3 β
GTP	guanosine 5'-triphosphate
GTP γ S	guanosine 5'-[γ -thio]triphosphate
H ₁ R, H ₂ R, H ₃ R, H ₄ R	histamine receptor subtypes
hH ₃ R	human histamine H ₃ -receptor
hH ₃ R-G α_{i2} , hH ₃ R-G α_{o1}	fusion proteins of histamine H ₃ -receptor and G protein α -subunits

HA	histamine
His ₆	hexahistidine tag
HDC	histidine decarboxylase
HNMT	histamine <i>N</i> -methyltransferase
i1, i2, i3	1 st , 2 nd , and 3 rd intracellular loops of a G protein-coupled receptor
IME	imetit
IMO	imoproxyfan
IMP	impentamine
IP ₃	inositol-1,4,5-trisphosphate
K _d	dissociation constant (saturation binding assay)
K _i	dissociation constant (competition binding assay)
mRNA	messenger ribonucleic acid
MAPK	mitogen-activated protein kinase
NAMH	<i>N</i> ^α -methylhistamine
NE	norepinephrine
N-term	extracellular amino terminus of a G protein-coupled receptor
OCT	organic cation transporter
PAGE	polyacrylamide gel electrophoresis
PCR	polymerase chain reaction
P _i	inorganic phosphate
pEC ₅₀	negative decadic logarithm of the EC ₅₀ value
PEI	polyethyleneimine
PI3K	phosphatidylinositol 3-kinase
PKA	protein kinase A
PKB	protein kinase B
PKC	protein kinase C
pK _i	negative decadic logarithm of the K _i value
PLA ₂	phospholipase A ₂
PLC	phospholipase C
PRO	proxifan
RAMH	(<i>R</i>)- α -methylhistamine
<i>r</i> ²	correlation coefficient
rH ₃ R	rat histamine H ₃ -receptor
RGS	regulator of G-protein signalling
RNA	ribonucleic acid

rpm	revolutions per minute
RT	reverse transcription
RT-PCR	combined reverse transcription and polymerase chain reaction
S. E. M.	standard error of the mean
SDS	sodiumdodecylsulfate
SDS-PAGE	sodiumdodecylsulfate-polyacrylamide gel electrophoresis
Sf9	insect cell line of <i>Spodoptera frugiperda</i>
THIO	thioperamide
TM	transmembrane domain of a G protein-coupled receptor
TM1-TM7	numbering of transmembrane domains of a G protein-coupled receptor
Tris	tris(hydroxymethyl)aminomethan
VACC	voltage activated calcium channel
VMAT2	vesicular monoamine transporter type 2
V_{\max}	maximum velocity of an enzymatic reaction

Author's Declaration

The author declares that the following work presented in this volume was written by none other than himself. **Chapters 2-4** were written in the format of original publications. Apart from were indicated all work was performed or supervised by the author.

The author would like to thank Mrs. K. Burleigh (supported by the “Research Internships in Science and Engineering (RISE) program” of the German Academic Exchange service (DAAD)) for her contribution to the development of the histamine H₃-receptor baculovirus/Sf9 cell system.

The author would like to thank Mrs. G. Wilberg and Mrs. A. Seefeld for their excellent technical assistance regarding immunoblots and GTPase experiments.

Human histamine H₃-receptor/G protein fusion constructs described in **Chapter 2.3.3** were generated by Mr. J. Trick (supported by the “Research Internships in Science and Engineering (RISE) program” of the German Academic Exchange service (DAAD); Current affiliation: Ontario Cancer Institute, Department of Medical Biophysics, University of Toronto, Ontario, Canada).

Molecular modelling described in **Chapter 3.4.6/3.5** and **Fig. 3.9** was performed by Dr. A. Strasser (Department of Pharmaceutical/Medicinal Chemistry I, University of Regensburg, D-93040 Regensburg, Germany).

Chapter 1

General Introduction

1.1 G protein coupled receptors

G protein coupled receptors (GPCRs) represent the largest and most versatile family of cell-surface receptors. The GPCR superfamily makes up nearly 2% of the human genome. About eighthundred genes have seven transmembrane characteristics, as assessed by hydrophobicity plots of amino acid sequences (Vassilatis et al., 2003). Approximately half of these are odorant receptors and for the remaining 360, the natural ligand has been identified for about 210, leaving 150 so-called “orphan GPCRs” with no known ligand or function.

As a superfamily of integral membrane proteins, GPCRs have a very high impact from a therapeutic point of view. Drugs binding to these receptors are beneficial across a wide range of human diseases, including pain, asthma, inflammation, obesity, cancer, as well as cardiovascular, metabolic, gastrointestinal and various CNS diseases. Approximately 50% of all modern drugs are targeted to GPCRs. Interestingly, however, the majority of these drugs exert their effects on about only 40 GPCRs (Wise et al., 2004; Jacoby et al., 2006; Lagerström and Schiöth, 2008). Thus, the remaining potential for drug discovery within this field is enormous.

Two major requirements define a protein to be classified as GPCR. The first is the existence of seven α -helical transmembrane (TM) domains and the second is the ability to interact with a G protein. The GPCR is able to bind a ligand from the extracellular side and transduce the signal via a G protein into the cell (Fredriksson et al., 2003). However, many GPCRs can modulate G protein-independent pathways. Therefore, the term seven transmembrane (7 TM) receptors would be more appropriate. Both terms are used by the International Union of Pharmacology Committee on Receptor Nomenclature and Drug Classification (NC-IUPHAR) (Foord et al., 2005). All 7 TM receptors share a common architecture: an extracellular amino terminus (N-term), seven α -helical TM domains that are connected by three extracellular (e1, e2 and e3) and three intracellular (i1, i2 and i3) loops, and an intracellular carboxyl terminus (C-term). Phylogenetically, GPCRs can be divided into six classes.

Family I (also referred to as family A or the rhodopsin-like family) represents by far the largest subgroup. Family I contains receptors for odorants, small molecules such as biogenic amines, peptides and glycoprotein hormones. The most important structural features of family I GPCRs are about 20 highly conserved amino acids and a disulphide bridge between the first and second extracellular loop (e1 and e2). Most of the conserved residues, including several proline residues and a conserved DRY (aspartate, arginine and tyrosine) motif adjacent to TM III, are located in the cytoplasmic half of the protein. The seven α -helices

span the cell membrane in a counter-clockwise manner when viewed from the extracellular side.

Family II or family B GPCRs are characterized by a relatively long N-terminus, containing several cysteine residues, which presumably form a network of disulphide bridges. Their morphology is similar to family I receptors, although they share only low sequence homology. Little is known about the exact three-dimensional arrangement of the TM domains, but given the divergence in amino acid sequence, it is likely quite dissimilar from that of family I receptors. Ligands for family II GPCRs include hormones, such as glucagon, gonadotropin-releasing hormone and parathyroid hormone.

Family III contains the metabotropic glutamate, the Ca^{2+} sensing and the γ -aminobutyric acid (GABA) B receptors. These GPCRs possess a long N- and C-terminus. The ligand binding domain is located in the amino terminus, which is often described as being like a “venus fly trap”. Except for two cysteines in e1 and e2 that form a putative disulphide bridge, family III receptors do not have any of the key features that characterize family I and II receptors. Unique among family III GPCRs is a short and highly conserved third intracellular loop (i3). Although the structure of the N-terminus is well characterized, similar to family II receptors, little is known about the exact three-dimensional arrangement of the TM domains.

The smaller, less characterized GPCR families comprise family IV pheromone receptors, while family V includes the “frizzled” and the smoothened receptors involved in embryonic development and in particular cell polarity and segmentation. Finally, the cAMP receptors have only been found in *D. discoideum*, but possible expression in vertebrates has not yet been reported (Bockaert and Pin, 1999).

A breakthrough in GPCR research was the determination of a high-resolution crystal structure of bovine rhodopsin by Palczewski in 2000, providing the first insight into the three-dimensional architecture of a mammalian family I receptor (Palczewski et al., 2000). More recently, the first crystal structure of a human GPCR, the β_2 -adrenoceptor ($\text{h}\beta_2\text{AR}$), was solved by Kobilka and co-workers (Rasmussen et al., 2007). This was possible due to truncation of the receptor and generation of an antibody as stabilizing element. More protein-engineering yielded an alternative high-resolution structure of $\text{h}\beta_2\text{AR}$ via construction of a receptor/T4-lysozyme fusion protein (Rosenbaum et al., 2007). These milestones in GPCR research provided the basis for other investigators to move on in the field of structural receptor biology. Another catecholamine receptor structure was determined for an engineered turkey $\beta_1\text{AR}$ (Warne et al., 2008) and Jaakola et al. (Jaakola et al., 2008) provided structural information about the human adenosine 2A receptor ($\text{hA}_{2\text{A}}\text{R}$). However, all these GPCR structures represent the receptors in an inactive state. Thus, the next major challenge in GPCR crystallography will be the determination of high-resolution *active-state*

receptor structures. Currently, much progress is being made towards this goal. Recent structures of opsin provide insight into active receptor states without G protein or bound to a G protein fragment (Park et al., 2008; Scheerer et al., 2008). The information provided by the new GPCR crystal structures and the lessons learned were very recently discussed and summarized in several articles (Kobilka and Schertler, 2008; Weis and Kobilka, 2008; Mustafi and Palczewski, 2009).

Nevertheless, GPCRs are dynamic in nature and crystal structures represent only snapshots of specific states, so in the future, X-ray crystallography will have to be complemented by sophisticated biophysical studies like NMR, to learn more about the activation process of GPCRs on an atomic level (Ratnala, 2006; Kofuku et al., 2009). In the meantime, it will still be necessary to combine several different classic experimental approaches and molecular modelling techniques to understand the processes of ligand binding, receptor activation and G protein/effector coupling for a given GPCR.

1.2 GPCR signal transduction

Based on our current knowledge, binding of an agonist from the extracellular side to a GPCR embedded in the cell membrane is followed by a conformational change. The resulting active state of the receptor protein then specifically interacts with a precoupled or free heterotrimeric G protein, consisting of a $G\alpha$ -subunit and a $G\beta\gamma$ -heterodimer, located at the cytosolic side of the membrane (Fig. 1.1). The interaction of the G protein with a receptor in the active state leads to the release of GDP bound to inactive G protein. Subsequently, a ternary complex between the agonist-bound active receptor and nucleotide-free G protein is formed, which is however unstable and dissociates or rearranges again (Bünemann et al., 2003). The nucleotide-free G protein can then bind GTP and a further conformational change occurs. In the GTP-bound state G proteins are activated. The heterotrimeric activated G protein complex then dissociates into GTP-bound $G\alpha$ -subunit and $G\beta\gamma$ -dimer, which can influence effector proteins.

Heterotrimeric G proteins are typically divided into four main classes: $G_{i/o}$, G_s , $G_{q/11}$ and $G_{12/13}$ based on sequence homology of their $G\alpha$ -subunits (Birnbauer, 2007). Different subtypes of activated $G\alpha$ -subunits can selectively inhibit ($G\alpha_{i/o}$) or stimulate ($G\alpha_s$) adenylyl cyclase (AC), activate phospholipase $C\beta$ ($G\alpha_{q/11}$), or interact with guanine nucleotide exchange factors ($G\alpha_{12/13}$). As a consequence, the production of second messengers such as cyclic 3',5'-adenosine monophosphate (cAMP), 1,2-diacylglycerol (DAG), and inositol-1,4,5-trisphosphate (IP_3) is modulated. The second messengers can induce a fast cellular response, such as change in intracellular ion concentrations or the regulation of enzyme

activity, or cause long-term effects by modulating transcription factors, thereby regulating gene expression. Moreover, activated $G\beta\gamma$ -dimers can also trigger cellular effects (Birnbaumer, 2007). For example, they can directly interact with phospholipase $C\beta$, AC or certain ion channels.

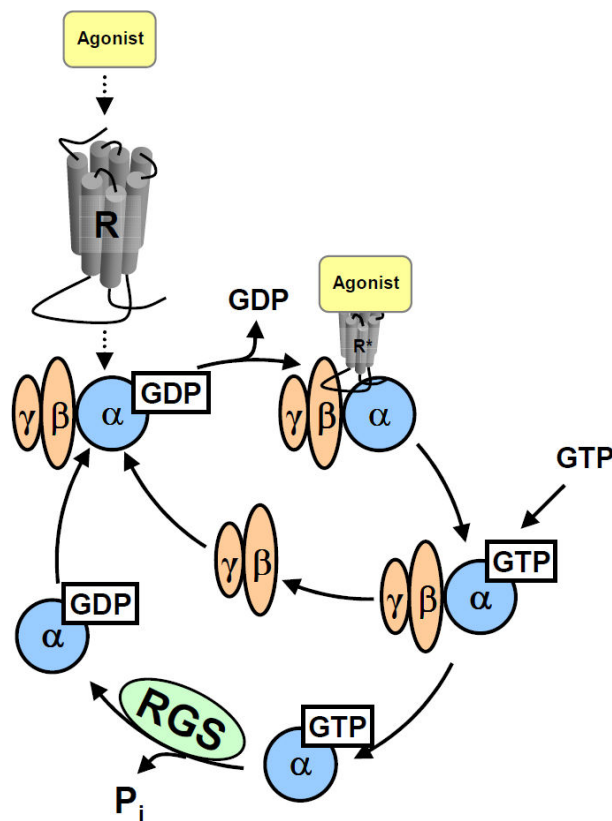


Fig. 1.1: $G\alpha$ protein activation/deactivation cycle after GPCR stimulation by an agonist. Adapted from Seifert, 2005.

After modulation of effector proteins, the intrinsic GTPase activity of the $G\alpha$ -subunit terminates the signal by cleavage of bound GTP into GDP and inorganic phosphate (P_i). The GDP-bound $G\alpha$ -subunit can then re-associate with the $G\beta\gamma$ -dimer again. The inactive GDP-bound heterotrimeric G protein complex is available for another round of activation.

Importantly, V_{max} -values of GTPases in reconstitution systems *in vitro* are often orders of magnitude higher than in tissue preparations. The reason for

these differences is the existence of GTPase-accelerating proteins. The so-called regulators of G protein signalling (RGS proteins) are guanine-nucleotide exchange factors (GEFs), which enhance the GTPase activity of $G\alpha$ -subunits (Neitzel and Hepler, 2006; Willars, 2006; Wieland et al., 2007). This family of proteins consists of at least 20 members that can be divided into 3 subfamilies. All RGS proteins share a common RGS domain, which stabilizes the transition state of the GTP hydrolysis at the $G\alpha$ -subunit. Thus, RGS proteins function as negative regulators of G proteins signalling *in vivo*.

Continuous or repeated stimulation of a GPCR by agonist leads to a loss of cellular sensitivity. This desensitisation process includes phosphorylation of the GPCR by G protein coupled receptor kinases (GRKs), followed by β -arrestin binding and uncoupling of the G protein. Subsequent internalization of the receptor via clathrin-coated vesicles leads to sorting of the receptor either back to the plasma membrane (receptor recycling) or to lysosomes for degradation (Hanyaloglu and von Zastrow, 2008).

1.3 Constitutive activity, models of GPCR activation and ligand classification

During the last decades, different models based on the law of mass action have been developed to mathematically describe the interaction of ligand (agonist), receptor and G protein. In the ternary complex model, binding of the agonist to the receptor is prerequisite to activate the G protein. However, GPCRs can be spontaneously active, a phenomenon which is referred to as constitutive activity (Seifert and Wenzel-Seifert, 2002). The existence of constitutive receptor activity resulted in the extended ternary complex (or two-state) model, which assumes that GPCRs isomerize from an inactive state (R) to an active state (R*), even in the absence of agonist (Fig. 1.2). A receptor in the R* state binds and activates G proteins, resulting in a cellular response.

According to the two-state model, ligands can be classified as agonists, neutral antagonists and inverse agonists (Fig. 1.3). Agonists stabilize the active R* state, inverse agonists the inactive R state of a GPCR. Neutral antagonists do not possess intrinsic activity but competitively antagonize the effects of agonists and inverse agonists. Partial agonists or inverse agonists possess a lower efficacy towards G protein activation or inhibition, relative to the endogenous (full) agonist.

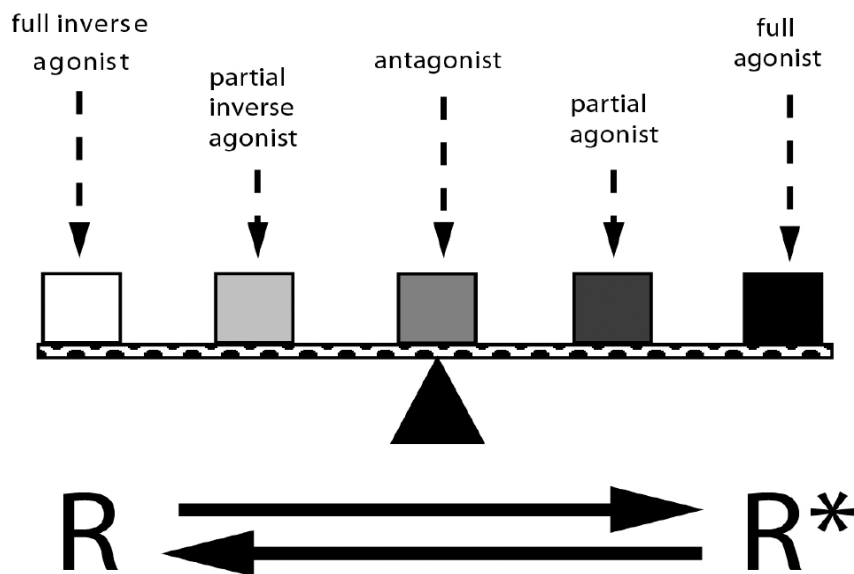


Fig. 1.2: The two state model of GPCR activation. GPCRs are able to isomerize from an inactive state (R) to an active state (R*). Ligands are classified according to their capability of shifting the equilibrium to either side of both states. Adapted from Seifert, 2005.

A thermodynamically more complete model is the cubic ternary complex model, including the formation of non-signalling complexes (RG and ARG). Based on evidence that multiple (most likely infinite) receptor states do exist and the increasing number of novel GPCR-interacting proteins (GIPs) identified, those models are continuously improved (Kenakin, 2004).

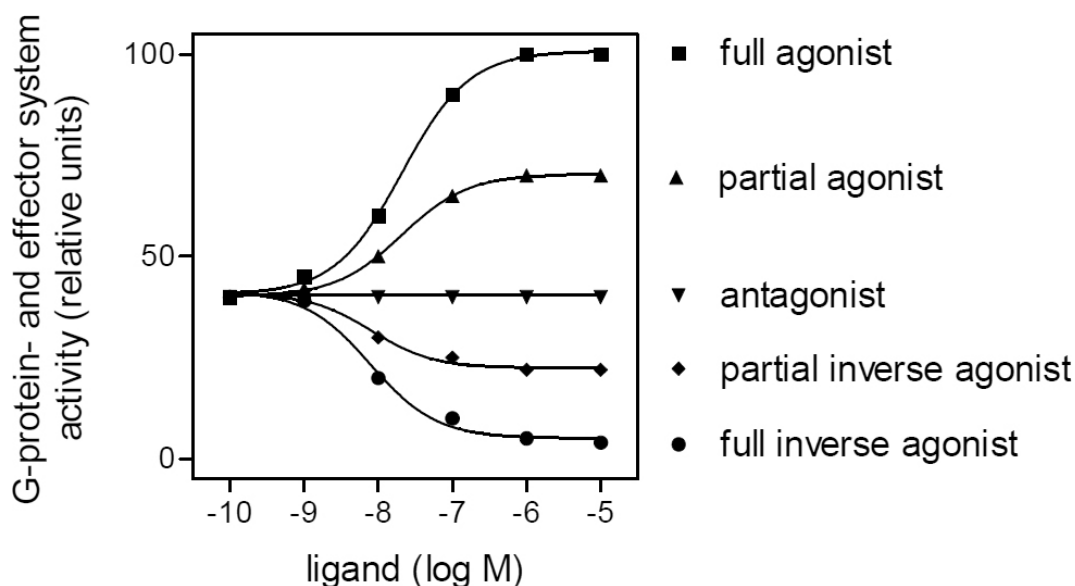


Fig. 1.3: Differential responses in an effector system upon binding of full agonists (■), partial agonists (▲), antagonists (●), partial inverse agonists (◆), and full inverse agonists (▼). Adapted from Seifert, 2005.

Moreover, the existence of allosteric GPCR modulators and the possibility of homo- and hetero-oligomerization further complicate the situation. Nonetheless, the models still can describe most scenarios based on the simple law of mass action. The application of the models goes far beyond their descriptive nature. They can be used in drug discovery to develop ligands with clearly defined cellular effects.

1.4 Histamine and the histamine receptor family

1.4.1 Historical perspective

The first report of histamine (HA, 2-(1*H*-imidazol-4-yl)ethanamine) was its synthesis by Windaus and Vogt in 1908 (Windaus and Vogt, 1908). Sir Henry Dale and colleagues were able to isolate this amine from ergot in 1910 (Barger and Dale, 1910). In the following years, HA was pharmacologically characterized (Dale and Laidlaw, 1910; Dale and Laidlaw, 1911; Dale and Laidlaw, 1919). These early studies elaborated the fundamental effects of

HA, such as stimulation of smooth muscles from the gut and respiratory tract, stimulation of cardiac contractility and induction of shock-like syndrome when injected into animals. The isolation from liver and lung was the first verification of HA as an endogenous substance (Best et al., 1927). The first compounds that blocked the action of HA in an anaphylactic response were identified in the 1930s (Fourneau and Bovet, 1933; Bovet and Staub, 1937). Some chemicals with similar activities (e. g. mepyramine or diphenhydramine) were introduced into the clinic for the treatment of allergic conditions. However, these prototypical “antihistamines” were not able to block certain HA-effects such as the stimulation of gastric acid secretion. Therefore, the existence of two distinct HA receptor subtypes was predicted (Ash and Schild, 1966). This was confirmed, when Black and co-workers developed burimamide, a compound that competitively antagonized HA-induced gastric acid secretion (Black et al., 1972). For the treatment of gastric and duodenal ulcer more potent derivatives were developed (Black et al., 1973; Brimblecombe et al., 1975) and have been used as blockbuster drugs for decades. In the early 1980s, the groups of Schwartz and Schunack showed that HA inhibits its own release from depolarized slices of rat cerebral cortex, an action that could not be blocked by known antihistaminergics (Arrang et al., 1983). A third HA receptor subtype was predicted and confirmed with a potent and selective agonist ((*R*)- α -methylhistamine) and antagonist (thioperamide) (Arrang et al., 1988). In the 1990s, progress in the field of molecular biology enabled cloning of the H₁R (Yamashita et al., 1991), the H₂R (Gantz et al., 1991) and, with substantial delay, of the H₃R (Lovenberg et al., 1999). At the turn of the millennium, Oda et al. identified and cloned the sequence of an additional HA receptor and termed it H₄R (Oda et al., 2000). The existence of a fourth HA receptor was confirmed independently by other groups (Nakamura et al., 2000; Liu et al., 2001; Morse et al., 2001; Nguyen et al., 2001; Zhu et al., 2001; O'Reilly et al., 2002). A detailed account on the history of HA and its receptors is given by Parsons and Ganellin (Parsons and Ganellin, 2006).

1.4.2 Histamine

HA is one of the most important local mediators and neurotransmitters. High concentrations of HA are found in the skin, lung, and the gastrointestinal tract. In the hematopoietic system, mast cells and basophils store HA in specific granules, closely associated with anionic proteoglycans and chondroitin-4-sulfate. In this form, it can be released in large amounts during degranulation in response to various immunological or non-immunological stimuli. Alternatively, HA is liberated upon destruction of these cells or by chemical substances (HA liberators). In the stomach, HA is produced in enterochromaffin-like cells (ECL) and regulates gastric acid secretion. In the central nervous system (CNS), HA is

stored in vesicles of histaminergic neurons, located exclusively in the tuberomammillary nucleus of the posterior hypothalamus (Haas and Panula, 2003). They are involved in the regulation of fundamental brain functions such as sleep/wakefulness, cognition and energy homeostasis (Haas and Panula, 2003). However, also other cellular sources of HA have been discovered, in which HA is immediately released without prior storage (Dy and Schneider, 2004). The production of the so-called “neo-synthesized HA” is modulated by cytokines and was identified in hematopoietic cells, macrophages, platelets, dendritic cells, and T cells.

The key enzyme for HA synthesis is *L*-histidine decarboxylase (HDC) (Fig. 1.4). This enzyme is located in the cytosol and decarboxylates the amino acid *L*-histidine. HDC requires binding of the cofactor pyridoxal-5-phosphate. The vesicular monoamine transporter VMAT2 is responsible for the transport of HA from the cytosol into the secretory granules (Kazumori et al., 2004). HA is inactivated by oxidative deamination or methylation to form imidazole-4-acetaldehyde and *N*^ε-methylhistamine.

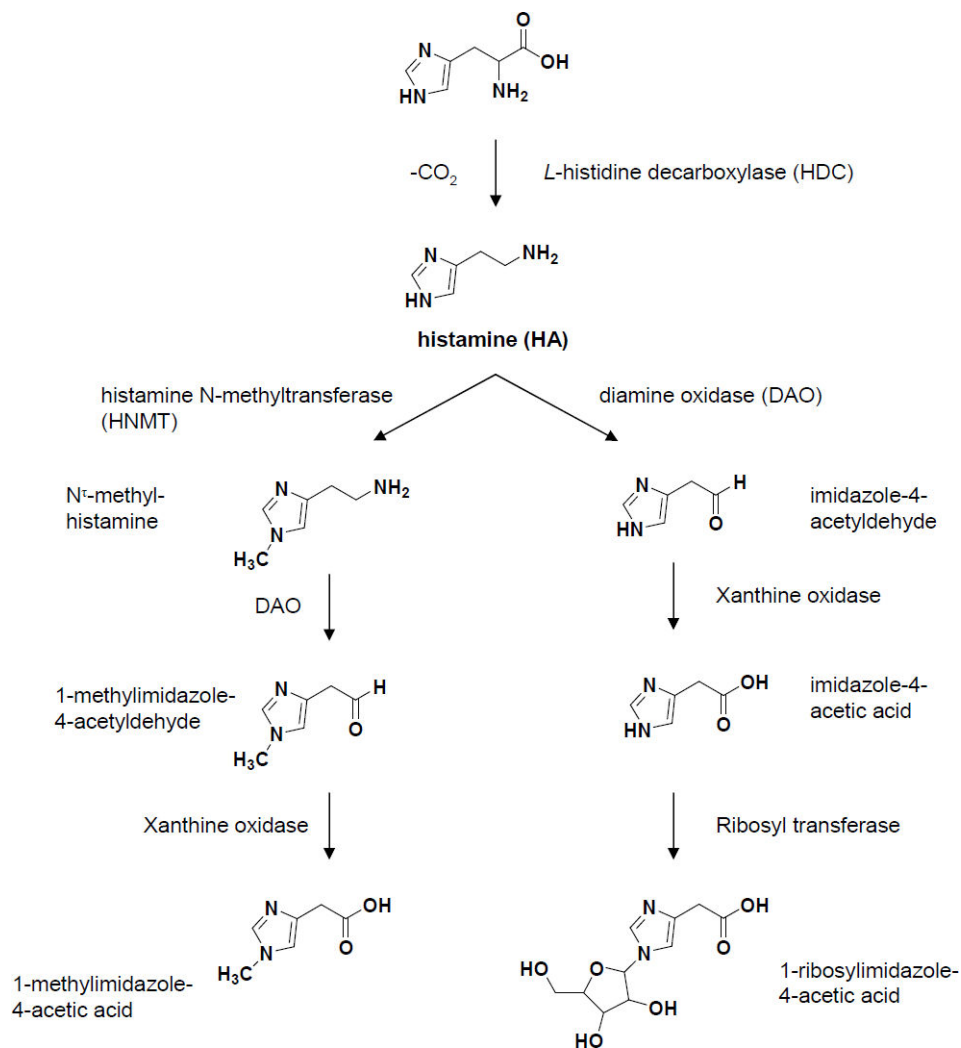


Fig. 1.4: Biosynthesis and metabolism of histamine.

These reactions are catalyzed by diamine oxidase (DAO) and histamine *N*-methyltransferase (HNMT), respectively. HNMT transfers a methyl group from *S*-adenosyl-*L*-methionine to the N^τ -nitrogen of the imidazole ring. Imidazole-4-acetaldehyde is oxidized to form imidazole-4-acetic acid. Imidazole-4-acetic acid and N^τ -methylhistamine are further metabolized to 1-ribosylimidazole-4-acetic acid and 1-methylimidazole-4-acetic acid, respectively. At present, it is not clear if HNMT is translocated to the plasma membrane to metabolize HA or if reuptake of HA occurs by means of organic cation transporters (OCT)-2 or -3 (Ogasawara et al., 2006). The inactive metabolites are excreted into the urine.

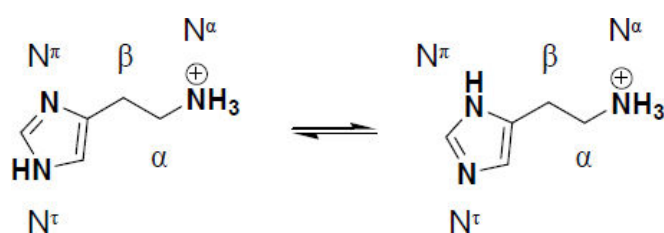


Fig. 1.5: Tautomerism of histamine in the monocationic form.

HA has two basic centres and fully protonated HA is a dication: the side chain amino group is a strong base ($pK_{a2} = 9.40$); the imidazole ring is a weak base ($pK_{a1} = 5.80$) (Fig. 1.5). Under physiological conditions ($pH = 7.4$) the monocation predominates and is the form most likely to be acting at histamine receptors. The imidazole ring of HA can exist in two tautomeric forms, with the proton on the N proximal (N^π -H tautomer) or distal (N^τ -H tautomer). In aqueous solution about 80% of HA monocation is in the N^τ -H tautomeric form (Ganellin, 1973).

1.4.3 Histamine receptors

Histamine receptors belong to family I and are classified in four subtypes: H_1R , H_2R , H_3R and H_4R . The average sequence homology between the subtypes is relatively low (~20%). H_3R and H_4R share the highest overall sequence homology of about 40% (~58% homology in the TM regions). An overview of the most important properties of histamine receptors is given in Table 1.1.

Table 1.1: Overview on histamine receptors.

H₁R	
Gene locus	3p25
Amino acids	487
Expression pattern	airway and vascular smooth muscle cells, neurons, hepatocytes, endothelial and epithelial cells, hematopoietic cells
Signal transduction (main pathways)	$G_{\alpha_{q/11}} \rightarrow \text{PLC}\uparrow, \text{DAG}\uparrow \text{ and } \text{IP}_3\uparrow; [\text{Ca}^{2+}]\uparrow; \text{PKC}\uparrow$
(Patho)physiological function	rhinitis, conjunctivitis, urticaria, asthma, anaphylaxis, bronchoconstriction and vascular permeability in the lung \uparrow , immune response \uparrow
Agonists	2-methylhistamine, 2-(3-trifluoromethylphenyl)histamine, histaprodifen(s)
Antagonists/inverse agonists	<u>1st generation</u> : chlorpromazine, chlorpheniramine, mepyramine, diphenhydramine, clemastine <u>2nd generation</u> : cetirizine, loratadine, astemizole, terfenadine, triprolidine
H₂R	
Gene locus	5q35.2
Amino acids	359
Expression pattern	gastric parietal, right atrial and ventricular muscle cells, airway and vascular smooth muscle cells, neurons, promyelocytic leukemic cells, hematopoietic cells
Signal transduction (main pathways)	$G_{\alpha_s} \rightarrow \text{AC}\uparrow, [\text{cAMP}]\uparrow; \text{protein kinases}\uparrow; [\text{Ca}^{2+}]\uparrow$
(Patho)physiological function	gastric acid secretion \uparrow , positive chronotropic and inotropic activity, cell differentiation \uparrow
Agonists	dimaprit, amthamine, impromidine, arpromidine
Antagonists/inverse agonists	cimetidine, raniditine, tiotidine, famotidine, aminopotentidine

<p>H₃R</p> <p>Gene locus</p> <p>Amino acids</p> <p>Expression pattern</p> <p>Signal transduction (main pathways)</p> <p>(Patho)physiological function</p> <p>Agonists</p> <p>Antagonists/inverse agonists</p>	<p>20q13.33</p> <p>445</p> <p>histaminergic neurons, low concentrations in peripheral tissues</p> <p>$G\alpha_{i/o} \rightarrow AC\downarrow, [cAMP]\downarrow; [Ca^{2+}]\downarrow$</p> <p>presynaptic autoreceptor (controlling HA release and synthesis\downarrow) and heteroreceptor (controlling release of other neurotransmitters\downarrow)</p> <p>(<i>R</i>)-α-methylhistamine, imetit, immepip</p> <p>thioperamide, ciproxyfan, clobenpropit, JNJ-5207852</p>
<p>H₄R</p> <p>Gene locus</p> <p>Amino acids</p> <p>Expression pattern</p> <p>Signal transduction (main pathways)</p> <p>(Patho)physiological function</p> <p>Agonists</p> <p>Antagonists/inverse agonists</p>	<p>18q11.2</p> <p>390</p> <p>hematopoietic and immunocompetent cells; low expression in brain, liver, and lung; neurons in the periphery</p> <p>$G\alpha_{i/o} \rightarrow AC\downarrow, [cAMP]\downarrow; PLC\uparrow; [Ca^{2+}]\uparrow$</p> <p>chemotaxis in mast cells and eosinophiles\uparrow; HA-induced itching\uparrow</p> <p>OUP-16, 4(5)-methylhistamine, UR-PI376</p> <p>JNJ-7777120, thioperamide</p>

1.4.4 The histamine H₃ receptor

1.4.4.1 Molecular and biochemical pharmacology

In 1983, Arrang et al. pharmacologically identified the H₃R as presynaptic autoreceptor inhibiting histamine release from histaminergic neurons in rat brain (Fig. 1.6). Histaminergic neurons are located exclusively in the tuberomammillary nucleus of the posterior hypothalamus, project to all major brain areas and are involved in fundamental brain functions such as sleep/wakefulness, energy homeostasis and cognition. Histaminergic neurotransmission was recently described in reviews by Panula and Haas (Haas and Panula, 2003; Haas et al., 2008). Although H₃Rs can also be found in the periphery, the great majority of H₃Rs are expressed in the brain, e. g. in cerebral cortex, hippocampus, amygdala, nucleus accumbens, globus pallidus, striatum and hypothalamus. H₃R expression is not restricted to histaminergic neurons. The H₃R is also known to function as a heteroreceptor, modulating the release of other important neurotransmitters, like norepinephrine, acetylcholine, dopamine, serotonin and GABA.

The H₃R was cloned in 1999 by Lovenberg and co-workers, almost 20 years after its pharmacological characterization (Lovenberg et al., 1999). The reason for this delay was an unexpectedly low sequence homology to H₁R and H₂R. In a search for orphan GPCRs, a potential GPCR-related expressed sequence tag (EST) with homology to α_2 -adrenergic receptors was identified *in silico* and used to clone a full-length cDNA from a human thalamus library. The cDNA contained an open reading frame of 445 amino acids with all features characteristic of a family I GPCR for a biogenic amine. The overall sequence homology of the H₃R to H₁R and H₂R is only 22% and 20%, respectively.

Due to the complex gene structure, a large number of H₃R isoforms exists (Hancock et al., 2003). This is possible through alternative splicing of H₃R mRNA. The H₃R gene consists of three exons and two introns. So far, at least 20 isoforms of the human H₃R have been identified on the basis of detection of varying mRNAs, but their regional expression and function remains largely unknown. The full-length H₃R (445 amino acids) is currently the best characterized isoform. Of interest, most splice variants have deletions in the e3 loop, an important region involved in G protein coupling (Bongers et al., 2007). In recombinant systems, it was already shown that these isoforms have altered signalling properties compared to the full-length receptor.

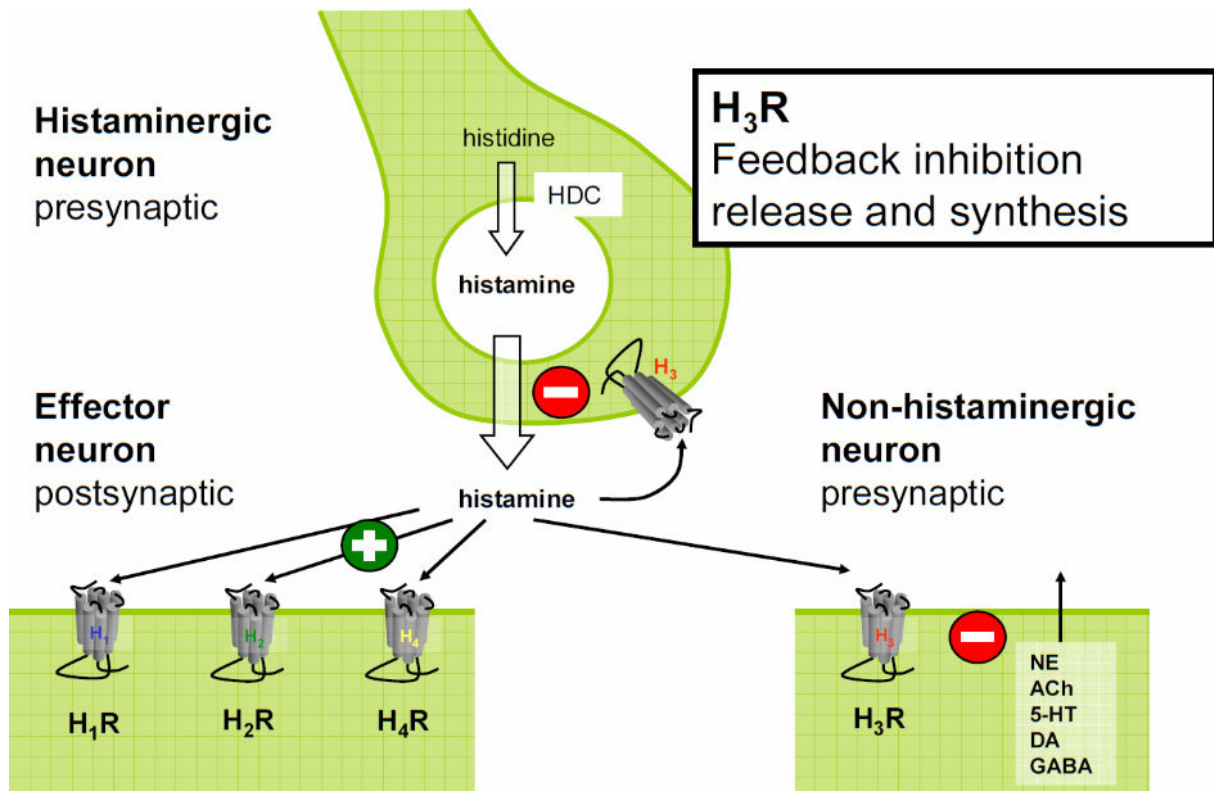


Fig. 1.6: H₃R auto- and heteroreceptor function in the nervous system.

In addition to H₃R splice variants, there is some evidence for genetic polymorphism within the H₃R gene. The amino acid at position 19 is reported to be either glutamic acid or aspartic acid (Lovenberg et al., 1999; Lovenberg et al., 2000a; Yao et al., 2003a). A second polymorphism, resulting from an alanine to valine substitution at amino acid 280 has been found in a patient with Shy-Drager syndrome (neurological orthostatic hypotension), a disease that is characterized by neuronal degeneration and autonomic failure (Wiedemann et al., 2002; Hancock et al., 2003). A third H₃R polymorphism, resulting from a tyrosine to a cysteine substitution at position 197, has also been identified (Hancock et al., 2003). However, at present there is no information available on the potential functional differences between polymorphic H₃R variants.

The H₃R was also cloned from various other species, including monkey (Yao et al., 2003b), guinea pig (Cassar, 2000; Tardivel-Lacombe et al., 2000), rat (Lovenberg et al., 2000b; Drutel et al., 2001) and mouse (Rouleau et al., 2004). The cDNA of these H₃R species homologs is very similar (>90%), but there are considerable pharmacological species differences. Most importantly, many antagonists have a higher affinity at rodent vs. human H₃Rs (Ireland-Denny et al., 2001; Stark et al., 2001) (Fig. 1.7). In addition, H₃R splice variants are not only limited to human H₃Rs, but also exist in other species (Hancock et al.,

2003). Moreover, the expression pattern of these isoforms also differs between species, adding another layer of complexity. The species-specificity of H₃R splicing events renders data translation to humans very difficult.

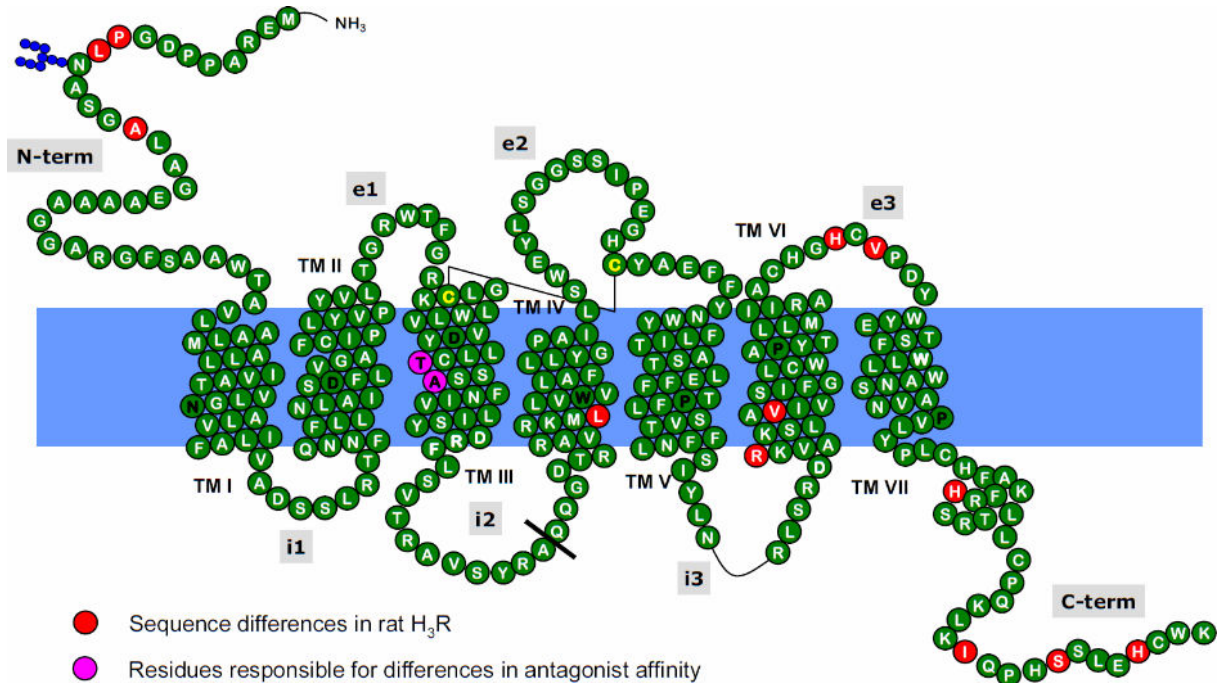


Fig. 1.7: Snake representation of the human H₃R.

After the cloning of H₃R, knock-out mice (H₃R^{-/-}) were generated by independent laboratories (Takahashi et al., 2002; Toyota et al., 2002). Collectively, the derived results confirmed data from previous pharmacological studies with H₃R ligands. However, the phenotype of H₃R^{-/-} mice was different from wild type mice treated with H₃R antagonists with respect to arousal and food intake. Since conditional H₃R^{-/-} mice are not yet available, compensatory mechanisms have been put forward to explain the apparent anomalies.

H₃Rs couple to G $\alpha_{i/o}$ -proteins (Fig. 1.8). This was originally shown by the pertussis toxin-sensitivity of H₃R agonist-dependent [³⁵S]GTP γ S binding in rat brain homogenate (Clark and Hill, 1996).

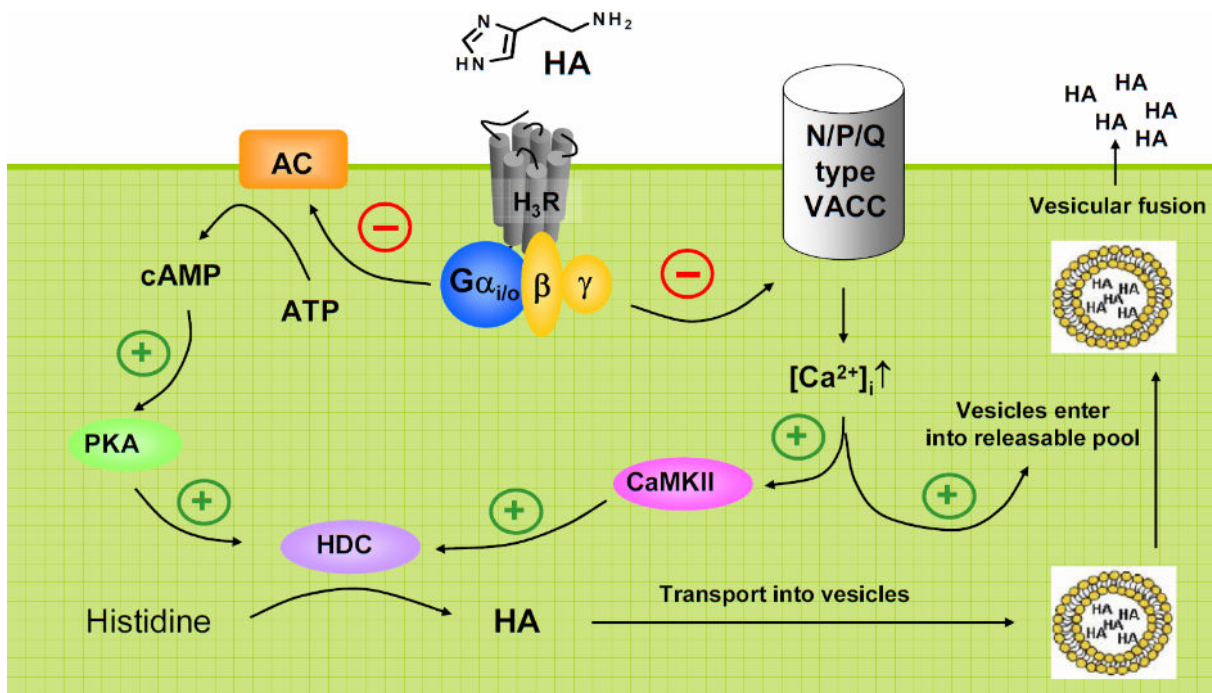


Fig. 1.8: H₃R-mediated signal transduction – HA synthesis and release. H₃R, histamine H₃-receptor; $G\alpha_{i/o}$, inhibitory G protein α -subunits of the $G\alpha_{i/o}$ -family; β , G protein β -subunits; γ , G protein γ -subunits; AC, adenylyl cyclase; PKA, protein kinase A; HDC, histidine decarboxylase; VACC, voltage-activated calcium channels; CaMKII, calmodulin kinase II.

It has been confirmed by heterologous expression of the H₃R in various mammalian cell lines, where H₃R-activation results in AC-inhibition (Lovenberg et al., 1999). AC catalyzes the formation of the second messenger cyclic AMP (cAMP). It was also shown, that a reduction of cAMP-levels leads to an inhibition of HDC and thus, to a decrease in HA synthesis in pre-synaptic histaminergic neurons (Gomez-Ramirez et al., 2002). However, an inhibition of HA release into the synaptic cleft is mainly triggered due to a decrease in intracellular Ca^{2+} -concentration (Moreno-Delgado et al., 2009). Here, an inhibition of voltage-gated ion channels plays a role. This differentiation was possible in studies with rat cortical miniprisms, leaving the natural environment of H₃Rs intact. For this purpose, cortical lobes of rat brains were dissected and sliced into small miniprisms (0.3 mm/side) using a special tissue chopper. Other signal transduction pathways modulated by the H₃R are for example activation of PLA₂, MAPK and the PI3K-PKB-GSK3 β axis (Leurs et al., 2005; Bongers et al., 2007). An activation of MAPK and PI3K results in a phosphorylation of extracellular signal-regulated kinases (ERKs) and protein kinase B (PKB or Akt), respectively. Active PKB phosphorylates and thereby inhibits glycogen synthase kinase 3 β (GSK3 β) activity, a major tau kinase in the brain. Activation of MAPK and PI3K are involved in memory consolidation, whereas the role of PKB/GSK3 β , modulated by the H₃R in the brain is less clear. However,

dysregulation of GSK3 β is associated with diabetes and/or insulin resistance and Alzheimer's disease.

H₃Rs are also constitutively active (Arrang et al., 2007). They can signal in the absence of an agonist, which was even shown *in vivo*. Using rat cortical miniprisms, it could be shown that HA-synthesis and -release are controlled by the constitutive activity of H₃R, although to a different extent (Gomez-Ramirez et al., 2002; Moreno-Delgado et al., 2009). Due to the high constitutive activity of H₃R, almost all H₃R antagonists had to be re-classified as inverse agonists.

Interestingly, there is also some evidence that H₃Rs can exist as homo- or heterodimers and/or -oligomers (Shenton et al., 2005). Functional interactions between the dopamine receptors (D₁R and D₂R) and H₃R have already been described in the literature (Sanchez-Lemus and Arias-Montano, 2004; Humbert-Claude et al., 2007; Ferrada et al., 2008). In recombinant systems, activation of MAPKs by H₃Rs did not occur until D₁Rs were co-expressed (Ferrada et al., 2009). Moreover, D₁Rs, usually coupled to G α_s , coupled to G $\alpha_{i/o}$ in co-transfected cells. Additionally, signalling *via* each receptor was not only blocked by a selective antagonist, but also by an antagonist of the partner receptor.

1.4.4.2 H₃R ligands

As above mentioned, the H₃R is an auto- and heteroreceptor. Thus, their activation reduces, whereas blockade increases, not only the release of HA but also several other neurotransmitters. Almost all H₃R agonists are small molecule derivatives of HA (De Esch and Belzar, 2004) (Fig. 1.9). So far, efforts to replace the imidazole-moiety in agonists have been unsuccessful. Methylation of the basic amine group yields *N*^ε-methylhistamine, a H₃R agonist that is frequently used as radioligand in its tritiated form. Methylation of the imidazole side chain results in (*R*)- α -methylhistamine, which is the archetypal H₃R agonist, used for the first pharmacological characterization of the H₃R. Relatively small structural changes lead to very potent and selective H₃R agonists like imetit or immepip. Methylation of the piperidine nitrogen of immepip gives methimepip, currently the most potent and selective H₃R agonist. Impentamine, a higher homolog of histamine, proxyfan and GT-2331 (cipralisant) were originally characterized to be H₃R antagonists. However, subsequent studies revealed the agonistic nature of the compounds. The first potent and selective H₃R antagonist was thioperamide (Stark et al., 2004). This compound and many other imidazole-containing H₃R antagonists, like ciproxyfan or clobenpropit, had to be re-classified as inverse agonists due to the constitutive activity of the H₃R. Thioperamide was the reference H₃R antagonist for almost two decades. Today, it is known that thioperamide, as well as many other imidazole-containing H₃R ligands, shows high antagonistic potency at the structurally related H₄R, 5-

HT₃R, α_{2A} AR and α_{2B} AR. These off-target effects, the low bioavailability and blood-brain barrier penetration, and CYP450-inhibition due to the imidazole-moiety of many H₃R ligands, lead to the development of more drug-like molecules as H₃R antagonists/inverse agonists (Fig. 1.10). The replacement of the imidazole-moiety was crucial towards more selective and drug-like H₃R antagonists.

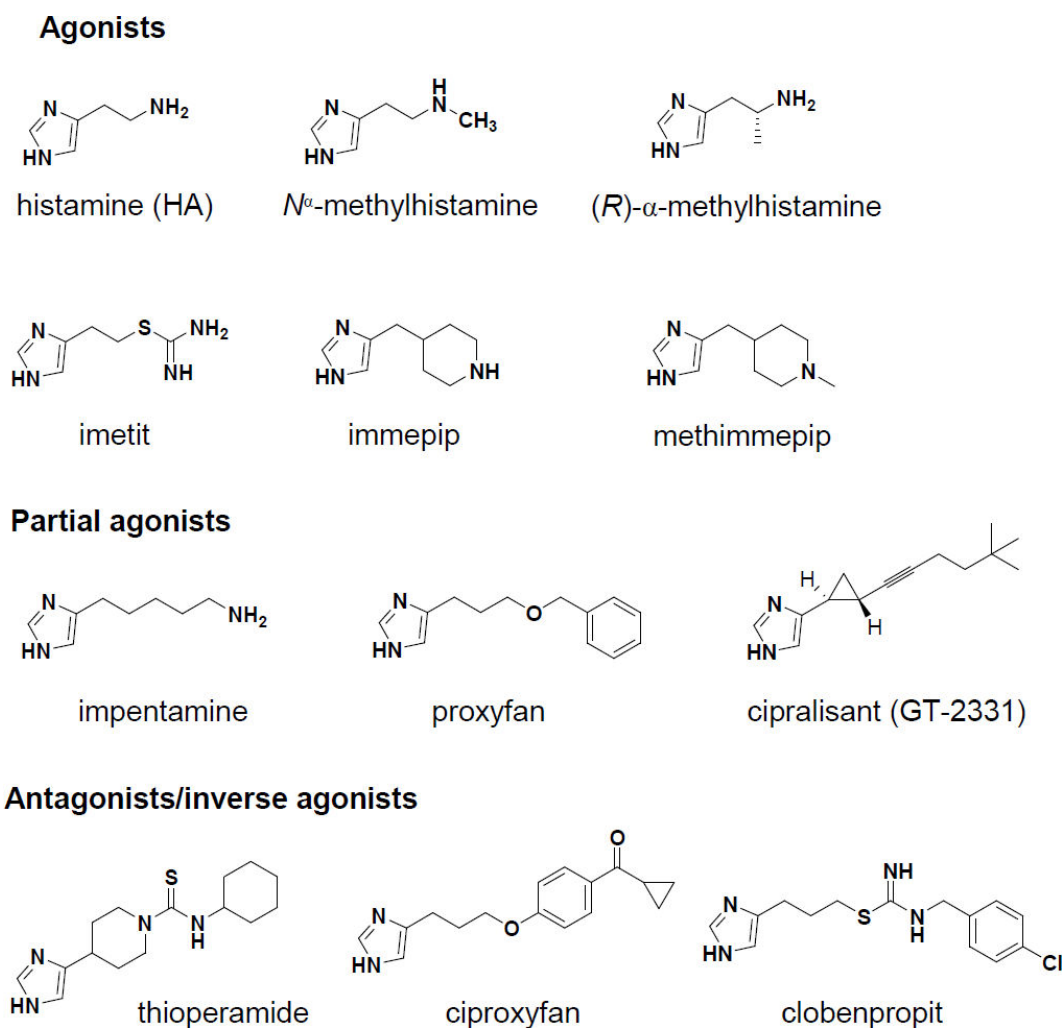
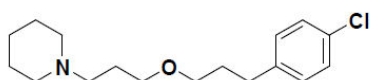
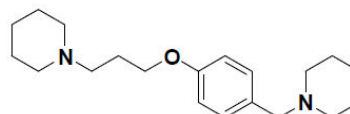


Fig. 1.9: Imidazole-containing H₃R-ligands.

Nonetheless, there are still problems in the preclinical development of these ligands, e. g. inappropriate pharmacokinetics or toxic effects like phospholipidiosis. In recent years, a very large variety of non-imidazole H₃R antagonists have been introduced and many of them are already in clinical trials. An interesting approach to fine tune the effects of H₃R ligands is also a combination of H₃R antagonism and selective inhibition of enzymes (Petroianu et al., 2006), like acetylcholine esterase (Bembenek et al., 2008), or parallel transporter blockade, for example serotonin reuptake (Barbier et al., 2007).

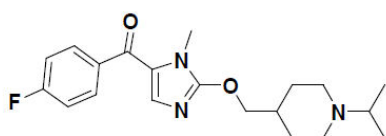
Non-imidazole H₃R antagonists/inverse agonists

tiprolisant (BF 2.649)



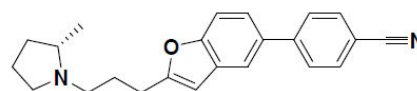
JNJ-5207852

(1-(4-(3-(piperidin-1-yl)
propoxy)benzyl)piperidine)



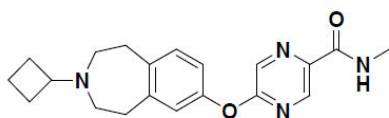
JNJ-7753707

(4-fluorophenyl)(1-methyl-2-((1-(1-methyl-
ethyl)piperidin-4-yl)methoxy)-1H-imidazol-
5-yl)methanone



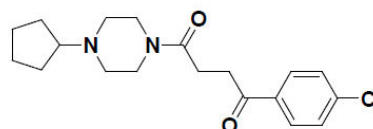
ABT-239

((S)-4-(2-(3-(2-methyl-pyrrolidin-1-yl)
propyl)benzofuran-5-yl)benzonitrile



GSK-207040

5-(3-cyclobutyl-2,3,4,5-tetrahydro-
1H-benzo[d]azepin-7-yloxy)-N-
methylpyrazine-2-carboxamide



NNC-381049

1-(4-chlorophenyl)-4-(4-cyclopentyl-
piperazin-1-yl)butane-1,4-dione

Fig. 1.10: Non-imidazole H₃R-antagonists/inverse agonists.

The preclinical development of non-imidazole H₃R antagonists/inverse agonists (Bonaventure et al., 2007; Esbenshade et al., 2008; Stocking and Letavic, 2008) and first reports on clinical trials are subjects of some excellent reviews (Wijtmans et al., 2007; Sander et al., 2008; Gemkow et al., 2009).

1.5 The baculovirus/Sf9 cell system

There are numerous methods to study ligand binding, receptor activation and G protein/effector coupling. Each methodological approach has its specific applications, advantages and disadvantages, and provides distinct information. Optimally, several different approaches should be used to obtain as much information as possible on a given GPCR. With a baculovirus/Sf9 cell expression system, various basic steps in GPCR signal transduction can be investigated (Seifert and Wieland, 2005).

Sf9 insect cells, derived from *Spodoptera frugiperda* pupal ovarian tissue, are very suitable for protein expression, especially GPCRs (Aloia et al., 2009). As expression vectors, recombinant baculoviruses have to be generated (Preuss et al., 2007a; Schneider et al., 2009). Baculoviruses are double-strained, filamentous DNA-viruses, which infect only non-vertebrate hosts. *Autographa californica* nuclear polyhedrosis virus (AcNPV) is the best characterized baculovirus and routinely used for protein expression. AcNPV infects the clonal tissue culture line Sf9 and can be genetically modified. Wild-type AcNPV-DNA possesses a strong polyhedrin promoter, facilitating the production of polyhedrin, a matrix protein in which virus particles are embedded. The polyhedrin gene, 3' to the promoter sequence, can be replaced by cDNA of interest, leading to a high expression level of the encoded protein. The BD BaculoGold™ linearized baculovirus DNA from BD Biosciences provides a tool for high recombination efficiencies. In principle, this modified type of baculovirus DNA contains a lethal deletion. The DNA does not code for viable virus. Only co-transfection of insect cells with the viral DNA and a complementing transfer vector construct reconstitutes viable virus. The foreign cDNA to be expressed has to be cloned into the transfer vector (Fig. 1.11).

If the engineered baculovirus encodes for a GPCR or G protein, high expression levels can be achieved (Seifert et al., 1998; Ratnala et al., 2004; Schneider et al., 2009). Baculovirus expression provides correct folding of recombinant protein as well as disulfide bond formation and other important post-translational modifications. Most mammalian family I receptors and G proteins expressed in Sf9 cells are properly integrated into the membranous lipid bilayer and thus, reconstitution of receptor/G protein-coupling is feasible. Sf9 cells do not express any constitutively active GPCRs or relevant amounts of other receptors. Another advantage of Sf9 cells as GPCR expression system is the limited endogenous G-protein signalling, which leads to excellent signal to noise ratios (Quehenberger et al., 1992; Wenzel-Seifert et al., 1998; Brys et al., 2000; Seifert and Wenzel-Seifert, 2003).

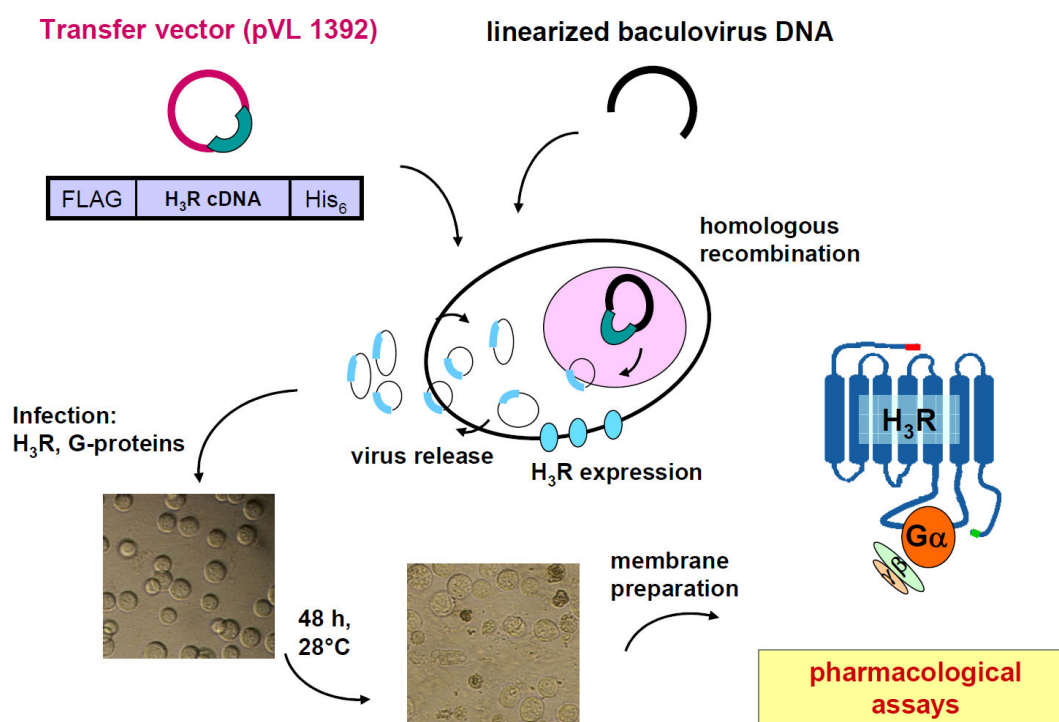


Fig. 1.11: Generation of recombinant H₃R-baculoviruses, protein expression and membrane preparation.

In this work, studies were only performed with broken-cell preparations (membranes) and not whole cells. Studies with membranes have many advantages, particularly when constitutive GPCR signalling is investigated. Contaminating agonists that may cause an apparent GPCR activation can be eliminated through multiple rounds of membrane centrifugation and resuspension. When working with whole cells or native brain tissue, an elimination of endogenous HA can be very difficult if not impossible. To ensure an absolute absence of endogenous HA one would have to study tissue derived from HDC^{-/-} mice, keep the animals under sterile conditions and provide HA-free food. In the case of Sf9 cell membranes, also a precise control of the concentrations of GTP, ions and pH, all of which have an effect on constitutive GPCR activity, is possible (Seifert et al., 1999, 2001; Ghanouni et al., 2000; Seifert and Wenzel-Seifert, 2001). This might be artificial, but given the unknown composition of the precise chemical microenvironment of GPCRs and G proteins near the plasma membrane, the importance of data derived from these experiments cannot be dismissed.

Studies with membranes are also crucial for study of the impact of G proteins on signalling properties of GPCRs. Experiments with membranes allow analysis of GPCR activity not only at the level of ligand binding, but also directly at the G protein level (i. e.,

GDP/GTP exchange and steady-state GTP hydrolysis). Moreover, using a baculovirus/Sf9 cell expression system the G protein coupling profile of a given GPCR can easily be elucidated (Wenzel-Seifert et al., 1999, 2001; Brys et al., 2000; Wenzel-Seifert and Seifert, 2000; Gazi et al., 2003). Again, studies with native tissue require the availability of several G protein knock-out mice (Albarran-Juarez et al., 2009). As an alternative, photoaffinity labelling using [α - 32 P]AA-GTP can be performed, if potent and selective GPCR ligands and selective antibodies are available (Klemke et al., 2000; Woo et al., 2009). Nevertheless, these methods are much more laborative than the reconstitution approach.

1.6 Scope and Objectives

The identification of the histamine H₃-receptor (H₃R) opened attractive perspectives for an exploitation of this new drug target. Since the initial cloning, a lot of knowledge about the molecular and biochemical pharmacology of this GPCR was accumulated. Numerous potent and selective H₃R-ligands were identified and serve as pharmacological tools or potential therapeutics. There are, however, still some ligand effects that cannot be easily explained, based on the currently available data.

The first aim of this thesis was to establish a sensitive, robust and uniform assay system to analyze all histamine receptors and their ligands under identical experimental conditions. So far, test systems to study these GPCRs are very heterogeneous and use many different pharmacological read-outs. Therefore, already existing baculovirus/Sf9 cell systems for the analysis of H₁R, H₂R and H₄R (Kelley et al., 2001; Houston et al., 2002; Schneider et al., 2009) were complemented by a new system to study H₃R. This system provides the basis for further molecular studies.

As a second aim, the G protein coupling-profile of the H₃R should be investigated. It is known, that H₃R couples to pertussis toxin-sensitive G proteins of the G_i/G_o-family, but detailed information about the interaction with specific G protein-subunits is not available. There are some ligands which show pleiotropic effects (Fox et al., 2002; Gbahou et al., 2003; Krueger et al., 2005; Ito et al., 2006). Therefore, the role of certain G protein α -subunits had to be investigated with respect to this matter.

Additionally, a system to study rat H₃R, a common laboratory animal to study H₃R-ligand effects, was generated. Deeper insights into the multiple functional species-differences of all histamine receptors in general, and H₃Rs in particular, will facilitate the development of more potent and selective ligands and increase our understanding of ligand-receptor interactions (Preuss et al., 2007b, c; Strasser et al., 2008b, 2009; Deml et al., 2009; Igel et al., 2009; Kraus et al., 2009; Wittmann et al., 2009). Moreover, for the design of a

suitable pharmacological tool, it is absolutely necessary to know its functional properties on every relevant GPCR species homolog in an unbiased manner (Pertz et al., 2006; Xie et al., 2006, 2007; Preuss et al., 2007a; Strasser et al., 2008a). The experimental studies should be complemented by molecular modelling approaches.

Finally, it is generally poorly understood how the ionic environment changes the pharmacological properties of a GPCR (Costa et al., 1990; Seifert, 2001; Schneider et al., 2009). Therefore, by using H₃R as a model system, the influence of different monovalent ions on receptor-to-G protein coupling were investigated. In particular, a potential interaction-site for Na⁺-ions, highly conserved among GPCRs, was mutated and studied (Horstman et al., 1990; Ceresa and Limbird, 1994).

In summary, this thesis further characterizes the structure and function of H₃R species homologs as well as the ligand-receptor interactions by an interdisciplinary approach comprising pharmacological assays, site-directed mutagenesis and molecular modelling.

1.7 References

- Albarran-Juarez J, Gilsbach R, Piekorz RP, Pexa K, Beetz N, Schneider J, Nürnberg B and Hein L (2009) Modulation of α_2 -adrenoceptor functions by heterotrimeric $G\alpha_i$ protein isoforms. *J Pharmacol Exp Ther* **331**:35-44.
- Aloia AL, Glatz RV, McMurchie EJ and Leifert WR (2009) GPCR expression using baculovirus-infected Sf9 cells. *Methods Mol Biol* **552**:115-129.
- Arrang JM, Garbarg M, Lancelot JC, Lecomte JM, Pollard H, Robba M, Schunack W and Schwartz JC (1988) Highly potent and selective ligands for a new class H_3 of histamine receptor. *Invest Radiol* **23 Suppl 1**:S130-132.
- Arrang JM, Garbarg M and Schwartz JC (1983) Auto-inhibition of brain histamine release mediated by a novel class H_3 of histamine receptor. *Nature* **302**:832-837.
- Arrang JM, Morisset S and Gbahou F (2007) Constitutive activity of the histamine H_3 receptor. *Trends Pharmacol Sci* **28**:350-357.
- Ash AS and Schild HO (1966) Receptors mediating some actions of histamine. *Br J Pharmacol Chemother* **27**:427-439.
- Barbier AJ, Aluisio L, Lord B, Qu Y, Wilson SJ, Boggs JD, Bonaventure P, Miller K, Fraser I, Dvorak L, Pudiak C, Dugovic C, Shelton J, Mazur C, Letavic MA, Carruthers NI and Lovenberg TW (2007) Pharmacological characterization of JNJ-28583867, a histamine H_3 receptor antagonist and serotonin reuptake inhibitor. *Eur J Pharmacol* **576**:43-54.
- Barger G and Dale HM (1910) The presence in ergot and physiological activity of Biminazoylethylamine. *J Physiol Paris* **40**:38-40.
- Bembenek SD, Keith JM, Letavic MA, Apodaca R, Barbier AJ, Dvorak L, Aluisio L, Miller KL, Lovenberg TW and Carruthers NI (2008) Lead identification of acetylcholinesterase inhibitors-histamine H_3 receptor antagonists from molecular modeling. *Bioorg Med Chem* **16**:2968-2973.
- Best CH, Dale HH, Dudley HW and Thorpe WV (1927) The nature of the vasodilator constituents of certain tissue extracts. *J Physiol* **62**:397-417.
- Birnbaumer L (2007) Expansion of signal transduction by G proteins. The second 15 years or so: from 3 to 16 alpha subunits plus betagamma dimers. *Biochim Biophys Acta* **1768**:772-793.
- Black JW, Duncan WA, Durant CJ, Ganellin CR and Parsons EM (1972) Definition and antagonism of histamine H_2 -receptors. *Nature* **236**:385-390.
- Black JW, Duncan WA, Emmett JC, Ganellin CR, Hesselbo T, Parsons ME and Wyllie JH (1973) Metiamide--an orally active histamine H_2 -receptor antagonist. *Agents Actions* **3**:133-137.
- Bockaert J and Pin JP (1999) Molecular tinkering of G protein-coupled receptors: an evolutionary success. *Embo J* **18**:1723-1729.

- Bonaventure P, Letavic M, Dugovic C, Wilson S, Aluisio L, Pudiak C, Lord B, Mazur C, Kamme F, Nishino S, Carruthers N and Lovenberg T (2007) Histamine H₃ receptor antagonists: from target identification to drug leads. *Biochem Pharmacol* **73**:1084-1096.
- Bongers G, Bakker RA and Leurs R (2007) Molecular aspects of the histamine H₃ receptor. *Biochem Pharmacol* **73**:1195-1204.
- Bovet D and Staub AM (1937) Action protectrice des éthers phénolique au cours de l'intoxication histaminique. *C R Soc Biol* **124**:547-549.
- Brimblecombe RW, Duncan WA, Durant GJ, Ganellin CR, Parsons ME and Black JW (1975) The pharmacology of cimetidine, a new histamine H₂-receptor antagonist. *Br J Pharmacol* **53**:435P-436P.
- Brys R, Josson K, Castelli MP, Jurzak M, Lijnen P, Gommeren W and Leysen JE (2000) Reconstitution of the human 5-HT_{1D} receptor-G-protein coupling: evidence for constitutive activity and multiple receptor conformations. *Mol Pharmacol* **57**:1132-1141.
- Bünemann M, Frank M and Lohse MJ (2003) G_i protein activation in intact cells involves subunit rearrangement rather than dissociation. *Proc Natl Acad Sci U S A* **100**:16077-16082.
- Cassar S (2000) Cloning of the guinea pig H₃ receptor. *Neuroreport* **11**:L3-4.
- Ceresa BP and Limbird LE (1994) Mutation of an aspartate residue highly conserved among G-protein-coupled receptors results in nonreciprocal disruption of α_2 -adrenergic receptor-G-protein interactions. A negative charge at amino acid residue 79 forecasts α_{2A} -adrenergic receptor sensitivity to allosteric modulation by monovalent cations and fully effective receptor/G-protein coupling. *J Biol Chem* **269**:29557-29564.
- Clark EA and Hill SJ (1996) Sensitivity of histamine H₃ receptor agonist-stimulated [³⁵S]GTP γ S binding to pertussis toxin. *Eur J Pharmacol* **296**:223-225.
- Costa T, Lang J, Gless C and Herz A (1990) Spontaneous association between opioid receptors and GTP-binding regulatory proteins in native membranes: specific regulation by antagonists and sodium ions. *Mol Pharmacol* **37**:383-394.
- Dale HH and Laidlaw PP (1910) The physiological action of beta-iminazolyethylamine. *J Physiol* **41**:318-344.
- Dale HH and Laidlaw PP (1911) Further observations on the action of beta-iminazolyethylamine. *J Physiol* **43**:182-195.
- Dale HH and Laidlaw PP (1919) Histamine shock. *J Physiol* **52**:355-390.
- De Esch IJ and Belzar KJ (2004) Histamine H₃ receptor agonists. *Mini Rev Med Chem* **4**:955-963.
- Deml KF, Beermann S, Neumann D, Strasser A and Seifert R (2009) Interactions of Histamine H₁-Receptor Agonists and Antagonists with the Human Histamine H₄-Receptor. *Mol Pharmacol* **76**(5):1019-30.

- Drutel G, Peitsaro N, Karlstedt K, Wieland K, Smit MJ, Timmerman H, Panula P and Leurs R (2001) Identification of rat H₃ receptor isoforms with different brain expression and signaling properties. *Mol Pharmacol* **59**:1-8.
- Dy M and Schneider E (2004) Histamine-cytokine connection in immunity and hematopoiesis. *Cytokine Growth Factor Rev* **15**:393-410.
- Esbenshade TA, Browman KE, Bitner RS, Strakhova M, Cowart MD and Brioni JD (2008) The histamine H₃ receptor: an attractive target for the treatment of cognitive disorders. *Br J Pharmacol* **154**:1166-1181.
- Ferrada C, Ferre S, Casado V, Cortes A, Justinova Z, Barnes C, Canela EI, Goldberg SR, Leurs R, Lluís C and Franco R (2008) Interactions between histamine H₃ and dopamine D₂ receptors and the implications for striatal function. *Neuropharmacology* **55**:190-197.
- Ferrada C, Moreno E, Casado V, Bongers G, Cortes A, Mallol J, Canela EI, Leurs R, Ferre S, Lluís C and Franco R (2009) Marked changes in signal transduction upon heteromerization of dopamine D₁ and histamine H₃ receptors. *Br J Pharmacol* **157**:64-75.
- Foord SM, Bonner TI, Neubig RR, Rosser EM, Pin JP, Davenport AP, Spedding M and Harmar AJ (2005) International Union of Pharmacology. XLVI. G protein-coupled receptor list. *Pharmacol Rev* **57**:279-288.
- Fourneau E and Bovet T (1933) Recherches sur l'action sympatholytique d'un nouveau dérivé du dioxane. *Arch Int Pharmacodyn* **46**:179-191.
- Fox GB, Pan JB, Esbenshade TA, Bitner RS, Nikkel AL, Miller T, Kang CH, Bennani YL, Black LA, Faghiih R, Hancock AA and Decker MW (2002) Differential in vivo effects of H₃ receptor ligands in a new mouse dipsogenia model. *Pharmacol Biochem Behav* **72**:741-750.
- Fredriksson R, Lagerstrom MC, Lundin LG and Schiöth HB (2003) The G-protein-coupled receptors in the human genome form five main families. Phylogenetic analysis, paralogon groups, and fingerprints. *Mol Pharmacol* **63**:1256-1272.
- Ganellin CR (1973) The tautomer ratio of histamine. *J Pharm Pharmacol* **25**:787-792.
- Gantz I, Schaffer M, DelValle J, Logsdon C, Campbell V, Uhler M and Yamada T (1991) Molecular cloning of a gene encoding the histamine H₂ receptor. *Proc Natl Acad Sci U S A* **88**:429-433.
- Gazi L, Nickolls SA and Strange PG (2003) Functional coupling of the human dopamine D₂ receptor with G α_{i1} , G α_{i2} , G α_{i3} and G α_o G proteins: evidence for agonist regulation of G protein selectivity. *Br J Pharmacol* **138**:775-786.
- Gbahou F, Rouleau A, Morisset S, Parmentier R, Crochet S, Lin JS, Ligneau X, Tardivel-Lacombe J, Stark H, Schunack W, Ganellin CR, Schwartz JC and Arrang JM (2003) Protean agonism at histamine H₃ receptors in vitro and in vivo. *Proc Natl Acad Sci U S A* **100**:11086-11091.
- Ghanouni P, Schambye H, Seifert R, Lee TW, Rasmussen SG, Gether U and Kobilka BK (2000) The effect of pH on β_2 -adrenoceptor function. Evidence for protonation-dependent activation. *J Biol Chem* **275**:3121-3127.

- Gemkow MJ, Davenport AJ, Harich S, Ellenbroek BA, Cesura A and Hallett D (2009) The histamine H₃ receptor as a therapeutic drug target for CNS disorders. *Drug Discov Today* **14**:509-515.
- Gomez-Ramirez J, Ortiz J and Blanco I (2002) Presynaptic H₃ autoreceptors modulate histamine synthesis through cAMP pathway. *Mol Pharmacol* **61**:239-245.
- Haas H and Panula P (2003) The role of histamine and the tuberomamillary nucleus in the nervous system. *Nat Rev Neurosci* **4**:121-130.
- Haas HL, Sergeeva OA and Selbach O (2008) Histamine in the nervous system. *Physiol Rev* **88**:1183-1241.
- Hancock AA, Esbenshade TA, Krueger KM and Yao BB (2003) Genetic and pharmacological aspects of histamine H₃ receptor heterogeneity. *Life Sci* **73**:3043-3072.
- Hanyaloglu AC and von Zastrow M (2008) Regulation of GPCRs by endocytic membrane trafficking and its potential implications. *Annu Rev Pharmacol Toxicol* **48**:537-568.
- Horstman DA, Brandon S, Wilson AL, Guyer CA, Cragoe EJ, Jr. and Limbird LE (1990) An aspartate conserved among G-protein receptors confers allosteric regulation of α_2 -adrenergic receptors by sodium. *J Biol Chem* **265**:21590-21595.
- Houston C, Wenzel-Seifert K, Bückstümmer T and Seifert R (2002) The human histamine H₂-receptor couples more efficiently to Sf9 insect cell G_s-proteins than to insect cell G_q-proteins: limitations of Sf9 cells for the analysis of receptor/G_q-protein coupling. *J Neurochem* **80**:678-696.
- Humbert-Claude M, Morisset S, Gbahou F and Arrang JM (2007) Histamine H₃ and dopamine D₂ receptor-mediated [³⁵S]GTP γ S binding in rat striatum: evidence for additive effects but lack of interactions. *Biochem Pharmacol* **73**:1172-1181.
- Igel P, Geyer R, Strasser A, Dove S, Seifert R and Buschauer A (2009) Synthesis and structure-activity relationships of cyanoguanidine-type and structurally related histamine H₄ receptor agonists. *J Med Chem* **52**:6297-6313.
- Ireland-Denny L, Parihar AS, Miller TR, Kang CH, Krueger KM, Esbenshade TA and Hancock AA (2001) Species-related pharmacological heterogeneity of histamine H₃ receptors. *Eur J Pharmacol* **433**:141-150.
- Ito S, Yoshimoto R, Miyamoto Y, Mitobe Y, Nakamura T, Ishihara A, MacNeil DJ, Kanatani A and Tokita S (2006) Detailed pharmacological characterization of GT-2331 for the rat histamine H₃ receptor. *Eur J Pharmacol* **529**:40-46.
- Jaakola VP, Griffith MT, Hanson MA, Cherezov V, Chien EY, Lane JR, Ijzerman AP and Stevens RC (2008) The 2.6 Å crystal structure of a human A_{2A} adenosine receptor bound to an antagonist. *Science* **322**:1211-1217.
- Jacoby E, Bouhelal R, Gerspacher M and Seuwen K (2006) The 7 TM G-protein-coupled receptor target family. *ChemMedChem* **1**:761-782.
- Kazumori H, Ishihara S, Rumi MA, Ortega-Cava CF, Kadowaki Y and Kinoshita Y (2004) Transforming growth factor- α directly augments histidine decarboxylase and vesicular monoamine transporter 2 production in rat enterochromaffin-like cells. *Am J Physiol Gastrointest Liver Physiol* **286**:G508-514.

- Kelley MT, Bürckstümmer T, Wenzel-Seifert K, Dove S, Buschauer A and Seifert R (2001) Distinct interaction of human and guinea pig histamine H₂-receptor with guanidine-type agonists. *Mol Pharmacol* **60**:1210-1225.
- Kenakin T (2004) Principles: receptor theory in pharmacology. *Trends Pharmacol Sci* **25**:186-192.
- Klemke M, Pasolli HA, Kehlenbach RH, Offermanns S, Schultz G and Huttner WB (2000) Characterization of the extra-large G protein α -subunit XL α_s . II. Signal transduction properties. *J Biol Chem* **275**:33633-33640.
- Kobilka B and Schertler GF (2008) New G-protein-coupled receptor crystal structures: insights and limitations. *Trends Pharmacol Sci* **29**:79-83.
- Kofuku Y, Yoshiura C, Ueda T, Terasawa H, Hirai T, Tominaga S, Hirose M, Maeda Y, Takahashi H, Terashima Y, Matsushima K and Shimada I (2009) Structural basis of the interaction between chemokine stromal cell-derived factor-1/CXCL12 and its G-protein-coupled receptor CXCR4. *J Biol Chem*.
- Kraus A, Ghorai P, Birnkammer T, Schnell D, Elz S, Seifert R, Dove S, Bernhardt G and Buschauer A (2009) N^G-acylated aminothiazolylpropylguanidines as potent and selective histamine H₂ receptor agonists. *ChemMedChem* **4**:232-240.
- Krueger KM, Witte DG, Ireland-Denny L, Miller TR, Baranowski JL, Buckner S, Milicic I, Esbenshade TA and Hancock AA (2005) G protein-dependent pharmacology of histamine H₃ receptor ligands: evidence for heterogeneous active state receptor conformations. *J Pharmacol Exp Ther* **314**:271-281.
- Lagerström MC and Schiöth HB (2008) Structural diversity of G protein-coupled receptors and significance for drug discovery. *Nat Rev Drug Discov* **7**:339-357.
- Leurs R, Bakker RA, Timmerman H and de Esch IJ (2005) The histamine H₃ receptor: from gene cloning to H₃ receptor drugs. *Nat Rev Drug Discov* **4**:107-120.
- Liu C, Ma X, Jiang X, Wilson SJ, Hofstra CL, Blevitt J, Pyati J, Li X, Chai W, Carruthers N and Lovenberg TW (2001) Cloning and pharmacological characterization of a fourth histamine receptor (H₄) expressed in bone marrow. *Mol Pharmacol* **59**:420-426.
- Lovenberg TW, Pyati J, Chang H, Wilson SJ and Erlander MG (2000) Cloning of rat histamine H₃ receptor reveals distinct species pharmacological profiles. *J Pharmacol Exp Ther* **293**:771-778.
- Lovenberg TW, Roland BL, Wilson SJ, Jiang X, Pyati J, Huvar A, Jackson MR and Erlander MG (1999) Cloning and functional expression of the human histamine H₃ receptor. *Mol Pharmacol* **55**:1101-1107.
- Moreno-Delgado D, Gomez-Ramirez J, Torrent-Moreno A, Gonzalez-Sepulveda M, Blanco I and Ortiz J (2009) Different role of cAMP dependent protein kinase and CaMKII in H₃ receptor regulation of histamine synthesis and release. *Neuroscience* **164**(3):1244-51.
- Morse KL, Behan J, Laz TM, West RE, Jr., Greenfeder SA, Anthes JC, Umland S, Wan Y, Hipkin RW, Gonsiorek W, Shin N, Gustafson EL, Qiao X, Wang S, Hedrick JA, Greene J, Bayne M and Monsma FJ, Jr. (2001) Cloning and characterization of a novel human histamine receptor. *J Pharmacol Exp Ther* **296**:1058-1066.

- Mustafi D and Palczewski K (2009) Topology of class A G protein-coupled receptors: insights gained from crystal structures of rhodopsins, adrenergic and adenosine receptors. *Mol Pharmacol* **75**:1-12.
- Nakamura T, Itadani H, Hidaka Y, Ohta M and Tanaka K (2000) Molecular cloning and characterization of a new human histamine receptor, HH4R. *Biochem Biophys Res Commun* **279**:615-620.
- Neitzel KL and Hepler JR (2006) Cellular mechanisms that determine selective RGS protein regulation of G protein-coupled receptor signaling. *Semin Cell Dev Biol* **17**:383-389.
- Nguyen T, Shapiro DA, George SR, Setola V, Lee DK, Cheng R, Rauser L, Lee SP, Lynch KR, Roth BL and O'Dowd BF (2001) Discovery of a novel member of the histamine receptor family. *Mol Pharmacol* **59**:427-433.
- O'Reilly M, Alpert R, Jenkinson S, Gladue RP, Foo S, Trim S, Peter B, Trevethick M and Fidock M (2002) Identification of a histamine H₄ receptor on human eosinophils--role in eosinophil chemotaxis. *J Recept Signal Transduct Res* **22**:431-448.
- Oda T, Morikawa N, Saito Y, Masuho Y and Matsumoto S (2000) Molecular cloning and characterization of a novel type of histamine receptor preferentially expressed in leukocytes. *J Biol Chem* **275**:36781-36786.
- Ogasawara M, Yamauchi K, Satoh Y, Yamaji R, Inui K, Jonker JW, Schinkel AH and Maeyama K (2006) Recent advances in molecular pharmacology of the histamine systems: organic cation transporters as a histamine transporter and histamine metabolism. *J Pharmacol Sci* **101**:24-30.
- Palczewski K, Kumasaka T, Hori T, Behnke CA, Motoshima H, Fox BA, Le Trong I, Teller DC, Okada T, Stenkamp RE, Yamamoto M and Miyano M (2000) Crystal structure of rhodopsin: A G protein-coupled receptor. *Science* **289**:739-745.
- Park JH, Scheerer P, Hofmann KP, Choe HW and Ernst OP (2008) Crystal structure of the ligand-free G-protein-coupled receptor opsin. *Nature* **454**:183-187.
- Parsons ME and Ganellin CR (2006) Histamine and its receptors. *Br J Pharmacol* **147 Suppl 1**:S127-135.
- Pertz HH, Gornemann T, Schurad B, Seifert R and Strasser A (2006) Striking differences of action of lisuride stereoisomers at histamine H₁ receptors. *Naunyn Schmiedeberg's Arch Pharmacol* **374**:215-222.
- Petroianu G, Arafat K, Sasse BC and Stark H (2006) Multiple enzyme inhibitions by histamine H₃ receptor antagonists as potential procognitive agents. *Pharmazie* **61**:179-182.
- Preuss H, Ghorai P, Kraus A, Dove S, Buschauer A and Seifert R (2007a) Constitutive activity and ligand selectivity of human, guinea pig, rat, and canine histamine H₂ receptors. *J Pharmacol Exp Ther* **321**:983-995.
- Preuss H, Ghorai P, Kraus A, Dove S, Buschauer A and Seifert R (2007b) Mutations of Cys-17 and Ala-271 in the human histamine H₂ receptor determine the species selectivity of guanidine-type agonists and increase constitutive activity. *J Pharmacol Exp Ther* **321**:975-982.

- Preuss H, Ghorai P, Kraus A, Dove S, Buschauer A and Seifert R (2007c) Point mutations in the second extracellular loop of the histamine H₂ receptor do not affect the species-selective activity of guanidine-type agonists. *Naunyn Schmiedebergs Arch Pharmacol* **376**:253-264.
- Quehenberger O, Prossnitz ER, Cochrane CG and Ye RD (1992) Absence of G_i proteins in the Sf9 insect cell. Characterization of the uncoupled recombinant *N*-formyl peptide receptor. *J Biol Chem* **267**:19757-19760.
- Rasmussen SG, Choi HJ, Rosenbaum DM, Kobilka TS, Thian FS, Edwards PC, Burghammer M, Ratnala VR, Sanishvili R, Fischetti RF, Schertler GF, Weis WI and Kobilka BK (2007) Crystal structure of the human β_2 -adrenergic G-protein-coupled receptor. *Nature* **450**:383-387.
- Ratnala VR (2006) New tools for G-protein coupled receptor (GPCR) drug discovery: combination of baculoviral expression system and solid state NMR. *Biotechnol Lett* **28**:767-778.
- Ratnala VR, Swarts HG, VanOostrum J, Leurs R, DeGroot HJ, Bakker RA and DeGrip WJ (2004) Large-scale overproduction, functional purification and ligand affinities of the His-tagged human histamine H₁ receptor. *Eur J Biochem* **271**:2636-2646.
- Rosenbaum DM, Cherezov V, Hanson MA, Rasmussen SG, Thian FS, Kobilka TS, Choi HJ, Yao XJ, Weis WI, Stevens RC and Kobilka BK (2007) GPCR engineering yields high-resolution structural insights into β_2 -adrenergic receptor function. *Science* **318**:1266-1273.
- Rouleau A, Heron A, Cochois V, Pillot C, Schwartz JC and Arrang JM (2004) Cloning and expression of the mouse histamine H₃ receptor: evidence for multiple isoforms. *J Neurochem* **90**:1331-1338.
- Sanchez-Lemus E and Arias-Montano JA (2004) Histamine H₃ receptor activation inhibits dopamine D₁ receptor-induced cAMP accumulation in rat striatal slices. *Neurosci Lett* **364**:179-184.
- Sander K, Kottke T and Stark H (2008) Histamine H₃ receptor antagonists go to clinics. *Biol Pharm Bull* **31**:2163-2181.
- Scheerer P, Park JH, Hildebrand PW, Kim YJ, Krauss N, Choe HW, Hofmann KP and Ernst OP (2008) Crystal structure of opsin in its G-protein-interacting conformation. *Nature* **455**:497-502.
- Schneider EH, Schnell D, Papa D and Seifert R (2009) High constitutive activity and a G-protein-independent high-affinity state of the human histamine H₄-receptor. *Biochemistry* **48**:1424-1438.
- Seifert R, Lee TW, Lam VT and Kobilka BK (1998) Reconstitution of β_2 -adrenoceptor-GTP-binding-protein interaction in Sf9 cells--high coupling efficiency in a β_2 -adrenoceptor-G α_s fusion protein. *Eur J Biochem* **255**:369-382.
- Seifert R, Gether U, Wenzel-Seifert K and Kobilka BK (1999) Effects of guanine, inosine, and xanthine nucleotides on β_2 -adrenergic receptor/G_s interactions: evidence for multiple receptor conformations. *Mol Pharmacol* **56**:348-358.
- Seifert R (2001) Monovalent anions differentially modulate coupling of the β_2 -adrenoceptor to G_s alpha splice variants. *J Pharmacol Exp Ther* **298**:840-847.

- Seifert R and Wenzel-Seifert K (2001) Unmasking different constitutive activity of four chemoattractant receptors using Na⁺ as universal stabilizer of the inactive (R) state. *Receptors Channels* **7**:357-369.
- Seifert R and Wenzel-Seifert K (2002) Constitutive activity of G-protein-coupled receptors: cause of disease and common property of wild-type receptors. *Naunyn Schmiedebergs Arch Pharmacol* **366**:381-416.
- Seifert R and Wenzel-Seifert K (2003) The human formyl peptide receptor as model system for constitutively active G-protein-coupled receptors. *Life Sci* **73**:2263-2280.
- Seifert R and Wieland T (2005) *G protein-coupled receptors as drug targets : analysis of activation and constitutive activity*. Wiley-VCH, Weinheim.
- Shenton FC, Hann V and Chazot PL (2005) Evidence for native and cloned H₃ histamine receptor higher oligomers. *Inflamm Res* **54 Suppl 1**:S48-49.
- Stark H, Kathmann M, Schlicker E, Schunack W, Schlegel B and Sippl W (2004) Medicinal chemical and pharmacological aspects of imidazole-containing histamine H₃ receptor antagonists. *Mini Rev Med Chem* **4**:965-977.
- Stark H, Sippl W, Ligneau X, Arrang JM, Ganellin CR, Schwartz JC and Schunack W (2001) Different antagonist binding properties of human and rat histamine H₃ receptors. *Bioorg Med Chem Lett* **11**:951-954.
- Stocking EM and Letavic MA (2008) Histamine H₃ antagonists as wake-promoting and pro-cognitive agents. *Curr Top Med Chem* **8**:988-1002.
- Strasser A, Striegl B, Wittmann HJ and Seifert R (2008a) Pharmacological profile of histaprodifens at four recombinant histamine H₁ receptor species isoforms. *J Pharmacol Exp Ther* **324**:60-71.
- Strasser A, Wittmann HJ and Seifert R (2008b) Ligand-specific contribution of the N terminus and E2-loop to pharmacological properties of the histamine H₁-receptor. *J Pharmacol Exp Ther* **326**:783-791.
- Strasser A, Wittmann HJ, Kunze M, Elz S and Seifert R (2009) Molecular basis for the selective interaction of synthetic agonists with the human histamine H₁-receptor compared with the guinea pig H₁-receptor. *Mol Pharmacol* **75**:454-465.
- Takahashi K, Suwa H, Ishikawa T and Kotani H (2002) Targeted disruption of H₃ receptors results in changes in brain histamine tone leading to an obese phenotype. *J Clin Invest* **110**:1791-1799.
- Tardivel-Lacombe J, Rouleau A, Heron A, Morisset S, Pillot C, Cochois V, Schwartz JC and Arrang JM (2000) Cloning and cerebral expression of the guinea pig histamine H₃ receptor: evidence for two isoforms. *Neuroreport* **11**:755-759.
- Toyota H, Dugovic C, Koehl M, Laposky AD, Weber C, Ngo K, Wu Y, Lee DH, Yanai K, Sakurai E, Watanabe T, Liu C, Chen J, Barbier AJ, Turek FW, Fung-Leung WP and Lovenberg TW (2002) Behavioral characterization of mice lacking histamine H₃ receptors. *Mol Pharmacol* **62**:389-397.
- Vassilatis DK, Hohmann JG, Zeng H, Li F, Ranchalis JE, Mortrud MT, Brown A, Rodriguez SS, Weller JR, Wright AC, Bergmann JE and Gaitanaris GA (2003) The G protein-coupled receptor repertoires of human and mouse. *Proc Natl Acad Sci U S A* **100**:4903-4908.

- Warne T, Serrano-Vega MJ, Baker JG, Moukhametzianov R, Edwards PC, Henderson R, Leslie AG, Tate CG and Schertler GF (2008) Structure of a β_1 -adrenergic G-protein-coupled receptor. *Nature* **454**:486-491.
- Weis WI and Kobilka BK (2008) Structural insights into G-protein-coupled receptor activation. *Curr Opin Struct Biol*.
- Wenzel-Seifert K, Hurt CM and Seifert R (1998) High constitutive activity of the human formyl peptide receptor. *J Biol Chem* **273**:24181-24189.
- Wenzel-Seifert K, Arthur JM, Liu HY and Seifert R (1999) Quantitative analysis of formyl peptide receptor coupling to $G_{\alpha_{i1}}$, $G_{\alpha_{i2}}$, and $G_{\alpha_{i3}}$. *J Biol Chem* **274**:33259-33266.
- Wenzel-Seifert K and Seifert R (2000) Molecular analysis of β_2 -adrenoceptor coupling to G_s -, G_i -, and G_q -proteins. *Mol Pharmacol* **58**:954-966.
- Wenzel-Seifert K, Kelley MT, Buschauer A and Seifert R (2001) Similar apparent constitutive activity of human histamine H_2 -receptor fused to long and short splice variants of G_{α_s} . *J Pharmacol Exp Ther* **299**:1013-1020.
- Wiedemann P, Bonisch H, Oerters F and Bruss M (2002) Structure of the human histamine H_3 receptor gene (HRH3) and identification of naturally occurring variations. *J Neural Transm* **109**:443-453.
- Wieland T, Lutz S and Chidiac P (2007) Regulators of G protein signalling: a spotlight on emerging functions in the cardiovascular system. *Curr Opin Pharmacol* **7**:201-207.
- Wittmann HJ, Seifert R and Strasser A (2009) Contribution of binding enthalpy and entropy to affinity of antagonist and agonist binding at human and guinea pig histamine H_1 -receptor. *Mol Pharmacol* **76**:25-37.
- Wijtmans M, Leurs R and de Esch I (2007) Histamine H_3 receptor ligands break ground in a remarkable plethora of therapeutic areas. *Expert Opin Investig Drugs* **16**:967-985.
- Willars GB (2006) Mammalian RGS proteins: multifunctional regulators of cellular signalling. *Semin Cell Dev Biol* **17**:363-376.
- Windaus A and Vogt W (1908) Synthesis of Imidazolylethylamine. *Ber Dtsch Ges* **40**:3691.
- Wise A, Jupe SC and Rees S (2004) The identification of ligands at orphan G-protein coupled receptors. *Annu Rev Pharmacol Toxicol* **44**:43-66.
- Woo AY, Wang TB, Zeng X, Zhu W, Abernethy DR, Wainer IW and Xiao RP (2009) Stereochemistry of an agonist determines coupling preference of β_2 -adrenoceptor to different G proteins in cardiomyocytes. *Mol Pharmacol* **75**:158-165.
- Xie SX, Ghorai P, Ye QZ, Buschauer A and Seifert R (2006) Probing ligand-specific histamine H_1 - and H_2 -receptor conformations with N^G -acylated Imidazolylpropylguanidines. *J Pharmacol Exp Ther* **317**:139-146.
- Xie SX, Schalkhauser F, Ye QZ, Seifert R and Buschauer A (2007) Effects of impromidine- and arpromidine-derived guanidines on recombinant human and guinea pig histamine H_1 and H_2 receptors. *Arch Pharm (Weinheim)* **340**:9-16.

- Yamashita M, Fukui H, Sugama K, Horio Y, Ito S, Mizuguchi H and Wada H (1991) Expression cloning of a cDNA encoding the bovine histamine H₁ receptor. *Proc Natl Acad Sci U S A* **88**:11515-11519.
- Yao BB, Hutchins CW, Carr TL, Cassar S, Masters JN, Bennani YL, Esbenshade TA and Hancock AA (2003a) Molecular modeling and pharmacological analysis of species-related histamine H₃ receptor heterogeneity. *Neuropharmacology* **44**:773-786.
- Yao BB, Sharma R, Cassar S, Esbenshade TA and Hancock AA (2003b) Cloning and pharmacological characterization of the monkey histamine H₃ receptor. *Eur J Pharmacol* **482**:49-60.
- Zhu Y, Michalovich D, Wu H, Tan KB, Dytko GM, Mannan IJ, Boyce R, Alston J, Tierney LA, Li X, Herrity NC, Vawter L, Sarau HM, Ames RS, Davenport CM, Hieble JP, Wilson S, Bergsma DJ and Fitzgerald LR (2001) Cloning, expression, and pharmacological characterization of a novel human histamine receptor. *Mol Pharmacol* **59**:434-441.

Chapter 2

No evidence for functional selectivity of proxyfan at the human histamine H₃-receptor coupled to defined G_i/G_o protein heterotrimers

This chapter is adapted from:

Schnell D, Burleigh K, Trick J and Seifert R (2009) No evidence for functional selectivity of proxyfan at the human histamine H₃-receptor coupled to defined G_i/G_o protein heterotrimers. *J Pharmacol Exp Ther* (published online: <http://jpet.aspetjournals.org/content/early/2009/12/03/jpet.109.162339.long>).

2.1 Abstract

Numerous structurally diverse ligands were developed to target the human histamine H₃-receptor (hH₃R), a presynaptic G_i/G_o-coupled auto- and heteroreceptor. Proxyfan was identified to be functionally selective, with different efficacies towards G_i/G_o-dependent hH₃R signalling pathways. However, the underlying molecular mechanism of functional selectivity of proxyfan is still unclear. In the current study, we investigated the role of different G $\alpha_{i/o}$ proteins in hH₃R signalling, using a baculovirus/Sf9 cell expression system. We tested the hypothesis that ligand-specific coupling differences to defined G_i/G_o-heterotrimers are responsible for functional selectivity of proxyfan at hH₃R. In Sf9 membranes, full-length hH₃R (445 amino acids) was expressed in combination with an excess of different mammalian G proteins (G α_{i1} , G α_{i2} , G α_{i3} or G α_{o1} , and $\beta_1\gamma_2$ dimers, respectively). Additionally, we constructed the fusion proteins hH₃R-G α_{i2} and hH₃R-G α_{o1} to ensure clearly defined receptor/G protein stoichiometries. Steady-state GTPase experiments were performed to directly measure the impact of each G protein on hH₃R signal transduction. The hH₃R coupled similarly to all G proteins. We also observed similar ligand-independent or constitutive activity. Proxyfan and various other imidazole-containing ligands, including full agonists, partial agonists and inverse agonists showed very similar pharmacological profiles, not influenced by the type of G protein co-expressed. Selected ligands, examined in membranes expressing the fusion proteins hH₃R-G α_{i2} and hH₃R-G α_{o1} (plus $\beta_1\gamma_2$ dimers), yielded very similar results. Collectively, our data indicate that hH₃R couples similarly to different G $\alpha_{i/o}$ subunits and that ligand-specific active receptor conformations, resulting in G-protein coupling preferences, do not exist for proxyfan or other imidazole compounds investigated.

2.2 Introduction

The histamine H₃-receptor (H₃R) is currently one of the most targeted biogenic amine receptors because it participates in important physiological processes like the sleep-wake cycle, eating behavior and cognition (Leurs et al., 2005). Discovered pharmacologically in the early 1980s and cloned almost 20 years later (Lovenberg et al., 2000), the H₃R was shown to be a presynaptic auto- and heteroreceptor, regulating the release of neurotransmitters including histamine, dopamine, norepinephrine, serotonin and acetylcholine via negative feedback mechanisms (Haas et al., 2008). Thus, the H₃R is a promising drug target for many diseases including obesity, sleep disorders such as narcolepsy and cognitive problems

associated with Alzheimer's disease, attention deficit-hyperactivity disorder and schizophrenia (Bonaventure et al., 2007; Esbenshade et al., 2008).

According to the two-state model of receptor activation, G protein-coupled receptors (GPCRs) isomerize from an inactive (R) state to an active (R*) state (Kenakin, 2001; Seifert and Wenzel-Seifert, 2002). In the R* state, GPCRs activate G proteins. Agonist-independent R to R* isomerization is referred to as constitutive activity and results in an increase in basal G protein activity. Agonists stabilize the R* state and further increase, whereas inverse agonists stabilize the R state and decrease, basal G protein activity. The H₃R is constitutively active (Leurs et al., 2005) and couples to G_i/G_o-proteins in native tissues (Clark and Hill, 1996).

Many GPCRs are able to signal through various intracellular pathways. Depending on the specific G proteins to which the GPCR is coupled functional ligand selectivity has been frequently observed (Kenakin, 2001, 2007). In this case, the ligand preferentially activates specific signaling pathways mediated by a single GPCR in a manner that challenges the above introduced two-state model. Based on such findings, a multiple-state model, implying the existence of ligand-specific conformational states, has been developed (Kenakin, 2001, 2007; Kobilka and Deupi, 2007). Interestingly, even stereoisomers of one and the same compound can show different functional selectivities, providing an additional opportunity to control receptor-mediated effects (Seifert and Dove, 2009).

Protean agonism is considered a special case of functional selectivity. A protean agonist presumably stabilizes a receptor conformation with a lower efficacy towards the G protein than the agonist-free constitutively active or agonist-stabilized GPCR state. The ligand then acts as an inverse agonist. In a quiescent system with low constitutive activity, the protean ligand can act as an agonist (Gbahou et al., 2003; Kenakin, 2007).

Numerous structurally diverse H₃R ligands have been synthesized as potential drug candidates or as pharmacological tools. Almost all H₃R agonists are imidazole-containing small molecules, derived from the endogenous agonist histamine (Leurs et al., 2005). H₃R antagonists/inverse agonists can be differentiated into imidazole-containing antagonists and non-imidazole antagonists (Cowart et al., 2004; Leurs et al., 2005). Proxyfan is a prototypical, imidazole-containing H₃R ligand that was initially characterized as an antagonist (Hüls et al., 1996) (Fig. 2.1). Subsequent studies revealed a more complex pharmacological profile and proxyfan was re-classified as a protean agonist (Gbahou et al., 2003). However, the systems examined were all very different, rendering data interpretation difficult. In brief, proxyfan was examined in different species and measuring various parameters. Additionally, the parameters were often quite distal and the G protein constructs used to transfect recombinant cell lines do not represent the physiological coupling partners or were chimeric to redirect the signaling cascade (Krueger et al., 2005). Collectively, due to the large

differences between the systems examined it is very difficult to precisely define the molecular mechanism for the pleiotropic effects of proxyfan.

By studying nine imidazole-containing H₃R ligands (Fig. 2.1), we wished to obtain more direct evidence for the existence of different ligand-specific H₃R conformations. Most importantly, we aimed at probing the hypothesis that the type of G_i/G_o-protein α -subunit to which H₃R couples is responsible for the differential effects of proxyfan. Therefore, we established a baculovirus/Sf9 cell expression system for the full-length hH₃R (445 aa), in which the receptor can be expressed either alone or co-expressed with different G_i/G_o-protein α -subunits (G α_{i1} , G α_{i2} , G α_{i3} or G α_{o1} , and $\beta_1\gamma_2$ dimers, respectively). Sf9 cells have already been successfully used for reconstitution of several G_i/G_o-coupled GPCRs (Wenzel-Seifert et al., 1998; Kleemann et al., 2008). The hH₃R-expressing membranes were then studied under identical experimental conditions, focusing on steady-state GTPase activity, a proximal parameter of GPCR/G-protein coupling. Moreover, we examined the fusion proteins hH₃R-G α_{i2} and hH₃R-G α_{o1} . GPCR-G α fusion proteins ensure close proximity and defined 1:1 stoichiometry of the signalling partners (Seifert et al., 1999b), ruling out the possibility that differences in receptor-to-G protein ratio account for potential differences in pharmacological properties of ligands at hH₃R.

2.3 Materials and methods

2.3.1 Materials

The cDNA for the hH₃R was kindly provided by Dr. T. Lovenberg (Johnson & Johnson Pharmaceutical R&D, San Diego, CA, USA). All restriction enzymes and T4 DNA ligase were from New England Biolabs (Frankfurt, Germany). M-MLV Reverse Transcriptase was from Invitrogen (Carlsbad, CA, USA). Cloned *Pfu* polymerase was obtained from Stratagene (La Jolla, CA, USA). The DNA primers for PCR were synthesized by MWG Biotech (Ebersberg, Germany). Baculoviruses for G α_{i1} , G α_{i2} and G α_{i3} were donated by Dr. A. G. Gilman (Department of Pharmacology, University of Southwestern Medical Center, Dallas, TX, USA). Baculovirus for rat G α_{o1} was donated by Dr. J. C. Garrison (University of Virginia, Charlottesville, VA, USA). Recombinant baculovirus encoding the unmodified version of G $\beta_1\gamma_2$ subunits was a kind gift of Dr. P. Gierschik (Dept. of Pharmacology and Toxicology, University of Ulm, Germany). Anti-hH₃R Ig was from Bio-Trend (Cologne, Germany). The anti-FLAG Ig (M1 monoclonal antibody) and anti-His₆ Ig were from Sigma (St. Louis, MO, USA). The antibodies recognizing G $\alpha_{i/o}$ -subunits (G α_{common} ; AS 266) and G β -subunits (G β_{common} ; AS 398/9), as well as purified G α_{i2} - and G α_{o2} -protein, were kindly provided by Dr. B. Nürnberg (Institute of Pharmacology, University of Tübingen, Germany). The G $\alpha_{i1/2}$ - and

G α_o -selective antibodies were from Calbiochem (San Diego, CA, USA). Histamine, (*R*)- α -methylhistamine, *N*^u-methylhistamine, imetit, clobenpropit and thioperamide were from Tocris (Avonmouth, Bristol, UK). Impentamine, imoproxyfan and ciproxyfan were kind gifts from Dr. S. Elz (Dept. of Pharmaceutical/Medicinal Chemistry I, University of Regensburg, Germany). Proxyfan was synthesized by Dr. P. Igel (Department of Pharmaceutical/Medicinal Chemistry II, University of Regensburg, Germany). Ligand structures are depicted in Fig. 2.1. Stock solutions (10 mM) of all H₃R ligands described in this paper were prepared in distilled water and stored at -20°C. [³H]JNJ-7753707 (= [³H]RWJ-422475) (30 Ci/mmol) was kindly donated by Dr. P. Bonaventure (Johnson & Johnson Pharmaceutical R&D, San Diego, CA, USA). [³H]Dihydroalprenolol (85-90 Ci/mmol) and [³⁵S]GTP γ S (1100 Ci/mmol) were obtained from Perkin Elmer (Boston, MA, USA). [γ -³²P]GTP was prepared using GDP and [³²P]P_i (8500-9120 Ci/mmol orthophosphoric acid) (Perkin Elmer Life and Analytical Sciences, Boston, MA, USA) according to a previously described enzymatic labelling procedure (Walseth and Johnson, 1979). Unlabeled nucleotides were from Roche (Indianapolis, IN, USA) and all other reagents were of the highest purity available and from standard suppliers.

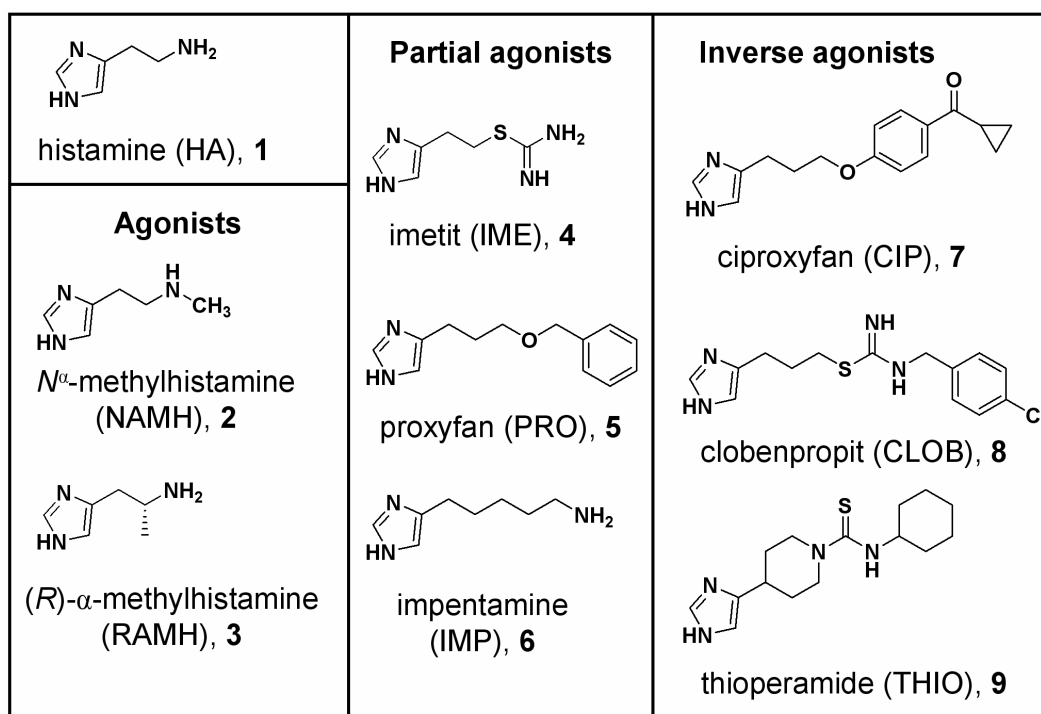


Fig. 2.1. Structures of imidazole-containing H₃R ligands: full agonists **1-3**, partial agonists **4-6** and antagonists/inverse agonists **7-9**.

2.3.2 Construction of FLAG epitope- and hexahistidine-tagged cDNA for hH₃R

The cDNA for the tagged receptor protein was generated by sequential overlap-extension PCR. With pGEM-3Z-SF-hH₄R-His₆ as template (Schneider et al., 2009), PCR 1A was used to amplify a DNA fragment consisting of the cleavable signal peptide from influenza hemagglutinin (S), the FLAG epitope (F) recognized by the monoclonal antibody M1 and a start codon. The sense primer F1a (5'-GAC CAT GAT TAC GCC AAG C-3') annealed with 19 bp of pGEM-3Z prior to the 5'-end of SF. The antisense primer C3 (5'-CAT GGC GTC ATC ATC GTC-3') annealed with 15 bp of the 3'-end of SF and with ATG. In PCR 1B, the cDNA encoding the hH₃R, followed by a hexahistidine tag (His₆) in 3'-position, was generated. The hexahistidine tag was included to allow future purification, to provide additional protection against proteolysis and to serve as a linker in fusion proteins between the hH₃R and G-proteins (Seifert et al., 1998). The sense primer HUMAN HRH3-F- (5'-GAC GAT GAT GAC GCC ATG GAG CGC GCG CCG CC-3') consisted of 15 bp of the 3'-end of SF and the first 17 bp of the 5'-end of the hH₃R. The antisense primer HUMAN HRH3-RV (5'-GA TCC TCT AGA TTA GTG ATG GTG ATG ATG GTG CTT CCA GCA GTG CTC-3') consisted of 15 bp of the C-terminus of the hH₃R, the hexahistidine tag, the *stop codon*, and an XbaI site. As template, a plasmid (pCIneo) containing the sequence of hH₃R was used. In PCR 2, the products of PCR 1A and PCR 1B annealed in the region encoding SF and ATG. Here, the sense primer of PCR 1a and the antisense primer of PCR 1b were used. In that way, a fragment encoding SF, the hH₃R sequence, the hexahistidine tag, the *stop codon*, and an XbaI site was obtained. The fragment was digested with Sac I and Xba I and cloned into pGEM-3Z-SF-hH₄R-His₆, digested with the same restriction enzymes, to yield pGEM-3Z-SF-hH₃R-His₆. After transformation of chemically competent bacteria (JM 109), amplification of the plasmids and analytical restriction digestion, the subcloned hH₃R construct was fully sequenced. Finally, the construct was cloned into the baculovirus transfer vector pVL1392-SF-hH₄R-His₆ (Schneider et al., 2009) via Sac I and Xba I restriction sites. Again, competent bacteria (Top 10) were transformed, the plasmid amplified and the accuracy of the resulting MaxiPrep-DNA checked by extensive restriction digestion analysis and sequencing.

2.3.3 Construction of the cDNAs for hH₃R-Gα_{i2} and hH₃R-Gα_{o1}

The cDNAs for the tagged fusion proteins were also generated by sequential overlap-extension PCR. With pGEM-3Z-SF-hH₃R-His₆ as template, a prolonged sense primer from PCR 1A F1b (5'-GAC CAT GAT TAC GCC AAG CTA TTT AGG TGA CAC TAT AGA ATA CTC AAG C-3') and an antisense primer a6His_H3R (5'-GTG ATG GTG ATG ATG GTG CTT CCA GCA GTG C-3'), in PCR 3A a fragment encoding SF, the cDNA for the hH₃R, and the hexahistidine tag was generated. In PCR 3B, a fragment encoding the hexahistidine tag, the cDNA for Gα_{i2} or Gα_{o1}, the *stop codon*, and an XbaI site was generated. Here, the sense

primer annealed with the hexahistidine tag, the *start codon* and 5 N-terminal codons of G α_{i2} , s6HGia2 (5'-CAC CAT CAT CAC CAT CAC ATG GGC TGC ACC GTG AGC-3'), or G α_{o1} , s6HGaoA (5'-CAC CAT CAT CAC CAT CAC ATG GGA TGT ACG CTG AGC-3'). The antisense primer annealed with the cDNA encoding the 5 C-terminal amino acids of G α_{i2} or G α_{o1} , the *stop codon*, and an XbaI site, aGia2Xbal (5'-GGT CGA CTC TAG AGG TCA GAA GAG GCC ACA GTC-3') and aGaoAXbal (5'-CGA CGG ATC CTC TAG AGG TCA GTA CAA GCC GCA GCC-3'). In PCR 4, the products of PCRs 3A and 3B annealed in the hexahistidine region, and the sense primer of PCR 1A and the antisense primers of PCR 3B were used. In that way, the complete cDNAs for the hH₃R-G α_{i2} and hH₃R-G α_{o1} fusion proteins, consisting of SF, the cDNA for the hH₃R, the hexahistidine tag, and the cDNAs of G α_{i2} or G α_{o1} were amplified. These fragments were digested with *Sac*I and *Xba*I and cloned into pGEM-3Z-SF-hH₄R-His₆, digested with the same restriction enzymes, to yield pGEM-3Z-SF-hH₃R-G α_{i2} -His₆ and pGEM-3Z-SF-hH₃R-G α_{o1} -His₆. After transformation of chemically competent bacteria (JM 109), amplification of the plasmids and analytical restriction digestion, the subcloned fusion constructs were fully sequenced. Finally, the constructs were cloned into the baculovirus transfer vector pVL1392-SF-hH₄R-His₆ via *Sac*I and *Xba*I restriction sites. Again, competent bacteria (Top 10) were transformed, the plasmids amplified and the accuracy of the resulting MaxiPrep-DNA checked by extensive restriction digestion analysis and sequencing.

2.3.4 Generation of recombinant baculoviruses, cell culture and membrane preparation

Baculoviruses encoding recombinant proteins were generated in Sf9 cells using the BaculoGOLD transfection kit (BD PharMingen, San Diego, CA, USA) according to the manufacturer's instructions. Sf9 cells were cultured in 250- or 500-ml disposable Erlenmeyer flasks at 28 °C under rotation at 150 rpm in SF 900 II medium (Invitrogen, Carlsbad, CA, USA) supplemented with 5 % (v/v) fetal calf serum (Biochrom, Berlin, Germany) and 0.1 mg/ml gentamicin (Cambrex Bio Science, Walkersville, MD, USA). Cells were maintained at a density of 0.5 – 6.0 x 10⁶ cells/ml. After initial transfection, high-titer virus stocks were generated by two sequential virus amplifications. In the first amplification, cells were seeded at 2.0 x 10⁶ cells/ml and infected with a 1:100 dilution of the supernatant from the initial transfection. Cells were cultured for 7 days, resulting in the death of virtually the entire cell population. The supernatant fluid of this infection was harvested and stored under light protection at 4 °C. In a second amplification, cells were seeded at 3.0 x 10⁶ cells/ml and infected with a 1:20 dilution of the supernatant fluid from the first amplification. Cells were cultured for 48 h, and the supernatant fluid was harvested. After the 48 h culture period, the majority of cells showed signs of infections (e.g. altered morphology, viral inclusion bodies),

but most of the cells were still intact. The supernatant fluid from the second amplification was stored under light protection at 4 °C and used as routine virus stock for membrane preparations. To ensure the purity and identity of the viruses, the total RNA of infected Sf9 cells was isolated (RNeasy Kit, Qiagen), the cDNA derived via reverse transcription, and fragments representative for the constructs PCR-amplified and analyzed by restriction digestion. For infection, cells were sedimented by centrifugation and suspended in fresh medium. Cells were seeded at 3.0×10^6 cells/ml and infected with a 1:100 dilution of high-titer baculovirus stocks encoding hH₃R constructs, G $\alpha_{i/o}$ -proteins and G $\beta_1\gamma_2$ -dimers. Cells were cultured for 48 h before membrane preparation. Sf9 membranes were prepared as described previously, using 1 mM EDTA, 0.2 mM phenylmethylsulfonyl fluoride, 10 µg/ml benzamidine, and 10 µg/ml leupeptine as protease inhibitors. Membranes were suspended in binding buffer (12.5 mM MgCl₂, 1 mM EDTA, and 75 mM Tris/HCl, pH 7.4) and stored at -80 °C until use.

2.3.5 SDS-PAGE and immunoblot analysis

Membrane proteins were diluted in Laemmli-buffer and separated on SDS polyacrylamide gels containing 12 % (w/v) acrylamide. The purified G protein standards were handled in dilution buffer (Tris-HCl 25 mM, pH 7.5, DTT 1mM, NaCl 100 mM, Lubrol PX 0.1% (m/v), MgCl₂ 25 mM, EDTA 1 mM). Proteins were transferred onto 0.45 µm nitrocellulose membranes (Bio-Rad, Hercules, CA, USA) and then reacted with anti-hH₃R (1:1000), M1 antibody (1:1000), anti-His₆ (1:5000), anti-G $\alpha_{i1/2}$ (1:1000), anti-G α_o (1:1000), anti-G α_{common} (1:500) and anti-G β_{common} (1:1200) Ig's. Immunoreactive bands were visualized by enhanced chemoluminescence (Pierce, Rockford, IL, USA), using anti-mouse and anti-rabbit Igs coupled to peroxidase (GE Healthcare, Little Chalfont, Buckinghamshire, UK). Electrochemoluminescence-stained blots were exposed to X-ray films (Amersham). The expression level of proteins were roughly estimated by using appropriate dilutions of a reference membrane expressing defined levels of h β_2 AR protein or purified G proteins. h β_2 AR expression levels were determined by radioligand binding with [³H]dihydroalprenolol. Immunoblots were scanned with a GS-710 calibrated imaging densitometer (Bio-Rad). The intensity of the bands was analyzed with the Quantity One 4.0.3 software (Bio-Rad).

2.3.6 [³H]JNJ-7753707 binding assay

Before experiments, membranes were sedimented by a 10-min centrifugation at 4°C and 15,000g and resuspended in binding buffer (12.5 mM MgCl₂, 1 mM EDTA, and 75 mM Tris-HCl, pH 7.4), to remove residual endogenous guanine nucleotides as much as possible. Each tube (total volume, 250 or 500 µl) contained 10 to 50 µg of protein. Non-specific binding was determined in the presence of [³H]JNJ-7753707 at various concentrations plus 10 µM

THIO and amounted to ~20 - 30% of total binding at saturating concentrations (10 nM). Incubations were conducted for 60 min at RT and shaking at 250 rpm. Saturation binding experiments were carried out using 0.3 to 10 nM [³H]JNJ-7753707. Bound [³H]JNJ-7753707 was separated from free [³H]JNJ-7753707 by filtration through 0.3% (m/v) polyethyleneimine-pretreated GF/C filters, followed by three washes with 2 ml of binding buffer (4°C). Filter-bound radioactivity was determined by liquid scintillation counting. The experimental conditions chosen ensured that not more than 10 % of the total amount of radioactivity added to binding tubes was bound to filters.

2.3.7 [³⁵S]GTP γ S binding assay

Membranes were thawed and sedimented by a 10-min centrifugation at 4°C and 15,000g to remove residual endogenous guanine nucleotides as far as possible. Membranes were resuspended in binding buffer, supplemented with 0.05% (m/v) BSA. Each tube (total volume of 250 or 500 μ l) contained 10 - 20 μ g of membrane protein. In saturation binding experiments, tubes contained 0.2 – 2 nM [³⁵S]GTP γ S plus unlabeled GTP γ S to give the desired final ligand concentrations (0.2 – 50 nM). Neither GDP nor H₃R ligands were included in assays. Non-specific binding was determined in the presence of 100 μ M unlabeled GTP γ S and amounted to less than 1% of total binding. Incubations were conducted for 90 minutes at 25°C and shaking at 250 rpm. Bound [³⁵S]GTP γ S was separated from free [³⁵S]GTP γ S by filtration through GF/C filters, followed by three washes with 2 ml of binding buffer (4°C). Filter-bound radioactivity was determined by liquid scintillation counting. The experimental conditions chosen ensured that not more than 10 % of the total amount of radioactivity added to binding tubes was bound to filters.

2.3.8 Steady-state GTPase activity assay

Membranes were thawed, sedimented and resuspended in 10 mM Tris/HCl, pH 7.4. Assay tubes contained Sf9 membranes (10 – 20 μ g of protein/tube), 5.0 mM MgCl₂, 0.1 mM EDTA, 0.1 mM ATP, 100 nM GTP, 0.1 mM adenylyl imidodiphosphate, 1.2 mM creatine phosphate, 1 μ g of creatine kinase, and 0.2% (w/v) bovine serum albumin in 50 mM Tris/HCl, pH 7.4, and H₃R ligands at various concentrations. Reaction mixtures (80 μ l) were incubated for 2 min at 25°C before the addition of 20 μ l of [γ -³²P]GTP (0.1 μ Ci/tube). All stock and work dilutions of [γ -³²P]GTP were prepared in 20 mM Tris/HCl, pH 7.4. Reactions were conducted for 20 min at 25°C. Reactions were terminated by the addition of 900 μ l of slurry consisting of 5% (w/v) activated charcoal and 50 mM NaH₂PO₄, pH 2.0. Charcoal absorbs nucleotides but not P_i. Charcoal-quenched reaction mixtures were centrifuged for 7 min at room temperature at 15,000g. Six hundred microliters of the supernatant fluid of reaction mixtures were removed, and ³²P_i was determined by liquid scintillation counting. Enzyme activities were

corrected for spontaneous degradation of [γ -³²P]GTP. Spontaneous [γ -³²P]GTP degradation was determined in tubes containing all of the above described components plus a very high concentration of unlabeled GTP (1 mM) that, by competition with [γ -³²P]GTP, prevents [γ -³²P]GTP hydrolysis by enzymatic activities present in Sf9 membranes. Spontaneous [γ -³²P]GTP degradation was <1% of the total amount of radioactivity added using 20 mM Tris/HCl, pH 7.4, as solvent for [γ -³²P]GTP. The experimental conditions chosen ensured that not more than 10% of the total amount of [γ -³²P]GTP added was converted to ³²P_i.

2.3.9 Miscellaneous

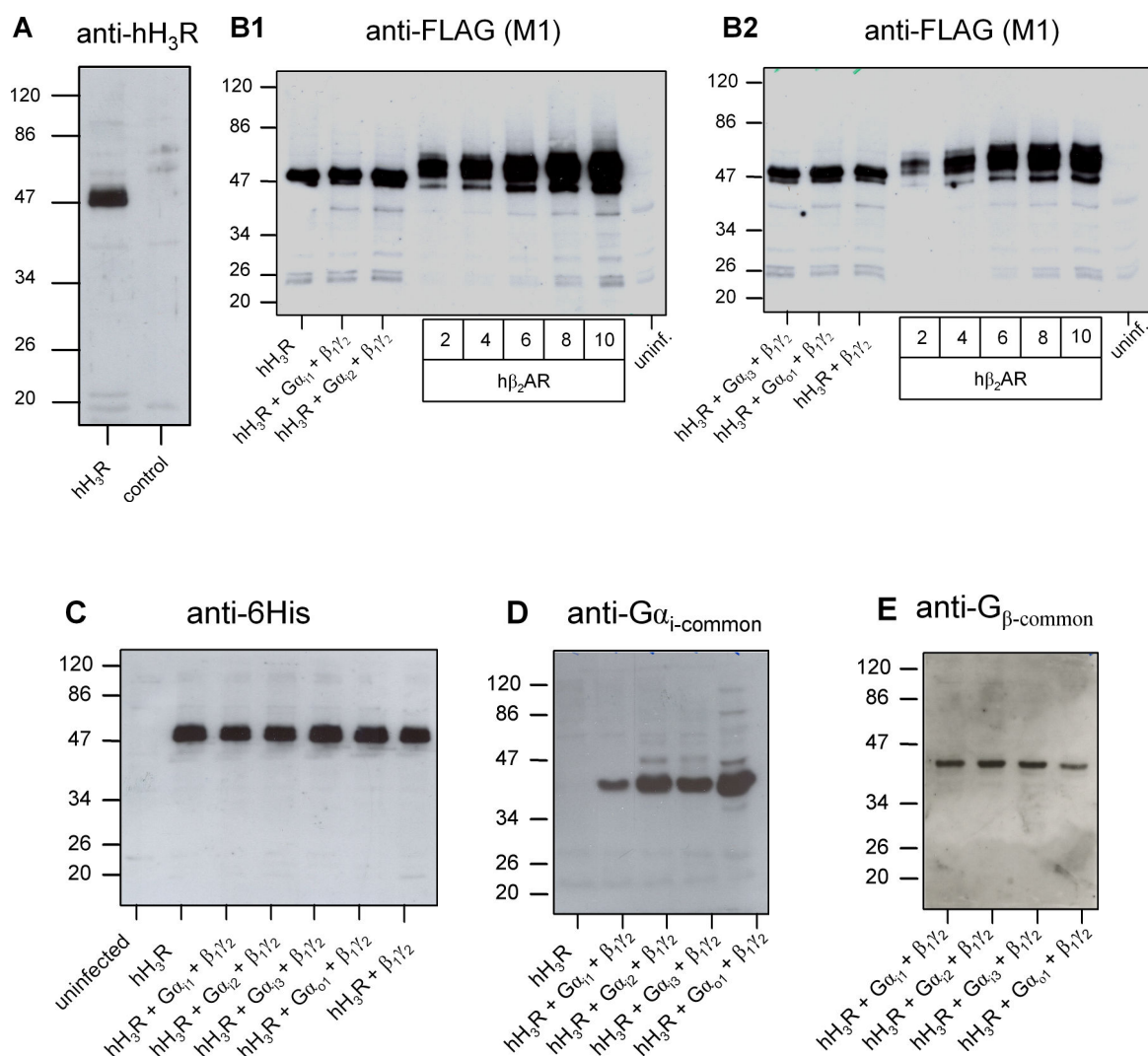
Molecular biology was planned with GCK 2.5 (Textco BioSoftware, West Lebanon, NH, USA). Ligand structures were illustrated using ChemDraw Ultra 8.0 (CambridgeSoft, Cambridge, MA, USA). Protein was determined using the DC protein assay kit (Bio-Rad, Hercules, CA, USA). [³H]Dihydroalprenolol saturation binding was performed as described previously (Seifert et al., 1998). All analyses of experimental data were performed with the Prism 5 program (GraphPad Software, San Diego, CA, USA). When expression levels of recombinant proteins were determined by western blot, the Bio-Rad GS-710 Calibrated Imaging Densitometer and the software tool Quantity One version 4.0.3 (Bio-Rad, Hercules, CA, USA) was used.

2.4 Results

2.4.1 Immunological detection of recombinant proteins expressed in Sf9 cell membranes

Membranes from the same batch of Sf9 cells infected with recombinant N- and C-terminally tagged hH₃R-baculoviruses alone or in combination with baculoviruses encoding different mammalian G proteins (G α _{i1}, G α _{i2}, G α _{i3} or G α _{o1} and/or $\beta_1\gamma_2$ dimers, respectively) were prepared and subjected to immunological analysis. The predicted molecular mass of the hH₃R is ~49 kDa. We used anti-hH₃R Ig, recognizing an 18 aa peptide within the extracellular N-terminus of the hH₃R to confirm expression (Fig. 2.2A). Indeed, hH₃R migrated as the expected band for a monomeric GPCR. The results were confirmed by the use of anti-FLAG Ig (Fig. 2.2B), recognizing the N-terminal FLAG-epitope and anti-His6 Ig (Fig. 2.2C), recognizing the C-terminal hexahistidine-tag. The bands were doublets, probably representing differently glycosylated forms of hH₃R. hH₃R possesses one putative N-glycosylation site (Asn11), located in the N-terminus. The receptor expression levels were similar in all membrane batches and estimated to be ~1-2 pmol/mg, using anti-FLAG Ig and h β_2 AR as standard (Fig. 2.2B). The expression level of the h β_2 AR was 7.5 pmol/mg, as

In order to visualize the co-expressed $G\alpha$ -subunits, we used an antibody recognizing all $G\alpha_{i/o}$ -proteins (Fig. 2.2D). $G\alpha_{i/o}$ -subunits appeared at the expected molecular mass (~40 – 41 kDa) as very intense bands, although the expression level of $G\alpha_{i1}$ was lower compared to the other ones. This is an intrinsic property of mammalian $G\alpha_{i1}$ heterologously expressed in Sf9 cells, as already shown in a previous study (Kleemann et al., 2008). Unfortunately, this problem could not be overcome by an optimization of the expression process. However, it was also shown that a low expression level of $G\alpha_{i1}$ does not influence its ability to effectively interact with GPCRs (Kleemann et al., 2008). Probably, $G\alpha_{i1}$ accumulates in GPCR-expressing membrane domains. $G\beta_1$ -subunits were expressed at similar levels in all membranes studied (Fig. 2.2E).



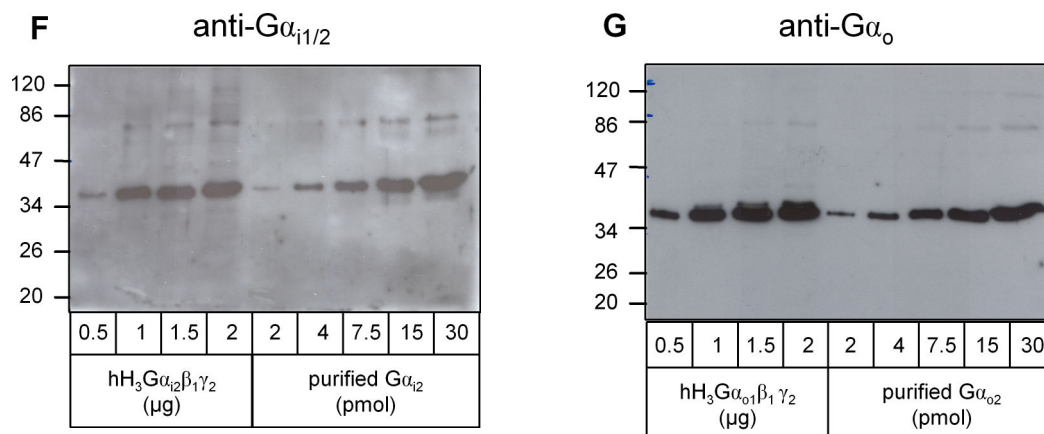


Fig. 2.2. Immunological detection of recombinant proteins expressed in Sf9 cells. Each lane of the gels was loaded with 10 μg of membrane protein, unless otherwise indicated below the film. Numbers on the left designate masses of marker proteins in kDa. In **A**, a membrane expressing the hH₃R alone was loaded onto the gels. In **B1** and **B2**, 2, 4, 6, 8 and 10 μg of protein of Sf9 membranes expressing h β_2 AR at 7.5 pmol/mg (as determined by [³H]dihydroalprenolol saturation binding) were used as standard to assess the expression levels of the hH₃R in different membrane preparations with anti-FLAG Ig. In **C**, the same membranes were reacted with anti-His6 Ig. In **D**, the membranes were reacted with anti-G $\alpha_{i\text{-common}}$ Ig. In **E**, the membranes were reacted with anti-G $\beta\text{-common}$ Ig. In **F**, 0.5, 1.0, 1.5 and 2.0 μg of a membrane expressing the hH₃R + G α_{i2} + $\beta_1\gamma_2$ was analyzed in order to quantify the G α -subunits, using 2, 4, 7.5, 15 and 30 pmol of purified G α_{i2} as standard. In **G**, 0.5, 1.0, 1.5 and 2.0 μg of a corresponding membrane of the same batch expressing hH₃R + G α_{o1} + $\beta_1\gamma_2$ was analyzed to quantify the G α -subunits, using 2, 4, 7.5, 15 and 30 pmol of purified G α_{o2} an almost identical splice variant of G α_{o1} as standard.

The GPCR/G protein ratio can alter the pharmacological properties of ligands (Kenakin, 1997). Therefore, we quantified G α_{i2} and G α_{o1} using purified protein as reference. These semi-quantitatively determined expression levels for the G α -subunits were in the range of 50-100 pmol/mg, resulting in receptor-to-G protein ratios of ~1:50 – 1:100 (Figs. 2.2F and 2.2G). This is in good agreement with ratios determined for other G $_{i/o}$ -coupled receptors in Sf9 cell membranes, for example the hH₄R (Schneider et al., 2009), human cannabinoid receptors CB₁ and CB₂ (Nickl et al., 2008) and the human formyl peptide receptor (Wenzel-Seifert et al., 1998).

2.4.2 [³H]JNJ-7753707 and [³⁵S]GTP γ S binding. Quantitative analysis of receptor-to-G protein stoichiometry

Due to the fact that the determination of expression levels by immunoblotting does not discriminate between functional and non-functional proteins, we also quantified the hH₃R and G α proteins by a combination of antagonist [³H]JNJ-7753707- and [³⁵S]GTP γ S-saturation binding and calculated the functional GPCR/G α protein ratios (Table 2.1). The membranes

were from the same batch as those studied by immunoblot to ensure maximal comparability and data accuracy.

Table 2.1: Quantification of hH₃R-to-G protein ratios via [³H]JNJ-7753707- and [³⁵S]GTP_γS-saturation binding.

$B_{\max} \pm \text{S. E. M. (pmol} \times \text{mg}^{-1})$				
membrane	hH ₃ R + $\beta_1\gamma_2$			
	+ G α_{i1}	+ G α_{i2}	+ G α_{i3}	+ G α_{o1}
[³ H]JNJ-7753707	0.6 ± 0.04	1.02 ± 0.07	1.2 ± 0.06	0.7 ± 0.03
[³⁵ S]GTP _γ S	1.40 ± 0.57	5.78 ± 0.67	4.02 ± 0.80	7.83 ± 0.77
R : G ratio	~1 : 2	~1 : 6	~1 : 3	~1 : 11

[³H]JNJ-7753707 saturation bindings were performed as described under *Materials and Methods*. [³⁵S]GTP_γS saturation bindings were performed, using Sf9 cell membranes from the same batch of preparation. Reaction mixtures contained membranes (10 - 20 μg of protein), 0.2 - 2 nM of [³⁵S]GTP_γS, and unlabeled GTP_γS to give the desired final ligand concentrations for saturation (0.2 – 50 nM). GDP or additional H₃R ligands were not present in the reaction mixtures. Data were analyzed by nonlinear regression and were best fitted to hyperbolic one-site saturation isotherms. The maximal number of GTP_γS binding sites in membranes expressing hH₃R plus G α_{i2} plus $\beta_1\gamma_2$ was corrected by the binding determined in hH₃R plus $\beta_1\gamma_2$. By this way, the number of functionally intact and heterologously expressed G protein α -subunits was quantified. Data shown are the means ± S. E. M. of 3 independent experiments performed in triplicate. Receptor-to-G protein ratios were calculated, using the B_{\max} values determined for the different membrane preparations.

In [³⁵S]GTP γ S-saturation binding experiments neither GDP nor H₃R ligands were present. The maximum number of G $\alpha_{i/o}$ -related GTP γ S binding sites in membranes expressing hH₃R plus G α -subunits plus $\beta_1\gamma_2$ was corrected by the binding determined in parallel in membranes expressing hH₃R plus $\beta_1\gamma_2$ alone. To ensure the same viral load in the reference membrane, Sf9 cells were infected with baculoviruses encoding hH₃R, $\beta_1\gamma_2$ and virus encoding no recombinant protein at all. In this manner, only the number of functionally intact and heterologously expressed mammalian G $\alpha_{i/o}$ -subunits was quantified.

The experiments revealed that the number of [³H]JNJ-7753707 binding sites was very similar to the hH₃R protein expression levels determined via immunoblot. Thus, most hH₃R molecules were correctly folded in Sf9 cell membranes. However, the number of specific [³⁵S]GTP γ S binding sites for mammalian G α -proteins was much smaller when compared with the G α -protein expression levels determined via immunoblot. Nevertheless, there were still more functionally intact mammalian G proteins than receptors in the membranes and the functional receptor-to-G protein ratios ranged between 1 : 2 and 1 : 11. Similar ratios were also found by other investigators, using the same methodology (Gazi et al., 2003). These data also fit to the linear and non-catalytic signal transfer observed for several GPCR/G-protein pairs in Sf9 cell membranes (Wenzel-Seifert et al., 1998, 1999; Wenzel-Seifert and Seifert, 2000).

2.4.3 Steady-state GTPase assay. hH₃R coupling to different G α -subunits

To investigate the G protein coupling profile of the hH₃R, we measured the receptor-dependent [γ -³²P]GTP hydrolysis of different G α -subunits. The experiments were performed under steady-state conditions. Thus, multiple G protein activation/deactivation cycles were assessed, eliminating the inherent bias of kinetic [³⁵S]GTP γ S binding studies. GTP hydrolysis was determined in parallel under basal conditions, maximal stimulation with the physiological (and full) agonist histamine (10 μ M) and a saturating concentration of the inverse agonist thioperamide (10 μ M) in Sf9 cell membranes expressing the hH₃R alone or co-expressing the hH₃R and different G proteins.

Table 2.2: GTPase activities in Sf9 membranes expressing hH₃R and different G $\alpha_{i/o}$ -proteins.

GTPase activity \pm S. E. M.	hH ₃ R + $\beta_1\gamma_2$				
	-	+ G α_{i1}	+ G α_{i2}	+ G α_{i3}	+ G α_{o1}
basal (pmol \times mg ⁻¹ \times min ⁻¹)	1.21 \pm 0.04	1.98 \pm 0.05	2.92 \pm 0.13	2.08 \pm 0.16	4.43 \pm 0.40
+ ago. (pmol \times mg ⁻¹ \times min ⁻¹)	1.36 \pm 0.03	2.56 \pm 0.03	4.24 \pm 0.22	3.10 \pm 0.30	5.65 \pm 0.47
Δ ago. (pmol \times mg ⁻¹ \times min ⁻¹)	0.15 \pm 0.03	0.57 \pm 0.07	1.31 \pm 0.12	1.02 \pm 0.20	1.21 \pm 0.09
Agonist stimulation (% of basal)	12.63 \pm 3.10	29.01 \pm 3.98	44.82 \pm 3.51	49.28 \pm 9.01	27.50 \pm 1.40
+ inv. ago. (pmol \times mg ⁻¹ \times min ⁻¹)	1.07 \pm 0.02	1.45 \pm 0.17	1.64 \pm 0.15	1.40 \pm 0.22	3.34 \pm 0.38
Δ inv. ago. (pmol \times mg ⁻¹ \times min ⁻¹)	0.14 \pm 0.05	0.53 \pm 0.13	1.29 \pm 0.17	0.68 \pm 0.10	1.09 \pm 0.10
Inverse agonist inhibition (% of basal)	11.70 \pm 4.25	27.20 \pm 6.85	44.13 \pm 3.57	33.45 \pm 5.83	24.88 \pm 2.59

Steady-state GTPase experiments were performed as described in *Materials and Methods*. Reaction mixtures contained 0.1 μ Ci [γ -³²P]GTP and 100 nM unlabeled GTP in the presence of solvent (basal), 10 μ M HA (+ ago.) or 10 μ M THIO (+ inv. ago.). Data shown are the means \pm S. E. M. of three to four independent experiments for each membrane preparation performed in duplicates. The absolute agonist-stimulation (Δ ago.) and inverse agonist-inhibition (Δ inv. ago.) of GTP hydrolysis, as well as the relative agonist-stimulation and inverse agonist-inhibition of GTP hydrolysis (% of basal), were calculated.

In membranes expressing the hH₃R alone, basal GTPase activity was low, and the stimulatory and inhibitory effects of histamine and thioperamide, respectively, were small (Table 2.2). This reflects only very weak coupling of the hH₃R to insect cell G proteins. The structurally related hH₄R also couples only weakly to insect cell G proteins (Schneider et al., 2009). hH₃R coupled efficiently to all co-expressed mammalian G $\alpha_{i/o}$ -subunits (G α_{i1} , G α_{i2} , G α_{i3} or G α_{o1} , and $\beta_1\gamma_2$ dimers, respectively) as was evident by the higher basal GTPase activity and the larger absolute stimulatory and inhibitory effects of histamine and thioperamide, respectively. The relative stimulatory effects of histamine and the relative inhibitory effects of thioperamide based on total ligand-regulated GTPase activity were similar for each of the five systems studied, indicating that the constitutive activity of hH₃R was comparable and not substantially influenced by the type of G protein (Seifert and Wenzel-Seifert, 2002). In contrast to hH₃R, the short and long splice variants of G α_s had a large impact on the constitutive activity of the h β_2 AR (Seifert et al., 1998; Seifert, 2001). The constitutive activity of hH₃R coupled to cognate G $_i$ /G $_o$ -proteins was rather high and comparable to the constitutive activity of hH₄R (Schneider et al., 2009) and the human formyl peptide receptor (Wenzel-Seifert et al., 1998, 1999). However, some G $_i$ /G $_o$ -coupled GPCRs expressed in Sf9 cells exhibit only low or no constitutive activity, indicating that the expression system per se does not give rise to high constitutive activity (Seifert and Wenzel-Seifert, 2002; Kleemann et al., 2008).

2.4.4 Ligand potencies and efficacies in the steady-state GTPase assay at hH₃R co-expressed with different G α -subunits

Next, we examined a variety of imidazole-based ligands, including the functionally selective proxyfan, in Sf9 cell membranes expressing the hH₃R and different G $\alpha_{i/o}$ -proteins in the steady-state GTPase assay (Fig. 2.1, Table 2.3).

Table 2.3: Ligand potencies and efficacies in the GTPase assay.

	hH ₃ R + G α_{i1} + $\beta_1\gamma_2$		hH ₃ R + G α_{i2} + $\beta_1\gamma_2$		hH ₃ R + G α_{i3} + $\beta_1\gamma_2$		hH ₃ R + G α_{o1} + $\beta_1\gamma_2$	
	pEC ₅₀ ± S. E. M.	E _{max} ± S. E. M.	pEC ₅₀ ± S. E. M.	E _{max} ± S. E. M.	pEC ₅₀ ± S. E. M.	E _{max} ± S. E. M.	pEC ₅₀ ± S. E. M.	E _{max} ± S. E. M.
HA	8.02 ± 0.07	1.00	7.90 ± 0.05	1.00	7.88 ± 0.09	1.00	7.85 ± 0.07	1.00
NAMH	8.95 ± 0.12	1.04 ± 0.07	8.86 ± 0.07	1.00 ± 0.04	8.83 ± 0.11	1.00 ± 0.06	8.84 ± 0.08	0.94 ± 0.04
RAMH	8.78 ± 0.21	1.08 ± 0.12	8.81 ± 0.16	1.16 ± 0.10	8.82 ± 0.12	1.07 ± 0.07	8.71 ± 0.19	0.89 ± 0.09
IME	9.61 ± 0.19	0.94 ± 0.09	9.68 ± 0.13	0.92 ± 0.06	9.63 ± 0.16	0.92 ± 0.07	9.38 ± 0.15	0.91 ± 0.06
PRO	8.34 ± 0.15	0.88 ± 0.06	8.19 ± 0.11	0.88 ± 0.05	8.26 ± 0.15	0.79 ± 0.06	8.14 ± 0.14	0.69 ± 0.05
IMP	8.68 ± 0.21	0.50 ± 0.05	8.25 ± 0.20	0.33 ± 0.03	8.97 ± 0.49	0.28 ± 0.08	8.87 ± 0.28	0.41 ± 0.06
CIP	7.21 ± 0.22	-0.71 ± 0.08*	7.03 ± 0.18	-1.08 ± 0.11	7.04 ± 0.19	-0.74 ± 0.08*	7.11 ± 0.09	-0.84 ± 0.04
CLOB	9.08 ± 0.22	-1.00 ± 0.11*	9.14 ± 0.12	-1.37 ± 0.08	9.18 ± 0.23	-0.83 ± 0.09**	9.05 ± 0.08	-1.14 ± 0.05
THIO	6.97 ± 0.13	-0.93 ± 0.06	6.93 ± 0.14	-1.02 ± 0.07	6.77 ± 0.18	-0.61 ± 0.05**	6.64 ± 0.12	-0.85 ± 0.05

Steady-state GTPase activity in Sf9 membranes expressing hH₃R, different G $\alpha_{i/o}$ subunits and $\beta_1\gamma_2$ was determined as described under *Materials and Methods*. Reaction mixtures contained ligands at concentrations from 0.1 nM to 10 μ M as appropriate to generate saturated concentration/response curves. Data were analyzed by nonlinear regression and were best fit to sigmoid concentration/response curves. Typical basal GTPase activities ranged between 2.0 and 5.0 pmol \times mg⁻¹ \times min⁻¹, and the maximal stimulatory effect of histamine (10 μ M) amounted to ~30 to ~50% above basal. The efficacy (E_{max}) of histamine was determined by nonlinear regression and was set to 1.00. The E_{max} values of other agonists and inverse agonists were referred to this value. Data shown are the means ± S. E. M. of three to four experiments performed in duplicates each. Statistical analysis was performed using one-way ANOVA, followed by Dunnett's multiple comparison test using the values determined at hH₃R, G α_{i2} and $\beta_1\gamma_2$ as a reference. Significant differences to the membrane expressing G α_{i2} are shown following comparison with other G $\alpha_{i/o}$ -subunits. (no symbol: not significant; *, $p < 0.05$; **, $p < 0.01$; ***, $p < 0.001$).

The endogenous agonist histamine (**1**) and the standard H₃R ligands *N*^α-methylhistamine (**2**) and (*R*)- α -methylhistamine (**3**) were full agonists and equally potent in all membranes. The highly potent standard H₃R agonist imetit (**4**) was almost a full partial agonist in this assay. Most interestingly, the protean agonist proxyfan (**5**) was a strong partial agonist in all systems, independent of the G protein subtype co-expressed (Fig. 2.3).

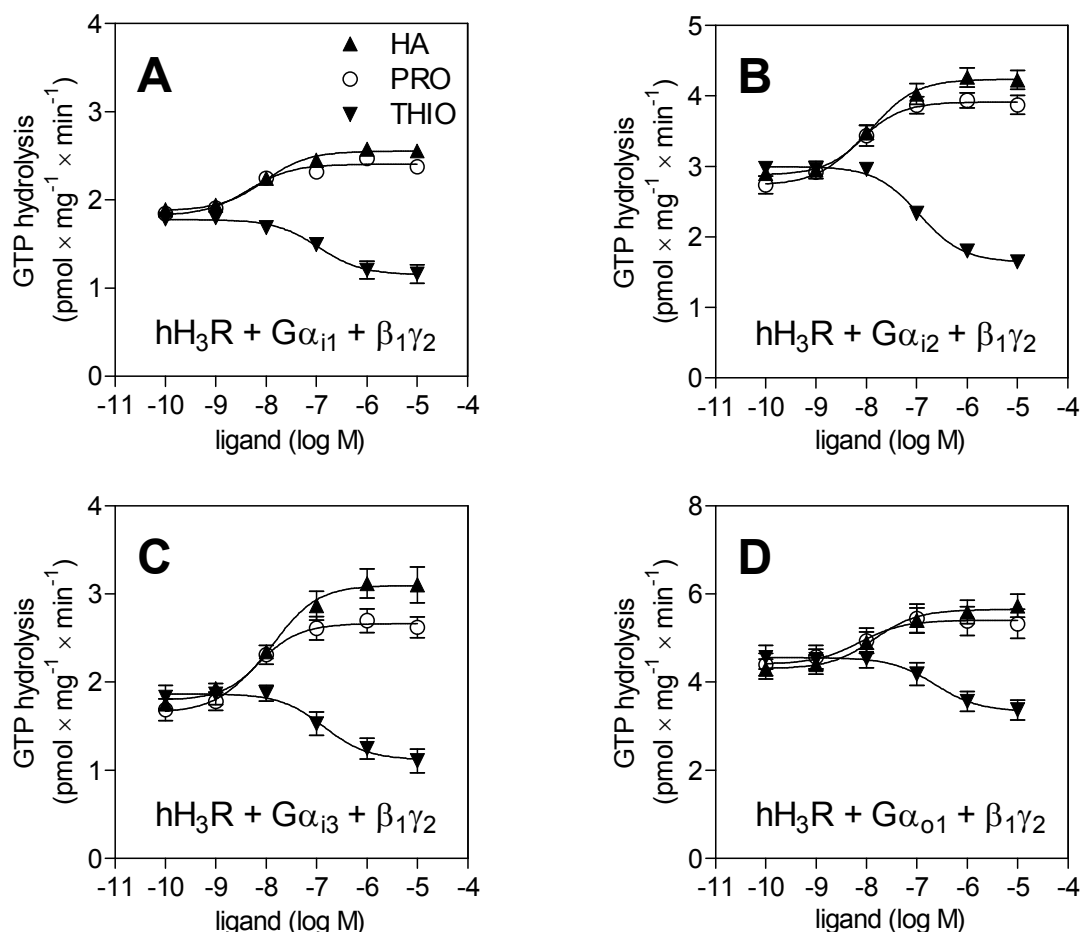


Fig. 2.3. Comparison of the effects of histamine, proxyfan and thioperamide in membranes expressing the hH₃R, different Gα_{i/o} subunits and β₁γ₂ dimers. Steady-state GTPase activity in Sf9 membranes was determined as described under *Materials and Methods*. Reaction mixtures contained histamine (HA), proxyfan (PRO) or thioperamide (THIO) at the concentrations indicated on the abscissa to achieve saturation. Data were analyzed by nonlinear regression and were best fit to sigmoidal concentration/response curves. Data points shown are the means ± S. E. M. of 3 - 4 independent experiments performed in duplicate. A summary of all results is shown in Table 2.3.

Impentamine (**6**) was a moderate partial agonist in all experimental settings. The inverse agonists ciproxyfan (**7**), clobenpropit (**8**) and thioperamide (**9**) each were also equally potent in the various systems, although they significantly differed in efficacy with the various G $\alpha_{i/o}$ -proteins. However, the rank orders of potency and efficacy of compounds **7** - **9** did not change under the various conditions. Thus, the pharmacological profile of the hH₃R is very similar under the various experimental conditions. Additionally, there is a strong linear correlation between potencies and efficacies of H₃R ligands at membranes expressing different G $\alpha_{i/o}$ -subunits (Fig. 2.4). An increase in constitutive activity of hH₃R coupled to one G protein relative to another G-protein would have been reflected in increased agonist potency and efficacy (Seifert and Wenzel-Seifert, 2002), but such an observation was not made. Moreover, differences in constitutive activity of hH₃R under the various conditions would have resulted in systematic changes of inverse agonist potency, i.e. an increase in constitutive activity would have resulted in decreased inverse agonist potency (Seifert and Wenzel-Seifert, 2002). Again, no such data were obtained. Collectively, these results corroborate the findings regarding the relative stimulatory and inhibitory effects of histamine and thioperamide, respectively (Table 2.2) based on total ligand-regulated GTPase activity and are indicative for similar constitutive activity of hH₃R under all experimental conditions (Seifert and Wenzel-Seifert, 2002).

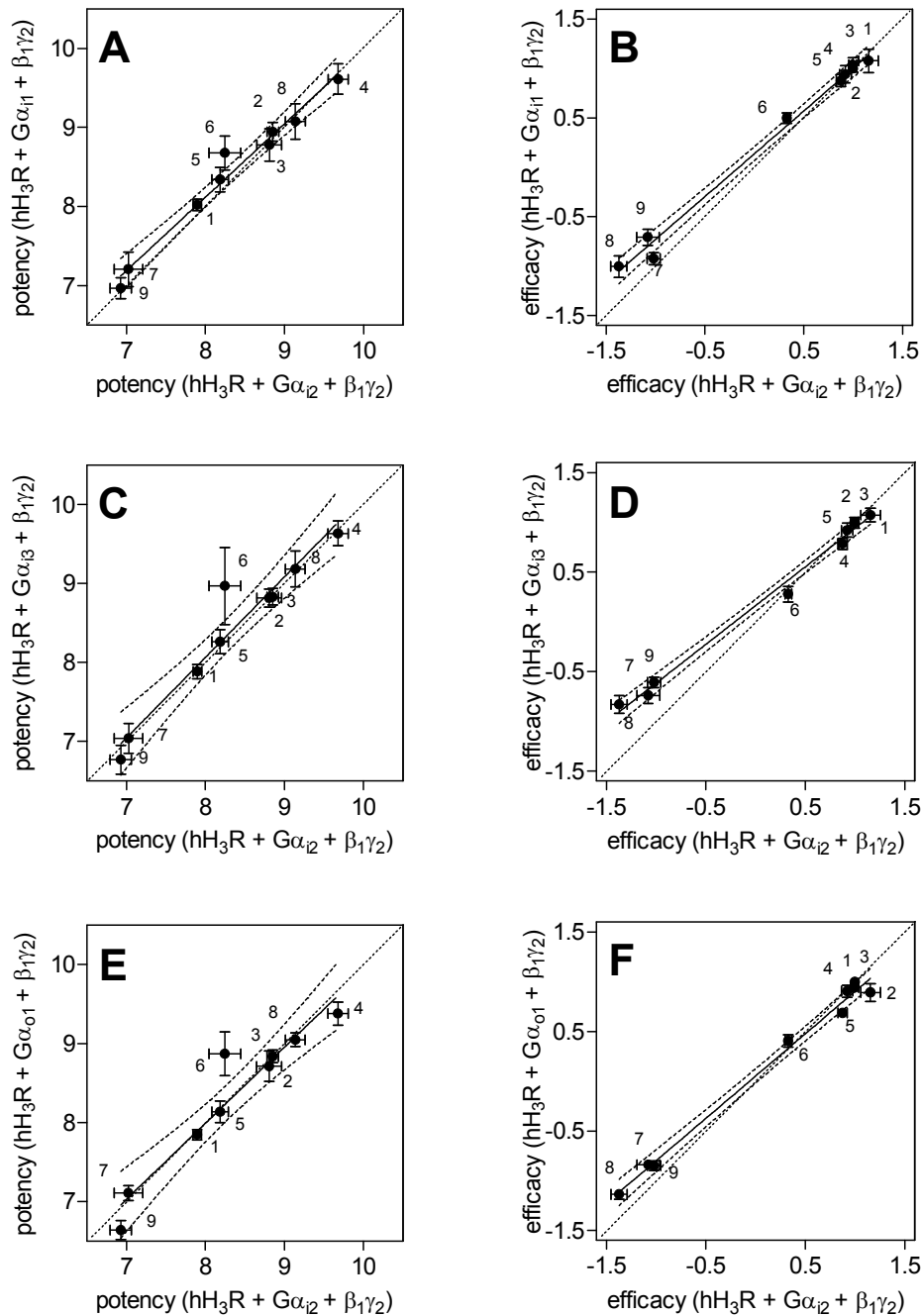


Fig. 2.4. Correlation of potency and efficacy of ligands at the hH₃R in the presence of different co-expressed $G\alpha_{i/o}$ -proteins. Data shown in Table 2.3 were analyzed by linear regression. In **A**, **C** and **E**, the potencies of ligands at membranes co-expressing the hH₃R, $G\alpha_{i1}$, $G\alpha_{i3}$ or $G\alpha_{o1}$, and $\beta_1\gamma_2$ dimers, respectively, were correlated with values determined at the reference membrane expressing $G\alpha_{i2}$. **A**, $r^2 = 0.97$; $slope = 0.93 \pm 0.06$. **C**, $r^2 = 0.93$; $slope = 1.02 \pm 0.10$. **E**, $r^2 = 0.92$; $slope = 0.96 \pm 0.11$. In **B**, **D** and **F**, the efficacies of ligands at membranes co-expressing the hH₃R, $G\alpha_{i1}$, $G\alpha_{i3}$ or $G\alpha_{o1}$, and $\beta_1\gamma_2$ dimers, respectively, were correlated with values determined at the reference membrane expressing $G\alpha_{i2}$. **B**, $r^2 = 0.99$; $slope = 0.87 \pm 0.03$. **D**, $r^2 = 0.99$; $slope = 0.78 \pm 0.03$. **F**, $r^2 = 0.99$; $slope = 0.85 \pm 0.03$. The dotted lines indicate the 95% confidence intervals of the regression lines. The diagonal dashed line has a slope of 1 and represents a theoretical curve for identical values.

2.4.5 Studies with hH₃R-G α_{i2} and hH₃R-G α_{o1} fusion proteins

The use of co-expression systems is often hampered by the fact that it is difficult, if not impossible, to control the expression levels of different signalling partners exactly (Fig. 2.2, Table 2.1) (Gille and Seifert, 2003; Kleemann et al., 2008). Table 2.1 shows that also for hH₃R, identical GPCR/G α ratios could not be achieved. The efficiency of interactions between GPCRs and heterotrimeric G proteins can be influenced by the absolute and relative densities of these proteins in the plasma membrane (Kenakin, 1997; Gille and Seifert, 2003). Fortunately, the analysis of these interactions is greatly facilitated by the use of GPCR-G α fusion proteins (Seifert et al., 1999b). Fusion proteins ensure a defined 1:1 stoichiometry of GPCR to G α and ensure physical proximity of the signalling partners. Nonetheless, fusion proteins are not physiologically occurring and therefore, the academically best procedure is to compare co-expression systems directly with fusion proteins (Wenzel-Seifert et al., 1998, 1999; Wenzel-Seifert and Seifert, 2000).

Pertussis toxin-sensitive G proteins consist of different G $\alpha_{i/o}$ -family members and $\beta\gamma$ -complexes (Birnbaumer, 2007). The three G α_i -subunits are all very similar in structure, whereas the two G α_o -splice variants are less conserved. The largest structural differences in this G protein family exist between G α_{i2} and G α_{o1} (Birnbaumer, 2007). Thus, we constructed hH₃R-G α_{i2} and hH₃R-G α_{o1} fusion proteins as representative pair to study hH₃R/G protein coupling in more detail. We hypothesized that, if there were any hH₃R/G protein coupling differences, then potencies and efficacies of ligands should diverge most prominently at this fusion protein pair. The assessment of GTPase activity at different GPCR-G α_x fusion proteins is the most accurate measure of the pharmacological profile of a given receptor because GTPase activities are determined under steady-state conditions, rendering potency and efficacy values of agonists and inverse agonists expression level-independent (Seifert et al., 1999a,b; Wenzel-Seifert et al., 1999; Wenzel-Seifert and Seifert, 2000). The pharmacological profiles of histamine, imetit, proxyfan, clobenpropit and thioperamide in the GTPase assay were very similar at the hH₃R-G α_{i2} and hH₃R-G α_{o1} fusion proteins both in terms of potency and efficacy (Table 2.4).

Table 2.4: Potencies and efficacies of selected ligands in the GTPase assay at fusion proteins.

	hH ₃ R-Gα _{i2} + β ₁ γ ₂		hH ₃ R-Gα _{o1} + β ₁ γ ₂	
	pEC ₅₀ ± S. E. M.	E _{max} ± S. E. M.	pEC ₅₀ ± S. E. M.	E _{max} ± S. E. M.
HA	7.40 ± 0.10	1.00	7.46 ± 0.11	1.00
IME	9.55 ± 0.19	0.96 ± 0.08	9.62 ± 0.09	0.95 ± 0.04
PRO	7.65 ± 0.23	0.81 ± 0.08	7.76 ± 0.13	0.74 ± 0.05
CLOB	8.72 ± 0.25	-0.60 ± 0.07	8.45 ± 0.25	-0.86 ± 0.09
THIO	7.00 ± 0.18	-0.76 ± 0.07	7.05 ± 0.15	-0.74 ± 0.05

Steady-state GTPase activity in Sf9 membranes expressing hH₃R-Gα_{i2} or hH₃R-Gα_{o1} plus β₁γ₂ was determined as described under *Materials and Methods*. Reaction mixtures contained ligands at concentrations from 0.1 nM to 10 μM as appropriate to generate saturated concentration/response curves. Data were analyzed by nonlinear regression and were best fit to sigmoid concentration/response curves. Typical basal GTPase activities ranged between 1.0 and 1.5 pmol × mg⁻¹ × min⁻¹, and the maximal stimulatory effect of HA (10 μM) amounted to ~50 to ~80% above basal. The efficacy (*E*_{max}) of HA was determined by nonlinear regression and was set to 1.00. The *E*_{max} values of other agonists and inverse agonists were referred to this value. Data shown are the means ± S. E. M. of three to four experiments performed in duplicates each. Statistical analysis was performed using the *t*-test (*p* < 0.05). Significant differences were not found for the data analyzed.

Moreover, there was no evidence for differences in constitutive activity of the two fusion proteins. These results fit very well to the data obtained with the corresponding co-expression systems (Table 2.3) and render it unlikely that the non-identical GPCR/Gα stoichiometries in the co-expression studies documented in Table 2.1 had a major impact on the pharmacological profile of hH₃R. Actually, the stoichiometry issue would have been of greater concern if the pharmacological profiles of the hH₃R had been different with the various co-expressed Gα_{i/o} proteins. This was, however, not the case (Table 2.3).

2.5 Discussion

The imidazole-containing H₃R ligand proxyfan exhibits pleiotropic effects, ranging from inverse agonism to agonism, depending on the system studied (Gbahou et al., 2003; Krueger et al., 2005). An explanation for these findings could be that the proxyfan-bound H₃R exhibits different affinities and efficacies for coupling to various G-proteins (Kenakin, 2001,

2007; Kobilka and Deupi, 2007). Thus, the observed proxyfan effects could be due to functional selectivity. We tested this hypothesis by studying coupling of the hH₃R to four different G $\alpha_{i/o}$ -proteins under clearly defined experimental conditions, measuring one and the same parameter of GPCR/G-protein coupling, i.e. steady-state GTPase activity. However, we did not obtain evidence for functional selectivity of proxyfan. In our hands, proxyfan was a strong partial agonist at the full-length hH₃R (445 aa) in all experimental settings. For eight other hH₃R ligands, we did not obtain evidence for functional selectivity either. Moreover, we could not find differences in constitutive activity of hH₃R coupled to G_i/G_o-proteins which would have been important for detecting protean agonism (Gbahou et al., 2003). Those “negative” data were obtained in a co-expression system and a fusion protein system. Thus, the crucial question is of how the discrepancies between our present study and the studies of Gbahou et al. (2003) and Krueger et al. (2005) could be explained.

Defined ligands stabilize distinct conformations in the human dopamine D₂-receptor that result in the activation of only one specific G $\alpha_{i/o}$ -subunit when expressed in Sf9 cells (Gazi et al., 2003). Additionally, endogenous catecholamines and synthetic ligands stabilize distinct ligand-specific active states in human β -adrenergic receptors (Seifert et al., 1999a; Wenzel-Seifert and Seifert, 2000; Weigl and Seifert, 2008). Moreover, ligand-specific conformations were readily unmasked for histamine H₁- and H₂-receptors expressed in Sf9 cells (Preuss et al., 2007; Wittmann et al., 2009). These data show that the baculovirus/Sf9 cell system is sufficiently sensitive at detecting ligand-specific GPCR conformations so that we should have been able to detect functional selectivity of proxyfan. However, it should also be emphasized that for some GPCRs expressed in Sf9 cells, e.g. the human formyl peptide receptor, no evidence for ligand-specific receptor conformations could be obtained despite intense efforts (Wenzel-Seifert et al., 1999). These data indicate that not all GPCRs exhibit ligand-specific conformations. Noteworthy, like hH₃R, the formyl peptide receptor couples to G_i/G_o-proteins (Wenzel-Seifert et al., 1999).

In the study of Gbahou et al. (2003), proxyfan was a partial agonist in [³⁵S]GTP γ S binding, cAMP accumulation and mitogen-activated protein kinase assays, but an inverse agonist in phospholipase A₂ assays, all parameters representing distal consequences of G $\alpha_{i/o}$ -protein activation. It is possible that different combinations of G $\alpha_{i/o}$ -proteins are involved in the responses, that the G-protein/effector stoichiometry is different in the pathways (Ostrom and Insel, 2004) and that there is cross-talk between the mitogen-activated protein kinase and phospholipase A₂. In contrast, we studied clearly defined G-protein heterotrimers (although at somewhat different GPCR/G-protein ratios) and a proximal parameter of GPCR/G-protein coupling, avoiding complications of G-protein/effector stoichiometry and cross-talk of signalling pathways.

In the study of Krueger et al. (2005), proxyfan exhibited little activity in neurotransmitter release assays, full agonism in cAMP accumulation assays and partial agonism in [³⁵S]GTP γ S binding assays. Additionally, in transfected HEK cells proxyfan displayed differential activity in cAMP accumulation- and calcium mobilization assays dependent on the type of G protein co-expressed (G α_{16} or G α_{qi5}). The authors concluded that the type of G protein determines the pharmacological properties of proxyfan. While it is known that G α_{16} has an impact on the pharmacological properties of GPCRs (Wenzel-Seifert and Seifert, 2000), G α_{16} is certainly not a cognate G-protein of hH₃R, but rather a G-protein expressed in hematopoietic cells and not in neuronal cells (Birnbaumer, 2007). Moreover, G α_{qi5} is not a physiological G protein, but a chimeric G protein used to direct G_i-coupled GPCRs towards G_q- and phospholipase C coupling (Coward et al., 1999). We studied only cognate G proteins of hH₃R, i.e. G $\alpha_{i/o}$ -proteins, and did not obtain evidence for ligand-specific hH₃R conformations.

Gbahou et al. (2003) expressed H₃R in CHO cells. These cells express some of the cognate G $\alpha_{i/o}$ -proteins of H₃R, but the specific expression pattern of G $\alpha_{i/o}$ -subunits was not defined in the previous study. Moreover, it is unknown whether the proxyfan-bound H₃R interacted differentially with various G $\alpha_{i/o}$ -proteins in CHO cells. Such an interaction can be studied by photoaffinity labelling with [α -³²P]GTP azidoanilide (Woo et al., 2009). However, such data are not available. Moreover, various $\beta_x\gamma_y$ -complexes impact on GPCR/G-protein coupling (Birnbaumer, 2007). However, in the previous studies on proxyfan $\beta_x\gamma_y$ -complexes were not defined. We studied a single $\beta\gamma$ -complex that is broadly expressed, i.e. $\beta_1\gamma_2$ (Birnbaumer, 2007), but we did not examine other $\beta_x\gamma_y$ -complexes. It is possible that distinct $\beta_x\gamma_y$ -complexes account for the protean agonism of proxyfan observed in the previous studies, but those $\beta_x\gamma_y$ -complexes remain to be identified. It is also possible that differential compartmentation of G-protein heterotrimers into specific membrane domains, resulting in different GPCR/G-protein stoichiometries (Ostrom and Insel, 2004) contributed to protean agonism of proxyfan observed in previous studies. In our co-expression system, we cannot exclude different compartmentation of signalling partners either, but the GPCR-G α fusion protein approach circumvented this problem (Seifert et al., 1999b). With hH₃R-G $\alpha_{i/o}$ fusion proteins, like with the corresponding co-expression systems, there was no evidence for ligand-specific GPCR conformations.

Another issue is the fact that some of the previous assays were performed with intact cells and some assays with membranes. In experiments with intact cells, the precise ionic and nucleotide environments of G-proteins are unknown, but both ionic and nucleotide composition can largely affect GPCR/G-protein coupling, constitutive GPCR activity and pharmacological GPCR profile (Seifert et al., 1999a; Seifert, 2001; Gille et al., 2002). Moreover, in intact cells, specifically native tissues, relevant for neurotransmitter release

studies, it cannot be excluded that endogenous histamine is present, thereby changing the apparent agonistic/inverse agonistic activities of ligands. We performed experiments with extensively washed membranes, excluding the presence of contaminating histamine and conducted experiments under clearly defined ionic conditions and nucleotide composition. We are aware of the fact that our experimental conditions do not represent physiological conditions, but our conditions are defined and allow direct comparison with data from our group for other GPCRs over a period of a decade (Seifert et al., 1999a; Seifert, 2001; Gille et al., 2002; Preuss et al., 2007; Schneider et al., 2009). Noteworthy, under our experimental conditions, different degrees of constitutive activity of a GPCR can be readily detected (Seifert, 2001; Wenzel-Seifert and Seifert, 2000; Preuss et al., 2007), supporting the principal suitability of our system for the hypothesis tested.

It should be also noted that the study of Gbahou et al. (2003) was performed with rH₃R. Species-specific pharmacology of the H₃R has been mainly attributed to two aa differences in transmembrane domain 3, which are part of the ligand binding site, and this leads to changes in antagonist affinities (Yao et al., 2003). However, it is possible that the rH₃R also shows a different G protein coupling profile compared to the hH₃R. Here, we studied only the full-length hH₃R (445 aa). Future studies will have to examine rH₃R as well.

Another point is the fact that Gbahou et al. (2003) used a truncated splice variant of the full-length rH₃R (413 aa) in their experiments. This short splice variant lacks 32 amino acids in the 3rd intracellular loop of the receptor, which is an important interaction site for G proteins (Seifert et al., 1999b; Leurs et al., 2005). It is possible that the truncated rH₃R possesses an altered G protein coupling profile compared to the full-length rH₃R. The detailed coupling profiles of various H₃R splice variants are not yet known, but should be addressed in future investigations. The pattern of H₃R splice variant expression differs between species and brain regions (Bongers et al., 2007) and splice variants differentially regulate signal transduction pathways (Drutel et al., 2001). These data are indicative for differences in G protein coupling of H₃R splice variants. We studied only the full-length hH₃R (445 aa) without considering splice variants.

In conclusion, we have shown that the full-length hH₃R (445 aa) couples similarly to four defined G_i/G_o-protein heterotrimers expressed in Sf9 cells. We did not obtain evidence in favor of the hypothesis that proxyfan or eight other H₃R ligands are functionally selective in a co-expression and a fusion protein system. Moreover, we did not find differences in constitutive activity of hH₃R under various experimental conditions. These “negative” results cannot be attributed to unsuitability of our expression system for exclusion of ligand functional selectivity. However, our system is not suitable to definitely exclude protean agonism at hH₃R, since that would require a systematic and precise variation of receptor-to-G protein stoichiometries (Kenakin 2001, 2007). Additionally, we discussed several

possibilities that could account, fully or partially, for the differences between the results of our study and the previous studies of Gbahou et al. (2003) and Krueger et al. (2005). Extensive systematic studies under clearly defined experimental conditions are required to reconcile the discrepancies. Thus, presently, a specific and generally applicable mechanistic explanation for the previously observed pleiotropic effects of proxyfan cannot yet be provided.

2.6 References

- Birnbaumer L (2007) Expansion of signal transduction by G proteins. The second 15 years or so: from 3 to 16 α subunits plus $\beta\gamma$ dimers. *Biochim Biophys Acta* **1768**:772-793.
- Bonaventure P, Letavic M, Dugovic C, Wilson S, Aluisio L, Pudiak C, Lord B, Mazur C, Kamme F, Nishino S, Carruthers N and Lovenberg T (2007) Histamine H₃ receptor antagonists: from target identification to drug leads. *Biochem Pharmacol* **73**:1084-1096.
- Bongers G, Bakker RA and Leurs R (2007) Molecular aspects of the histamine H₃ receptor. *Biochem Pharmacol* **73**:1195-1204.
- Clark EA and Hill SJ (1996) Sensitivity of histamine H₃ receptor agonist-stimulated [³⁵S]GTP γ S binding to pertussis toxin. *Eur J Pharmacol* **296**:223-225.
- Coward P, Chan SD, Wada HG, Humphries GM and Conklin BR (1999) Chimeric G proteins allow a high-throughput signaling assay of G_i-coupled receptors. *Anal Biochem* **270**:242-248.
- Cowart M, Altenbach R, Black L, Faghieh R, Zhao C and Hancock AA (2004) Medicinal chemistry and biological properties of non-imidazole histamine H₃ antagonists. *Mini Rev Med Chem* **4**:979-992.
- Drutel G, Peitsaro N, Karlstedt K, Wieland K, Smit MJ, Timmerman H, Panula P and Leurs R (2001) Identification of rat H₃ receptor isoforms with different brain expression and signaling properties. *Mol Pharmacol* **59**:1-8.
- Esbenshade TA, Browman KE, Bitner RS, Strakhova M, Cowart MD and Brioni JD (2008) The histamine H₃ receptor: an attractive target for the treatment of cognitive disorders. *Br J Pharmacol* **154**:1166-1181.
- Gazi L, Nickolls SA and Strange PG (2003) Functional coupling of the human dopamine D₂ receptor with G α_{i1} , G α_{i2} , G α_{i3} and G α_o G proteins: evidence for agonist regulation of G protein selectivity. *Br J Pharmacol* **138**:775-786.
- Gbahou F, Rouleau A, Morisset S, Parmentier R, Crochet S, Lin JS, Ligneau X, Tardivel-Lacombe J, Stark H, Schunack W, Ganellin CR, Schwartz JC and Arrang JM (2003) Protean agonism at histamine H₃ receptors *in vitro* and *in vivo*. *Proc Natl Acad Sci USA* **100**:11086-11091.
- Gille A and Seifert R (2003) Co-expression of the β_2 -adrenoceptor and dopamine D₁-receptor with G_{s α} proteins in Sf9 insect cells: limitations in comparison with fusion proteins. *Biochim Biophys Acta* **1613**:101-114.
- Gille A, Liu HY, Sprang SR and Seifert R (2002) Distinct interactions of GTP, UTP, and CTP with G_s-proteins. *J Biol Chem* **277**:34434-34442.
- Haas HL, Sergeeva OA and Selbach O (2008) Histamine in the nervous system. *Physiol Rev* **88**:1183-1241.
- Hüls A, Purand K, Stark H, Reidemeister S, Ligneau X, Arrang JM, Schwartz JC and Schunack W (1996) Novel histamine H₃-receptor antagonists with benzyl ether structure or related moieties: synthesis and structure-activity relationships. *Arch Pharm (Weinheim)* **329**:379-385.

- Kenakin T (1997) Differences between natural and recombinant G protein-coupled receptor systems with varying receptor/G protein stoichiometry. *Trends Pharmacol Sci* **18**:456-464.
- Kenakin T (2001) Inverse, protean, and ligand-selective agonism: matters of receptor conformation. *FASEB J* **15**:598-611.
- Kenakin T (2007) Functional selectivity through protean and biased agonism: who steers the ship? *Mol Pharmacol* **72**:1393-1401.
- Kleemann P, Papa D, Vigil-Cruz S and Seifert R (2008) Functional reconstitution of the human chemokine receptor CXCR4 with G_i/G_o-proteins in Sf9 insect cells. *Naunyn-Schmiedeberg's Arch Pharmacol* **378**:261-274.
- Kobilka BK and Deupi X (2007) Conformational complexity of G-protein-coupled receptors. *Trends Pharmacol Sci* **28**:397-406.
- Krueger KM, Witte DG, Ireland-Denny L, Miller TR, Baranowski JL, Buckner S, Milicic I, Esbenshade TA and Hancock AA (2005) G protein-dependent pharmacology of histamine H₃ receptor ligands: evidence for heterogeneous active state receptor conformations. *J Pharmacol Exp Ther* **314**:271-281.
- Leurs R, Bakker RA, Timmerman H and de Esch IJ (2005) The histamine H₃ receptor: from gene cloning to H₃ receptor drugs. *Nat Rev Drug Discov* **4**:107-120.
- Lovenberg TW, Pyati J, Chang H, Wilson SJ and Erlander MG (2000) Cloning of rat histamine H₃ receptor reveals distinct species pharmacological profiles. *J Pharmacol Exp Ther* **293**:771-778.
- Nickl K, Gardner EE, Geiger S, Heilmann J and Seifert R (2008) Differential coupling of the human cannabinoid receptors hCB₁R and hCB₂R to the G-protein G $\alpha_{i2}\beta_1\gamma_2$. *Neurosci Lett* **447**:68-72.
- Ostrom RS and Insel PA (2004) The evolving role of lipid rafts and caveolae in G protein-coupled receptor signalling: implications for molecular pharmacology. *Br J Pharmacol* **143**:235-245.
- Preuss H, Ghorai P, Kraus A, Dove S, Buschauer A and Seifert R (2007) Constitutive activity and ligand selectivity of human, guinea pig, rat and canine histamine H₂ receptors. *J Pharmacol Exp Ther* **321**:983-995.
- Schneider EH, Schnell D, Papa D and Seifert R (2009) High constitutive activity and a G-protein-independent high-affinity state of the human histamine H₄-receptor. *Biochemistry* **48**:1424-1438.
- Seifert R (2001) Monovalent anions differentially modulate coupling of the β_2 -adrenoceptor to G_{s α} splice variants. *J Pharmacol Exp Ther* **298**:840-847.
- Seifert R and Dove S (2009) Functional selectivity of GPCR ligand stereoisomers: new pharmacological opportunities. *Mol Pharmacol* **75**:13-18.
- Seifert R, Gether U, Wenzel-Seifert K and Kobilka BK (1999a) Effects of guanine, inosine, and xanthine nucleotides on β_2 -adrenergic receptor/G_s interactions: evidence for multiple receptor conformations. *Mol Pharmacol* **56**:348-358.

- Seifert R and Wenzel-Seifert K (2002) Constitutive activity of G-protein-coupled receptors: cause of disease and common property of wild-type receptors. *Naunyn Schmiedebergs Arch Pharmacol* **366**:381-416.
- Seifert R, Wenzel-Seifert K and Kobilka BK (1999b) GPCR-G α fusion proteins: molecular analysis of receptor-G-protein coupling. *Trends Pharmacol Sci* **20**:383-389.
- Seifert R, Wenzel-Seifert K, Lee TW, Gether U, Sanders-Bush E and Kobilka BK (1998) Different effects of G $_{s\alpha}$ splice variants on β_2 -adrenoreceptor-mediated signaling. The β_2 -adrenoreceptor coupled to the long splice variant of G $_{s\alpha}$ has properties of a constitutively active receptor. *J Biol Chem* **273**:5109-5116.
- Walseth TF and Johnson RA (1979) The enzymatic preparation of [α -³²P]nucleoside triphosphates, cyclic [³²P]AMP, and cyclic [³²P]GMP. *Biochim Biophys Acta* **562**:11-31.
- Weitl N and Seifert R (2008) Distinct interactions of human β_1 - and β_2 -adrenoceptors with isoproterenol, epinephrine, norepinephrine, and dopamine. *J Pharmacol Exp Ther* **327**:760-769.
- Wenzel-Seifert K, Arthur JM, Liu HY and Seifert R (1999) Quantitative analysis of formyl peptide receptor coupling to G $_{i\alpha_1}$, G $_{i\alpha_2}$, and G $_{i\alpha_3}$. *J Biol Chem* **274**:33259-33266.
- Wenzel-Seifert K, Hurt CM and Seifert R (1998) High constitutive activity of the human formyl peptide receptor. *J Biol Chem* **273**:24181-24189.
- Wenzel-Seifert K and Seifert R (2000) Molecular analysis of β_2 -adrenoceptor coupling to G $_{s-}$, G $_{i-}$, and G $_{q-}$ proteins. *Mol Pharmacol* **58**:954-966.
- Wittmann HJ, Seifert R and Strasser A (2009) Contribution of binding enthalpy and entropy to antagonist and agonist binding at human and guinea pig histamine H₁-receptor. *Mol Pharmacol* **76**:25-37.
- Woo AY, Wang TB, Zeng X, Zhu W, Abernethy DR, Wainer IW and Xiao RP (2009) Stereochemistry of an agonist determines coupling preference of β_2 -adrenoceptor to different G proteins in cardiomyocytes. *Mol Pharmacol* **75**:158-165.
- Yao BB, Hutchins CW, Carr TL, Cassar S, Masters JN, Bennani YL, Esbenshade TA and Hancock AA (2003) Molecular modeling and pharmacological analysis of species-related histamine H₃ receptor heterogeneity. *Neuropharmacology* **44**:773-786.

Chapter 3

Comparison of the pharmacological properties of human and rat histamine H₃-receptors

This chapter is adapted from:

Schnell D, Strasser A and Seifert R (2009) Comparison of the pharmacological properties of human and rat histamine H₃-receptors. *J Pharmacol Exp Ther* (submitted).

3.1 Abstract

Ligand pharmacology at histamine H₃-receptors is species-dependent. In previous studies, two amino acids in transmembrane domain 3 (TM III) were shown to play a significant role. In this study, we characterized human and rat histamine H₃-receptors (hH₃R and rH₃R, respectively), co-expressed with mammalian G proteins in Sf9 insect cell membranes. We compared a series of imidazole-containing H₃R ligands in radioligand binding and steady-state GTPase assays. H₃Rs similarly coupled to G $\alpha_{i/o}$ -proteins. Affinities and potencies of the agonists histamine, *N*^L-methylhistamine and *R*-(α)-methylhistamine were in the same range. Imetit was only a partial agonist. The pharmacology of imetit and proxyfan was similar at both species. However, impentamine was more potent and efficacious at rH₃R. The inverse agonists ciproxyfan and thioperamide showed higher potency but lower efficacy at rH₃R. Clobenpropit was not species-selective. Strikingly, imoproxifan was almost full agonist at hH₃R, but an inverse agonist at rH₃R. Imoproxifan was docked into the binding pocket of inactive and active hH₃R- and rH₃R-models and molecular dynamic simulations were performed. Imoproxifan bound to hH₃R and rH₃R in *E*-configuration, which represents the *trans*-isomer of the oxime-moiety as determined in crystallization studies, and stabilized active hH₃R-, but inactive rH₃R-conformations. Large differences in electrostatic surfaces between TM III and TM V cause differential orientation of the oxime-moiety of imoproxifan, which then differently interacts with the rotamer toggle switch Trp^{6.48} in TM VI. Collectively, the substantial species differences at H₃Rs are explained at a molecular level by the use of novel H₃R active-state models.

3.2 Introduction

Histamine (HA) exhibits its biological effects through the activation of four different G protein-coupled receptors (GPCRs). The histamine H₁-receptor (H₁R) is associated with inflammatory and allergic reactions, e. g. it increases vascular permeability and NO production (Hill et al., 1997). The histamine H₂-receptor (H₂R) regulates gastric acid production, but also shows a positive inotropic effect on the heart (Hill et al., 1997). The histamine H₃-receptor (H₃R) is a presynaptic auto- and heteroreceptor, regulating the release of HA and various other neurotransmitters in the nervous system, and is involved in important physiological processes like the sleep-wake cycle, eating behaviour and cognition (Leurs et al., 2005). The histamine H₄-receptor (H₄R) mediates inflammatory and immunological processes, e. g. chemotaxis of eosinophils, mast cells and dendritic cells, but

it is also present on neurons mediating HA-induced itching (Leurs et al., 2009; Zampeli and Tiligada, 2009). H₁R and H₂R antagonists have been used as therapeutics for decades, H₃R and H₄R are still explored and promising new drug targets (Tiligada et al., 2009).

The H₃R was pharmacologically identified in the early 1980s, but cloned almost 20 years later in 1999 as an orphan GPCR (Leurs et al., 2005). The reason for this delay was that it only shares ~20% homology to the H₁R and H₂R. The complex gene structure of the human H₃R (hH₃R) gives rise to many possible splice variants. To date about 20 hH₃R splice variants are known (Bongers et al., 2007a), but their function still remains elusive. The H₃R displays high constitutive, i. e. ligand-independent, activity in many experimental systems (Arrang et al., 2007). The H₃R is one of the very few GPCRs for which constitutive activity has also been demonstrated *in vivo* (Morisset et al., 2000).

For the H₃R it has also been shown that species-differences exist (Ireland-Denny et al., 2001; Wulff et al., 2002). Fig. 3.1 shows the amino acid sequences of hH₃R and rH₃R. Although the H₃R sequence has a high degree of similarity among species, differences located in key regions of the receptor protein account for differences in antagonist affinity (Ligneau et al., 2000; Yao et al., 2003). Additionally, splice variants differ in composition and expression pattern between species, and there are potential differences in signal transduction processes between either tissues and/or species (Hancock et al., 2003). Nevertheless, there are still unresolved questions about species differences of the full-length and un-spliced H₃Rs (445 amino acids), especially regarding the detailed molecular mechanisms involved in ligand-receptor interactions.

In the present study, we systematically compared the pharmacological properties of hH₃R and rH₃R. Fig. 3.2 shows the structures of the compounds studied, all of them being imidazole-containing ligands. We co-expressed hH₃R and rH₃R in Sf9 cells together with mammalian G proteins in a defined stoichiometry, determined the affinity of ligands in radioligand binding studies, and their potency and efficacy in steady-state GTPase assays. The baculovirus/Sf9 cell system is very suitable for the analysis of G_i/G_o-coupled receptors and in particular constitutively active receptors, because in Sf9 cells no endogenous G_i/G_o-proteins or GPCRs with constitutive activity are present. The controlled expression of receptor and G proteins in Sf9 cell membranes represents more the physiological situation than, for example, the construction of GPCR-G α fusion proteins, because fusion proteins do not exist physiologically and the mobility of the G proteins is not restricted in the co-expression system. Moreover, the use of very proximal read-outs, like radioligand binding or steady-state GTPase assays prevent possible bias in later steps of the signal transduction cascade.

Many studies of ligand-receptor interactions come to a point where structural information on the atomic level is needed to explain experimental results. In the case of

GPCRs, this is a very challenging and time-consuming process, and at the end only snapshots of static ligand-receptor complexes are resolved (Kobilka and Schertler, 2008). However, more and more high-resolution crystal structures of inactive- and active-state GPCR-ligand complexes are becoming available and can be used to generate better homology models (Rasmussen et al., 2007; Jaakola et al., 2008; Park et al., 2008). Since active-state models for H₃Rs do not yet exist, we generated and used those models to explain the pharmacological species differences at hH₃R and rH₃R on the basis of experimental data. These new models combine the information of previous studies on H₃Rs (Schlegel et al., 2007), and were complemented with sophisticated studies on the activation process of H₁Rs (Strasser and Wittmann, 2007; Strasser et al., 2009).

3.3 Materials and Methods

3.3.1 Materials

The cDNAs of the hH₃R and rH₃R were kindly provided by Dr. T. Lovenberg (Johnson & Johnson Pharmaceutical R&D, San Diego, CA, USA). An alignment of the corresponding amino acid sequences is given in Fig. 3.1. Anti-hH₃R Ig and anti-rH₃R Ig were from Bio-Trend (Cologne, Germany). The antibody recognizing both species homologs was from GeneWay (San Diego, CA, USA). All other antibodies, purified G proteins, reagents for molecular biology, recombinant baculoviruses encoding mammalian G protein subunits, and the sources of test compounds were described before (Schnell et al., 2009). Chemical structures of H₃R ligands are depicted in Fig. 3.2. Stock solutions (10 mM) of all H₃R ligands described in this paper were prepared in distilled water and stored at -20°C. [³H]JNJ-7753707 (= [³H]RWJ-422475) (30 Ci/mmol) was kindly donated from Dr. P. Bonaventure (Johnson & Johnson Pharmaceutical R&D, San Diego, CA, USA). [³H]*N*^α-methylhistamine (74-85 Ci/mmol) and [³⁵S]GTPγS (1100 Ci/mmol) were obtained from Perkin Elmer (Boston, MA, USA). [^γ-³²P]GTP was synthesized as described (Schnell et al., 2009). Unlabeled nucleotides were from Roche (Indianapolis, IN, USA) and all other reagents were of the highest purity available and from standard suppliers.

3.3.2 Construction of FLAG epitope- and hexahistidine-tagged cDNAs for hH₃R and rH₃R

The cDNA for the tagged rH₃R protein was generated by sequential overlap-extension PCR in analogy to the procedure described recently for hH₃R (Schnell et al., 2009). In the case of rH₃R, the sense primer RAT HRH3-F- (5'- GAC GAT GAT GAC GCC ATG GAG CGC GCG CCG CC-3') consisted of 15 bp of the 3'-end of SF and the first 17 bp of the 5'-

end of the rH₃R. The antisense primer RAT HRH3-RV (5'- GA TCC TCT AGA TTA GTG ATG GTG ATG ATG GTG CTT CCA GCA CTG CTC -3') consisted of 15 bp of the C-terminus of the rH₃R, and encoded a hexahistidine tag, the *stop codon*, and a Xba I site. As template, a plasmid (pCIneo) containing the sequence of rH₃R was used.

3.3.3 Generation of recombinant baculoviruses, cell culture and membrane preparation, SDS-PAGE and immunoblot analysis

The protocols for virus amplification, protein expression and western blot analysis were described before (Schnell et al., 2009). Proteins transferred to nitrocellulose membranes were reacted with anti-hH₃R (N-term) (1:1000), anti-rH₃R (C-term) (1:1000) and anti-H₃R (i3) (1:1000) Igs.

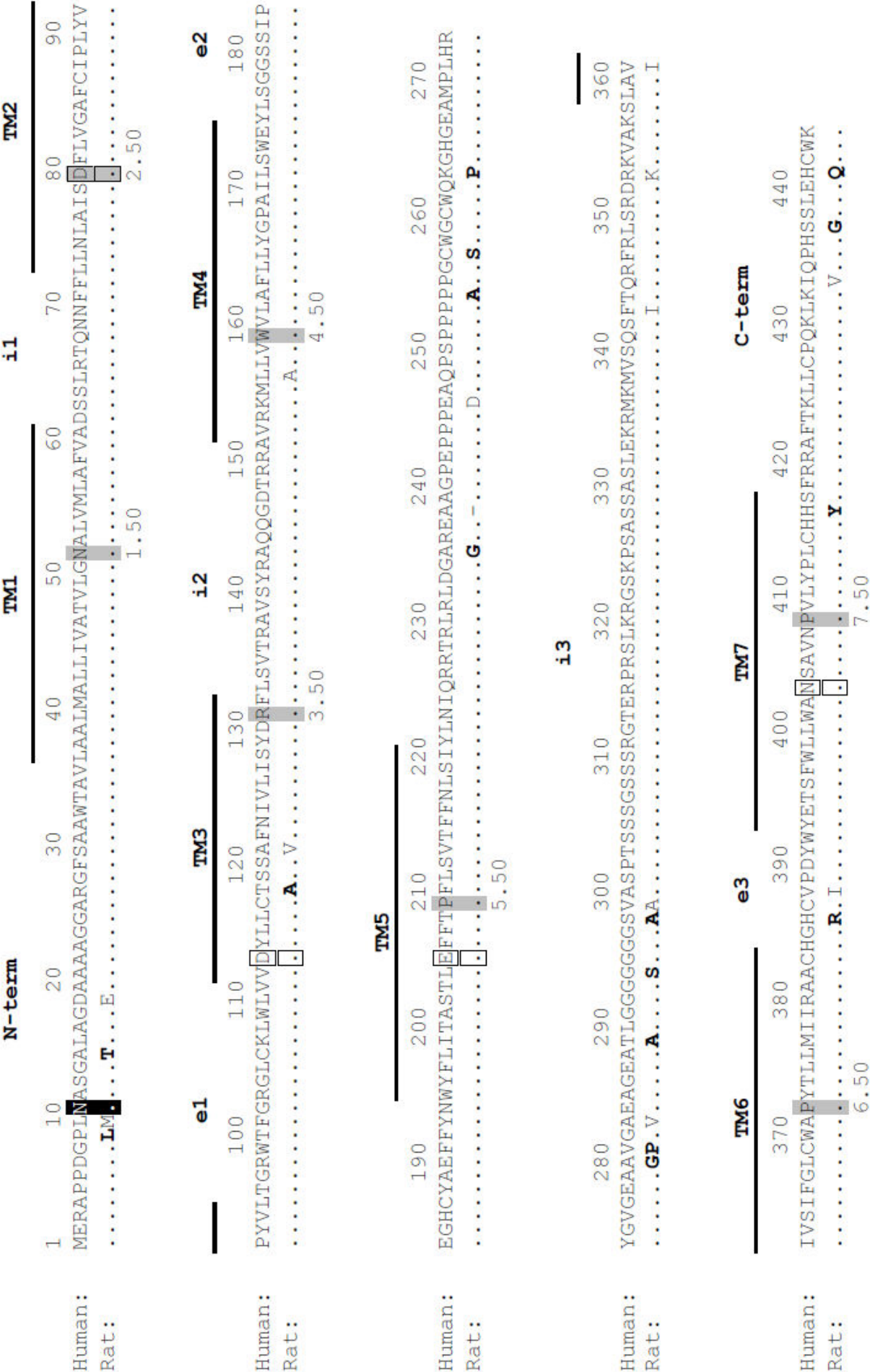


Fig. 3.1. Comparison of the amino acid sequences of hH₃R (GeneBank Accession No. AF140538) and rH₃R (GeneBank Accession No. AF237919). Putative transmembrane domains are stated above the sequences and indicated by a solid line. N-term, extracellular N-terminal domain of H₃Rs; C-term, intracellular C-terminal domain of H₃Rs; i1, i2, and i3, first, second, and third intracellular loops; e1, e2, e3, first, second, and third extracellular loops, respectively. Dots in the sequence of rH₃R indicate identity with hH₃R. Amino acids shown in regular fonts in the sequence of rH₃R represent conservative differences, those shown in bold represent non-conservative differences. The most conserved residues in each TM domain are indicated in grey shading. Residues within TM domains are named according to the Ballesteros/Weinstein nomenclature. The most conserved residue in each TM is numbered as X.50, where X is the number of the respective TM domain (Ballesteros and Weinstein, 1995). Amino acids shown in white with black shading represent a putative glycosylation site of the H₃R. Amino acids in frame represent putative interaction sites of HA with the H₃R (Uveges et al., 2002; Yao et al., 2003).

3.3.4 [³⁵S]GTP γ S saturation binding assay

Experiments were performed in analogy to the assay described in Schnell et al. (2009). Membranes were thawed and sedimented by a 10-min centrifugation at 4°C and 15,000g to remove residual endogenous guanine nucleotides as far as possible. Membranes were resuspended in binding buffer (12.5 mM MgCl₂, 1 mM EDTA, and 75 mM Tris-HCl, pH 7.4), supplemented with 0.05% (m/v) BSA. Each tube (total volume of 250 or 500 μ l) contained 10 - 20 μ g of membrane protein. Tubes contained 0.2 – 2 nM [³⁵S]GTP γ S plus unlabeled GTP γ S to give the desired final ligand concentrations (0.2 – 50 nM). Neither GDP nor H₃R ligands were included in assays. Non-specific binding was determined in the presence of 100 μ M unlabeled GTP γ S and amounted to less than 1% of total binding. Incubations were conducted for 90 minutes at 25°C and shaking at 250 rpm. Bound [³⁵S]GTP γ S was separated from free [³⁵S]GTP γ S by filtration through GF/C filters, followed by three washes with 2 ml of binding buffer (4°C). Filter-bound radioactivity was determined by liquid scintillation counting. The experimental conditions chosen ensured that not more than 10 % of the total amount of radioactivity added to binding tubes was bound to filters. The maximum number of G $\alpha_{i/o}$ -related GTP γ S binding sites in membranes expressing H₃Rs plus G α -subunits plus $\beta_1\gamma_2$ was corrected by the binding determined in parallel in membranes expressing H₃Rs plus $\beta_1\gamma_2$ alone. These reference membranes were always prepared under exactly the same conditions as the other ones. To ensure the same viral load in the reference membranes, Sf9 cells were infected with baculoviruses encoding H₃Rs, $\beta_1\gamma_2$ and virus encoding no recombinant protein at all. In this manner, only the number of functionally intact and heterologously expressed mammalian G $\alpha_{i/o}$ -subunits was quantitated.

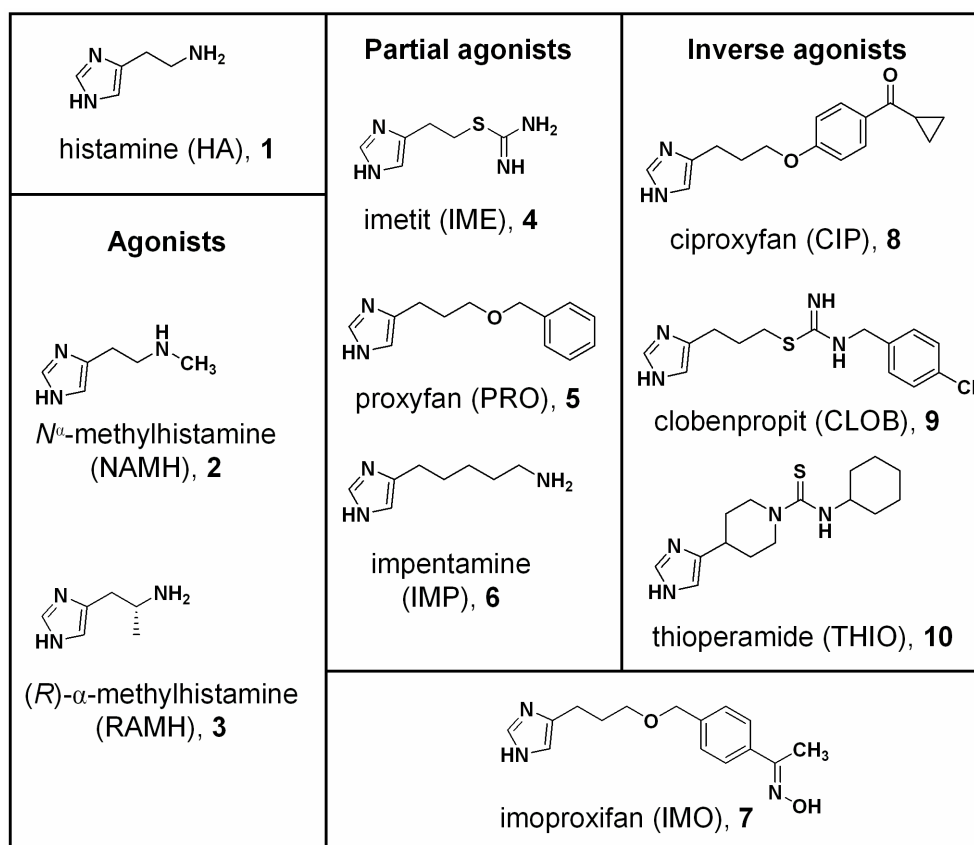


Fig. 3.2. Structures of imidazole-containing H₃R-ligands: full agonists **1-3**, partial agonists **4-6**, imoproxifan **7**, and antagonists/inverse agonists **8-10**.

3.3.5 Steady-state GTPase activity assay

Experiments were performed in analogy to the assay described in Schnell et al. (2009). Briefly, membranes were thawed, sedimented and resuspended in 10 mM Tris/HCl, pH 7.4. Assay tubes contained Sf9 membranes (10 – 20 μ g of protein/tube), 5.0 mM MgCl₂, 0.1 mM EDTA, 0.1 mM ATP, 100 nM GTP, 0.1 mM adenylyl imidodiphosphate, 1.2 mM creatine phosphate, 1 μ g of creatine kinase, and 0.2% (w/v) bovine serum albumin in 50 mM Tris/HCl, pH 7.4, and H₃R ligands at various concentrations. Reaction mixtures (80 μ l) were incubated for 2 min at 25°C before the addition of 20 μ l of [γ -³²P]GTP (0.1 μ Ci/tube). All stock and work dilutions of [γ -³²P]GTP were prepared in 20 mM Tris/HCl, pH 7.4. Reactions were conducted for 20 min at 25°C. Reactions were terminated by the addition of 900 μ l of slurry consisting of 5% (w/v) activated charcoal and 50 mM NaH₂PO₄, pH 2.0. Charcoal absorbs nucleotides but not P_i. Charcoal-quenched reaction mixtures were centrifuged for 7 min at room temperature at 15,000g. Six hundred microliters of the supernatant fluid of reaction mixtures were removed, and ³²P_i was determined by liquid scintillation counting. Enzyme activities were corrected for spontaneous degradation of [γ -³²P]GTP. Spontaneous [γ -³²P]GTP degradation was determined in tubes containing all of the above described components plus a very high concentration of unlabeled GTP (1 mM) that, by competition

with [γ -³²P]GTP, prevents [γ -³²P]GTP hydrolysis by enzymatic activities present in Sf9 membranes. Spontaneous [γ -³²P]GTP degradation was <1% of the total amount of radioactivity added using 20 mM Tris/HCl, pH 7.4, as solvent for [γ -³²P]GTP. The experimental conditions chosen ensured that not more than 10% of the total amount of [γ -³²P]GTP added was converted to ³²P_i.

3.3.6 Radioligand binding assays

Experiments were performed in analogy to the assay described in Schnell et al. (2009). Membranes were thawed and sedimented by a 10-min centrifugation at 4°C and 15,000g and resuspended in binding buffer (12.5 mM MgCl₂, 1 mM EDTA, and 75 mM Tris-HCl, pH 7.4), to remove residual endogenous guanine nucleotides as much as possible. In [³H]NAMH binding assays, each tube (total volume, 250 or 500 µl) contained 10 to 50 µg of protein. Non-specific binding was determined in the presence of [³H]NAMH at various concentrations plus 10 µM THIO and amounted to ~10% of total binding at saturating concentrations (10 nM). Incubations were conducted for 60 min at RT and shaking at 250 rpm. Saturation binding experiments were carried out using 0.3 to 10 nM [³H]NAMH in the presence or absence of 10 µM GTP γ S. In competition binding experiments, tubes contained 1 nM [³H]NAMH and unlabeled ligands at various concentrations. Bound [³H]NAMH was separated from free [³H]NAMH by filtration through GF/C filters pretreated with 0.3% (m/v) polyethyleneimine, followed by three washes with 2 ml of binding buffer (4°C). [³H]JNJ-7753707 (= [³H]RWJ-422475) binding experiments were performed using the same procedure as described above for [³H]NAMH. With [³H]JNJ-7753707 as radioligand, non-specific binding was about 20-30% of total binding at saturating concentrations (10 nM). Filter-bound radioactivity was determined by liquid scintillation counting. The experimental conditions chosen ensured that not more than 10 % of the total amount of radioactivity added to binding tubes was bound to filters.

3.3.7 Construction of inactive and active models of hH₃R and rH₃R

Based on the crystal structure of the human β_2 -adrenergic receptor (Cherezov et al., 2007; Rasmussen et al., 2007), a homology model of the inactive rH₃R was generated. Based on the active state model of guinea pig H₁R (gpH₁R) (Strasser and Wittmann, 2007; Strasser et al., 2008b), an active model of hH₃R was constructed by homology modelling. All models were refined and energetically minimized with SYBYL 7.0 (Tripos, St. Louis, MO), as described (Igél et al., 2009). Imoproxifan was docked manually into the binding pocket of the active hH₃R and the inactive rH₃R. Thereby, previous results of similar compounds were taken into account (Schlegel et al., 2007). The resulting structures were embedded in a simulation box, including lipid bilayer, water, sodium and chlorine ions, as described

(Strasser et al., 2008a). Subsequently, molecular dynamic simulations with GROMACS 3.3.1 (van der Spoel et al., 2004) were performed, using a simulation protocol, previously described (Strasser et al., 2008a).

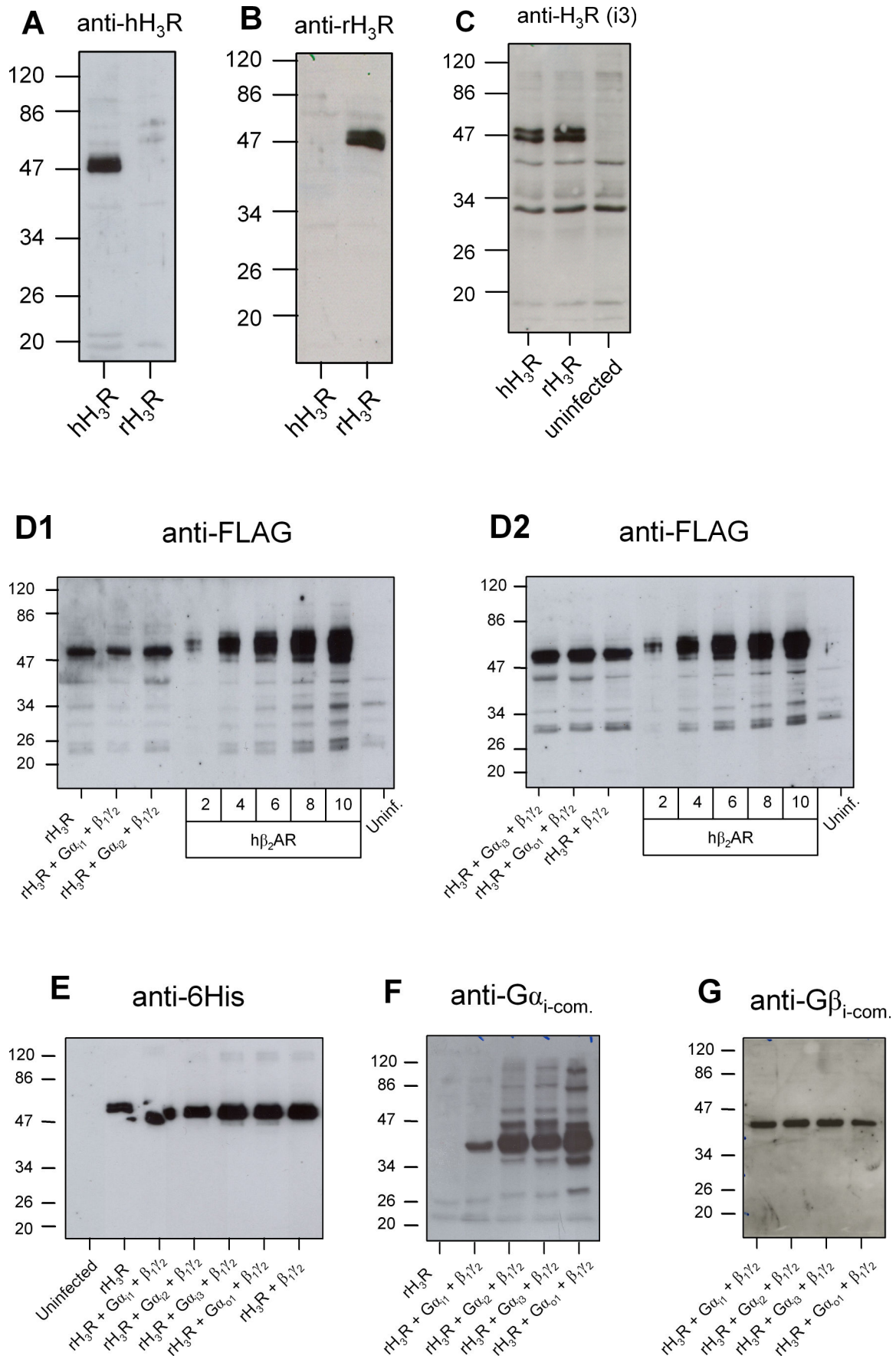
3.3.8 Miscellaneous

Molecular biology was planned with GCK 2.5 (Textco BioSoftware, West Lebanon, NH, USA). Ligand structures were illustrated using ChemDraw Ultra 8.0 (CambridgeSoft, Cambridge, MA, USA). The sequence alignment was performed using ClustalX (2.0), which is a windows interface based on the Clustal W algorithm (Thompson et al., 1994). Protein was determined using the DC protein assay kit (Bio-Rad, Hercules, CA, USA). [³H]Dihydroalprenolol was obtained from Perkin Elmer (Boston, MA, USA) and protein quantification via western blot performed as described in Schnell et al. (2009). All analyses of experimental data were performed with the Prism 5 program (GraphPad Software, San Diego, CA, USA).

3.4 Results

3.4.1 Western blot analysis of hH₃R and rH₃R expressed in Sf9 insect cell membranes

Membranes of Sf9 cells expressing hH₃R or rH₃R plus mammalian G proteins were prepared and analyzed via immunoblot. It has to be mentioned, that membranes co-expressing rH₃R plus different mammalian G proteins were prepared in parallel and under exactly the same conditions as the membranes expressing hH₃R (Schnell et al., 2009). Thus, the comparison of hH₃R and rH₃R pharmacology in this system is not based on historical data but direct. Both hH₃R and rH₃R bands were doublets, probably representing differently glycosylated forms (Fig. 3.3). H₃R species homologs presumably exhibit similar glycosylation patterns since the putative N-glycosylation site for the H₃R (Asn11) is fully conserved within their sequences (Fig. 3.1). The H₃R species homologs could be clearly discriminated by anti-hH₃R Ig, raised against an 18 amino acid peptide within the extracellular N-terminus of the hH₃R, and anti-rH₃R Ig, raised against an 18 amino acid peptide within the cytoplasmatic C-terminus of the rH₃R (Figs. 3.3A and 3.3B).



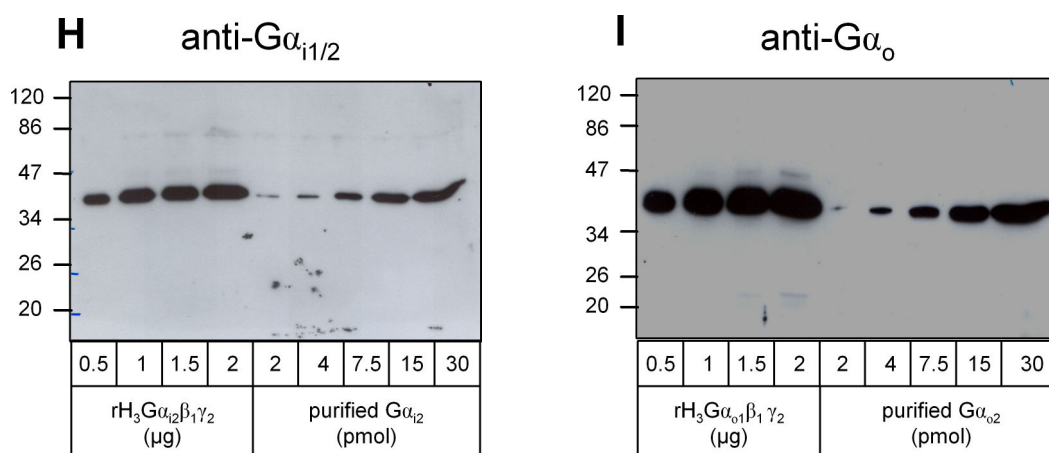


Fig. 3.3. Immunological detection of hH₃R and rH₃R expressed in Sf9 cells. Each lane of the gels was loaded with 10 μg of membrane protein, unless otherwise indicated below the film. Numbers on the left designate masses of marker proteins in kDa. In **A** and **B**, membranes expressing the hH₃R and rH₃R alone were loaded onto the gels. Proteins separated in **A** were reacted with anti-hH₃R Ig and in **B** with anti-rH₃R Ig. In **C**, membranes of **A** and **B** plus control were analyzed. Here, the proteins were reacted with the non-species-selective anti-hH₃R (i3) Ig. In **D1** and **D2**, 2, 4, 6, 8 and 10 μg of protein of Sf9 membranes expressing hβ₂AR at 7.5 pmol/mg (as determined by [³H]dihydroalprenolol saturation binding) were used as standard to assess the expression levels of the rH₃R in different membrane preparations with anti-FLAG Ig. In **E**, the same membranes were reacted with anti-His6 Ig. In **F**, the membranes were reacted with anti-G $\alpha_{i\text{-common}}$ Ig. In **G**, the membranes were reacted with anti-G $\alpha_{\beta\text{-common}}$ Ig. In **H**, 0.5, 1.0, 1.5 and 2.0 μg of a membrane expressing the rH₃R + G α_{i2} + β₁γ₂ was analyzed in order to quantify the G α -subunits, using 2, 4, 7.5, 15 and 30 pmol of purified G α_{i2} as standard. In **I**, 0.5, 1.0, 1.5 and 2.0 μg of a corresponding membrane of the same batch expressing rH₃R + G α_{o1} + β₁γ₂ was analyzed to quantify the G α -subunits, using 2, 4, 7.5, 15 and 30 pmol of purified G α_{o2} an almost identical splice variant of G α_{o1} as standard.

Additionally, anti-H₃R (i3) Ig was used to confirm the above mentioned results (Fig. 3.3C). This antibody was raised against a peptide sequence within the third intracellular loop (i3) of the hH₃R, but turned out to be not species-selective. Again, all H₃R bands occurred as doublets at ~49 kDa. However, there were some additional bands at lower molecular weight, which are presumably non-specific, since they also appeared at the control lane loaded with uninfected Sf9 cell membranes. Thus, our data indicate that hH₃R and rH₃R were equally well and properly expressed in Sf9 cells. In analogy to our recent publication (Schnell et al., 2009), the rH₃R was also co-expressed with different mammalian G proteins (G α_{i1} , G α_{i2} , G α_{i3} or G α_{o1} , and β₁γ₂ dimers, respectively) to analyze the coupling profile. All proteins were properly detected by different selective antibodies (Fig. 3.3). Moreover, we also quantified the expression levels of receptors and G proteins by immunoblot, using hβ₂AR or purified G protein subunits as standards (Fig. 3.3D and 3.3H, I). The results of these studies are summarized in Table 3.1.

3.4.2 Quantitative analysis of receptor-to-G protein stoichiometries

Protein quantification via western blot is semi-quantitative and does not discriminate between functional and non-functional proteins. Therefore, we directly used a recently described combination of antagonist [³H]JNJ-7753707- and [³⁵S]GTP γ S-saturation binding (Schnell et al., 2009) and calculated the functional GPCR/G α protein ratios (Table 3.1). Similar to the membranes expressing hH₃R, we detected an excess of mammalian G proteins in the case of rH₃R, confirming the previously reported results (Schnell et al., 2009). Thus, G protein expression level is not limiting in this experimental system, too.

3.4.3 hH₃R and rH₃R coupling to different G α -subunits

The G protein coupling profile of rH₃R (Table 3.2) was also investigated as for the hH₃R (Schnell et al., 2009). Briefly, receptor-dependent [γ -³²P]GTP hydrolysis of different G α -subunits was measured under steady-state conditions. GTPase activities were determined in parallel under basal conditions, maximal stimulation with the physiological (and full) agonist histamine (10 μ M) and a saturating concentration of the inverse agonist thioperamide (10 μ M) in Sf9 cell membranes co-expressing the rH₃R and different G proteins.

Table 3.1: Quantification of rH₃R-to-G protein ratios via western blot, [³H]JNJ-7753707- and [³⁵S]GTP_γS-saturation binding.

membrane	$B_{\max} \pm \text{S. E. M. (pmol} \times \text{mg}^{-1})$			
	rH ₃ R + $\beta_1\gamma_2$			
	+ G α_{i1}	+ G α_{i2}	+ G α_{i3}	+ G α_{o1}
immunoblot:				
anti-FLAG Ig	~1.5 – 2.5	~1.5 – 2.5	~1.5 – 2.5	~1.5 – 2.5
anti-G α Igs	n. d.	~50 - 100	n. d.	~50 - 100
[³ H]JNJ-7753707	0.67 ± 0.03	0.77 ± 0.02	1.05 ± 0.04	1.25 ± 0.04
[³⁵ S]GTP _γ S	3.40 ± 0.80	4.43 ± 0.53	2.52 ± 0.37	8.19 ± 1.27
R : G ratio	~1 : 5	~1 : 6	~1 : 2	~1 : 7

The quantification of receptors and G proteins via immunoblot was performed as described in Schnell et al. (2009). [³H]JNJ-7753707 saturation bindings were performed as described under *Methods*. [³⁵S]GTP_γS saturation bindings were performed, using Sf9 cell membranes from the same batch of preparation. Reaction mixtures contained membranes (10 - 20 µg of protein), 0.2 - 2 nM of [³⁵S]GTP_γS, and unlabeled GTP_γS to give the desired final ligand concentrations for saturation (0.2 – 50 nM). GDP or additional H₃R ligands were not present in the reaction mixtures. Data were analyzed by nonlinear regression and were best fitted to hyperbolic one-site saturation isotherms. The maximal number of GTP_γS binding sites in membranes expressing rH₃R plus G α_{i2} plus $\beta_1\gamma_2$ was corrected by the binding determined in rH₃R plus $\beta_1\gamma_2$. By this way, the number of functionally intact and heterologously expressed G protein α -subunits was quantified. Data shown are the means ± S. E. M. of 3 independent experiments performed in triplicate. Receptor-to-G protein ratios were calculated, using the B_{\max} values determined for the different membrane preparations.

Like hH₃R, rH₃R coupled efficiently to all co-expressed mammalian G $\alpha_{i/o}$ -subunits (G α_{i1} , G α_{i2} , G α_{i3} or G α_{o1} , and $\beta_1\gamma_2$ dimers, respectively), as was evident by the high basal GTPase activities and the large absolute stimulatory and inhibitory effects of histamine and thioperamide, respectively (Table 3.2). Also, the relative stimulatory effects of histamine and the relative inhibitory effects of thioperamide based on total ligand-regulated GTPase activity were similar for each of the four systems studied, indicating that the constitutive activity of rH₃R was comparable and not substantially influenced by the type of G protein (Table 3.2). The constitutive activity of rH₃R coupled to cognate G_i/G_o-proteins was rather high and comparable to the constitutive activity of hH₃R, rendering the two systems suitable for an

analysis of species-specific ligand effects, without possible bias due to differences in basal activity between membranes.

Table 3.2: Analysis of rH₃R/G protein coupling - GTPase activities in Sf9 membranes expressing rH₃R and different G $\alpha_{i/o}$ -proteins.

GTPase activity \pm S. E. M.	rH ₃ R + $\beta_1\gamma_2$			
	+ G α_{i1}	+ G α_{i2}	+ G α_{i3}	+ G α_{o1}
basal (pmol \times mg ⁻¹ \times min ⁻¹)	1.22 \pm 0.21	1.75 \pm 0.22	1.12 \pm 0.04	4.29 \pm 0.12
+ ago. (pmol \times mg ⁻¹ \times min ⁻¹)	2.01 \pm 0.26	3.17 \pm 0.37	2.13 \pm 0.14	5.95 \pm 0.14
Δ ago. (pmol \times mg ⁻¹ \times min ⁻¹)	0.79 \pm 0.07	1.42 \pm 0.15	1.01 \pm 0.10	1.66 \pm 0.09
Agonist stimulation (% of basal)	67.44 \pm 0.09	81.78 \pm 2.32	89.38 \pm 5.14	38.78 \pm 2.38
+ inv. ago. (pmol \times mg ⁻¹ \times min ⁻¹)	0.71 \pm 0.10	0.85 \pm 0.12	0.59 \pm 0.03	2.86 \pm 0.14
Δ inv. ago. (pmol \times mg ⁻¹ \times min ⁻¹)	0.51 \pm 0.13	0.90 \pm 0.10	0.53 \pm 0.02	1.43 \pm 0.13
Inverse agonist inhibition (% of basal)	40.32 \pm 5.93	51.66 \pm 0.96	47.4 \pm 0.82	33.29 \pm 2.88

Steady-state GTPase experiments were performed as described in *Methods*. Reaction mixtures contained 0.1 μ Ci [γ -³²P]GTP and 100 nM unlabeled GTP in the presence of solvent (basal), 10 μ M HA (+ ago.) or 10 μ M THIO (+ inv. ago.). Data shown are the means \pm S. E. M. of three to four independent experiments for each membrane preparation performed in duplicates. The absolute agonist-stimulation (Δ ago.) and inverse agonist-inhibition (Δ inv. ago.) of GTP hydrolysis, as well as the relative agonist-stimulation and inverse agonist-inhibition of GTP hydrolysis (% of basal), were calculated.

3.4.4 Ligand potencies and efficacies in the steady-state GTPase assay at rH₃R compared to hH₃R co-expressed with different G α -subunits

Next, we examined a series of imidazole-based ligands in Sf9 cell membranes expressing rH₃R and different G $\alpha_{i/o}$ -proteins in the steady-state GTPase assay. The data (Table 3.3) were then compared with the results for hH₃R (Schnell et al., 2009).

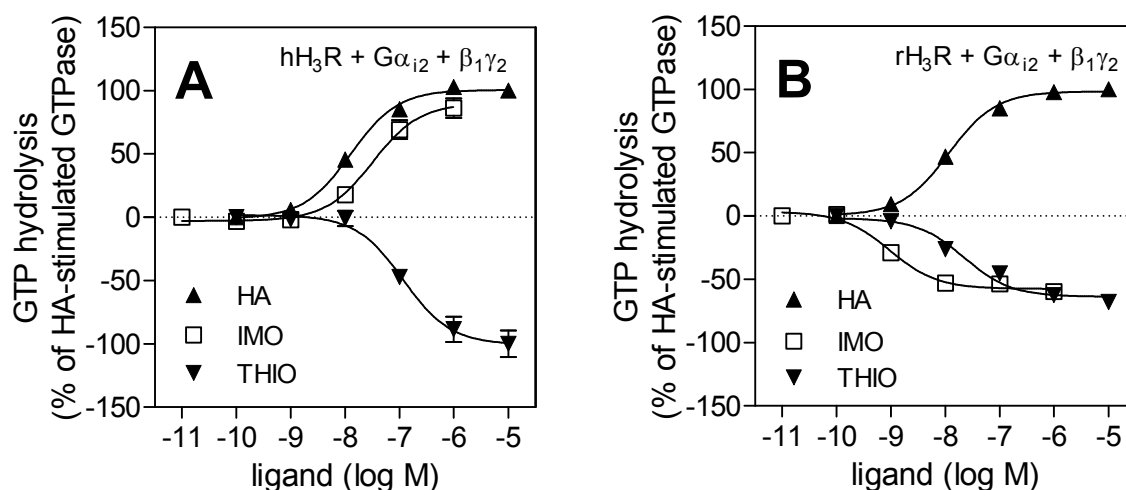


Fig. 3.4. Comparison of the effects of histamine, imoproxifan and thioperamide in membranes co-expressing the hH₃R or rH₃R, G α_{i2} subunits and $\beta_1\gamma_2$ dimers. Steady-state GTPase activity in Sf9 membranes was determined as described under *Methods*. Reaction mixtures contained HA, IMO or THIO at the concentrations indicated on the abscissa to achieve saturation. Data are expressed as percentage change in GTPase activity induced by the ligands compared to the GTPase activity stimulated by HA (10 μM), which was defined to be 100%. Data were analyzed by nonlinear regression and were best fit to sigmoidal concentration/response curves. Data points shown are the means \pm S. E. M. of 3 - 4 independent experiments performed in duplicate. A summary of all results is shown in Table 3.3.

The endogenous agonist histamine (**1**) and the standard H₃R ligands *N* $^{\alpha}$ -methylhistamine (**2**) and (*R*)- α -methylhistamine (**3**) were full agonists and equally potent in all membranes. There were essentially no species-differences. The highly potent standard H₃R agonist imetit (**4**) was almost a full agonist at rH₃R, too. Interestingly, proxyfan (**5**) was again a strong partial agonist in all systems, independent of the G protein subtype co-expressed, corroborating the notion that this ligand does not show functional selectivity at H₃R_s (Schnell et al., 2009). In contrast to hH₃R, impentamine (**6**) was a strong and more potent partial agonist at rH₃R in all experimental settings. Strikingly, imoproxifan (**7**) was an inverse agonist at rH₃R, but almost full agonist at hH₃R (Fig. 3.4). The type of G protein subunit did not change the pharmacological profile of imoproxyfan (Table 3.3). The inverse agonists ciproxyfan (**8**) and thioperamide (**10**) were more potent but less efficacious at rH₃R than at hH₃R and again, the G protein subtype caused no changes in their profiles. Clobenpropit (**9**)

was neither species-specific nor did the G protein subtype change its pharmacology. Moreover, there is also a strong linear correlation between potencies and efficacies of imidazole-based ligands at membranes expressing rH₃R and different G $\alpha_{i/o}$ -subunits, as was found for the hH₃R (Fig. 3.5; Table 3.3). Thus, the pharmacological profile of the rH₃R is also very similar under the various experimental conditions and, like at hH₃R, ligand-specific receptor conformations leading to coupling differences do not exist for the compounds investigated (Schnell et al., 2009).

Table 3.3: Ligand potencies and efficacies in the GTPase assay at Sf9 cell membranes expressing the rH₃R and different G proteins.

	rH ₃ R + G α_{11} + $\beta_1\gamma_2$		rH ₃ R + G α_{12} + $\beta_1\gamma_2$		rH ₃ R + G α_{13} + $\beta_1\gamma_2$		rH ₃ R + G α_{o1} + $\beta_1\gamma_2$	
	pEC ₅₀ ± S. E. M.	E _{max} ± S. E. M.	pEC ₅₀ ± S. E. M.	E _{max} ± S. E. M.	pEC ₅₀ ± S. E. M.	E _{max} ± S. E. M.	pEC ₅₀ ± S. E. M.	E _{max} ± S. E. M.
HA	7.64 ± 0.07*	1.00	7.94 ± 0.05	1.00	7.88 ± 0.06	1.00	7.72 ± 0.05	1.00
NAMH	8.30 ± 0.23	0.91 ± 0.10	8.98 ± 0.12	1.06 ± 0.07	9.11 ± 0.30	1.16 ± 0.21	8.88 ± 0.18	1.10 ± 0.11
RAMH	8.06 ± 0.17	0.88 ± 7.14	8.54 ± 0.10	0.91 ± 0.05	8.50 ± 0.08	0.90 ± 0.03	8.21 ± 0.10	0.84 ± 0.04
IME	9.86 ± 0.19	0.95 ± 0.10	9.76 ± 0.13	0.89 ± 0.06	10.14 ± 0.36	1.39 ± 0.30	9.78 ± 0.12	0.99 ± 0.07
PRO	8.12 ± 0.22	0.48 ± 0.05	8.52 ± 0.12	0.66 ± 0.04	8.42 ± 0.10	0.64 ± 0.04	8.19 ± 0.16	0.66 ± 0.05
IMP	8.33 ± 0.15	0.72 ± 0.05	8.94 ± 0.20	0.91 ± 0.10	8.99 ± 0.26	0.95 ± 0.14	8.76 ± 0.12	0.84 ± 0.06
IMO	9.03 ± 0.26	-0.61 ± 0.08	9.03 ± 0.13	-0.61 ± 0.04	9.05 ± 0.23	-0.46 ± 0.05	8.93 ± 0.16	-0.96 ± 0.08**
CIP	8.71 ± 0.27	-0.81 ± 0.10	8.64 ± 0.10	-0.75 ± 0.03	8.64 ± 0.15	-0.61 ± 0.04	8.58 ± 0.16	-1.01 ± 0.07
CLOB	9.04 ± 0.26	-0.43 ± 0.05	8.95 ± 0.16	-0.44 ± 0.03	8.77 ± 0.13	-0.41 ± 0.02	8.68 ± 0.11	-0.69 ± 0.03**
THIO	7.82 ± 0.24	-0.66 ± 0.07	7.66 ± 0.12	-0.62 ± 0.03	7.61 ± 0.13	-0.50 ± 0.03	7.64 ± 0.08	-0.99 ± 0.03***
<i>r</i> ²	0.77	0.99	1.00	1.00	0.97	0.96	0.96	0.996
<i>slope</i>	0.99 ± 0.19	0.97 ± 0.04	1.00	1.00	1.17 ± 0.07	0.99 ± 0.07	1.05 ± 0.07	1.20 ± 0.03

Steady-state GTPase activity in Sf9 membranes expressing rH₃R, different G $\alpha_{i/o}$ subunits and $\beta_1\gamma_2$ was determined as described under *Materials and Methods*. Reaction mixtures contained ligands at concentrations from 0.1 nM to 10 μ M as appropriate to generate saturated concentration/response curves. Data were analyzed by nonlinear regression and were best fit to sigmoid concentration/response curves. Typical basal GTPase activities ranged between 1.0 and 4.0 pmol * mg⁻¹ * min⁻¹, and the maximal stimulatory effect of histamine (10 μ M) amounted to ~40 to ~90% above basal. The efficacy (E_{max}) of histamine was determined by nonlinear regression and was set to 1.00. The E_{max} values of other agonists and inverse agonists were referred to this value. Data shown are the means \pm S. E. M. of three to four experiments performed in duplicates each. Statistical analysis was performed using one-way ANOVA, followed by Dunnett's multiple comparison test using the values determined at hH₃R, G α_{i2} and $\beta_1\gamma_2$ as a reference. Significant differences to the membrane expressing G α_{i2} are shown following comparison with other G $\alpha_{i/o}$ subunits. (no symbol: not significant; *, $p < 0.05$; **, $p < 0.01$; ***, $p < 0.001$). Additionally, data shown were correlated and analyzed by linear regression. The potencies and efficacies of ligands at membranes co-expressing the rH₃R, G α_{i1} , G α_{i3} or G α_{o1} , and $\beta_1\gamma_2$ dimers, respectively, were correlated with values determined at the reference membrane expressing G α_{i2} . The correlation coefficients (r^2) and the slopes are presented at the bottom of the table.

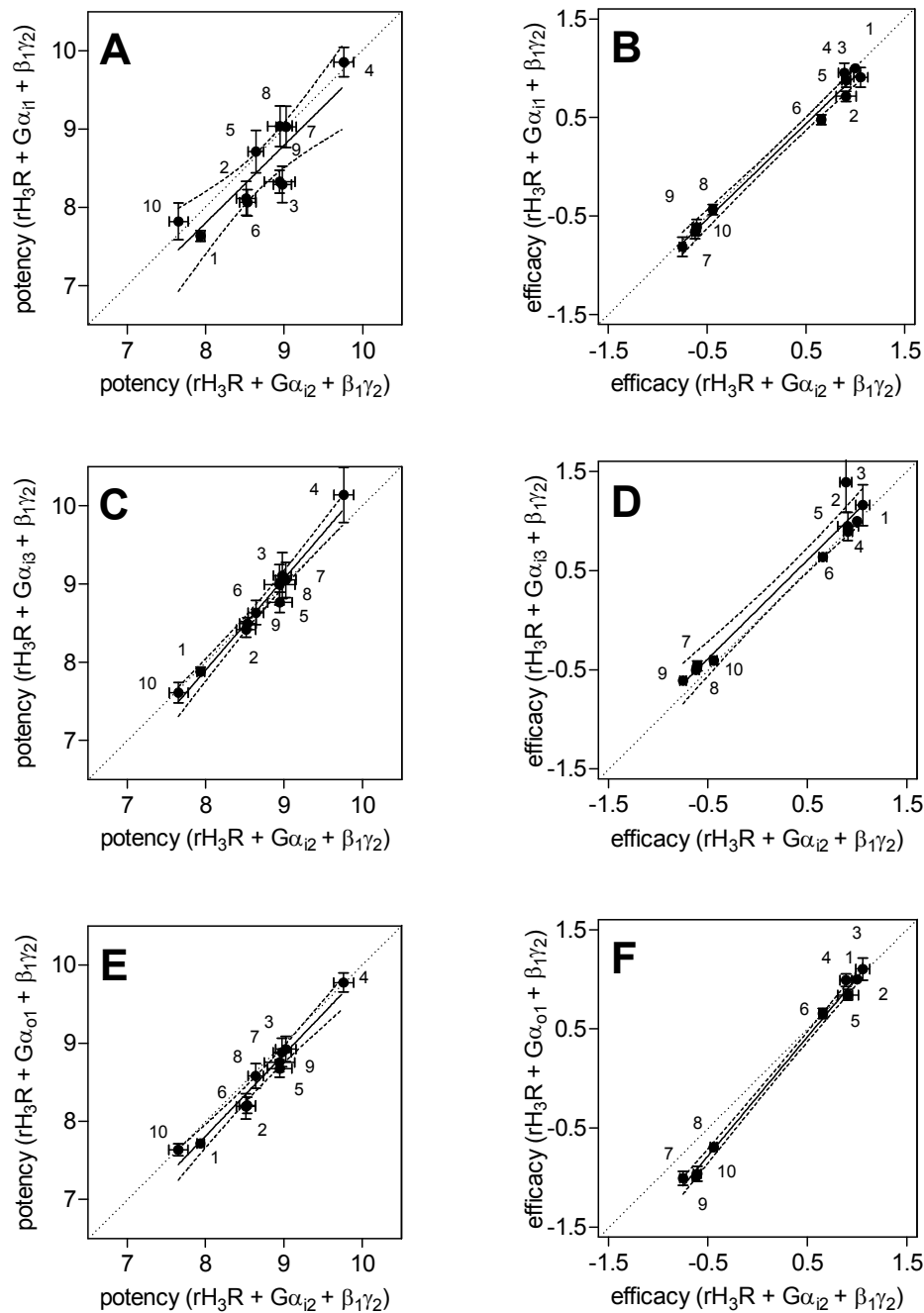


Fig. 3.5. Correlation of potency and efficacy of ligands at the rH₃R in the presence of different co-expressed Gα_{i/o}-proteins. Data shown in Table 3.3 were analyzed by linear regression. Numbers designate individual ligands decoded in Fig. 3.2. In **A**, **C** and **E**, the potencies of ligands at membranes co-expressing the rH₃R, Gα_{i1}, Gα_{i3} or Gα_{o1}, and β₁γ₂-dimers, respectively, were correlated with values determined at the reference membrane expressing Gα_{i2}. **A**, $r^2 = 0.77$; $slope = 0.99 \pm 0.19$. **C**, $r^2 = 0.97$; $slope = 1.17 \pm 0.07$. **E**, $r^2 = 0.96$; $slope = 1.05 \pm 0.07$. In **B**, **D** and **F**, the efficacies of ligands at membranes co-expressing the rH₃R, Gα_{i1}, Gα_{i3} or Gα_{o1}, and β₁γ₂ dimers, respectively, were correlated with values determined at the reference membrane expressing Gα_{i2}. **B**, $r^2 = 0.99$; $slope = 0.97 \pm 0.04$. **D**, $r^2 = 0.96$; $slope = 0.99 \pm 0.07$. **F**, $r^2 = 0.996$; $slope = 1.20 \pm 0.03$. The dotted lines indicate the 95% confidence intervals of the regression lines. The diagonal dashed line has a slope of 1 and represents a theoretical curve for identical values.

Collectively, these results confirm the findings regarding the relative stimulatory and inhibitory effects of histamine and thioperamide, respectively (Table 3.2), based on total ligand-regulated GTPase activity and are indicative for similar constitutive activity of hH₃R and rH₃R under all experimental conditions. If there had been differences in constitutive activity between hH₃R and rH₃R, then systematic changes in the potencies of full agonists as well as potencies and efficacies of partial agonists and inverse agonists would have occurred. This, however, was not the case. In contrast, the behaviour of ligands, e. g. impentamine or imoproxifan, at one H₃R species homolog often opposed each other, against every expectation. Thus, these ligand effects are solely species-specific and not due to differences in constitutive activity of hH₃R and rH₃R.

3.4.5 [³H]NAMH binding studies at hH₃R and rH₃R

Since the type of G protein co-expressed did not change the pharmacology of ligands at both hH₃R and rH₃R in the steady-state GTPase assay, we performed radioligand binding experiments for a further characterization only at membranes expressing hH₃R or rH₃R plus Gα_{i2} plus β₁γ₂ dimers.

At first, we addressed the formation of a high-affinity ternary complex between the agonist [³H]NAMH, the hH₃R or rH₃R and nucleotide-free G protein in saturation binding experiments (Fig. 3.6). The K_d of [³H]NAMH at hH₃R was 0.62 ± 0.21 nM ($n = 3$). At rH₃R, the K_d value was 1.37 ± 0.36 nM ($n = 3$). Interestingly, binding of [³H]NAMH was only partially GTPγS-sensitive in both cases. The K_d values of [³H]NAMH in the presence of GTPγS (10 μM) were about 2-fold lower, but the B_{max} values did not change significantly (Fig. 3.6).

In competition binding experiments (Fig. 3.7), histamine (**1**), *N*^α-methylhistamine (**2**), (*R*)-α-methylhistamine (**3**), imetit (**4**) and proxyfan (**5**) had essentially the same affinities at hH₃R and rH₃R. Impentamine (**6**), imoproxifan (**7**), ciproxyfan (**8**) and thioperamide (**10**) bound with higher affinity to rH₃R. Clobenpropit (**9**) also bound with similar affinity to both receptors. The pharmacological profiles, determined in [³H]NAMH competition binding (Table 3.4) and steady-state GTPase assays (Table 3.3), compared with the literature, were very similar (Lim et al., 2005; Bongers et al., 2007b).

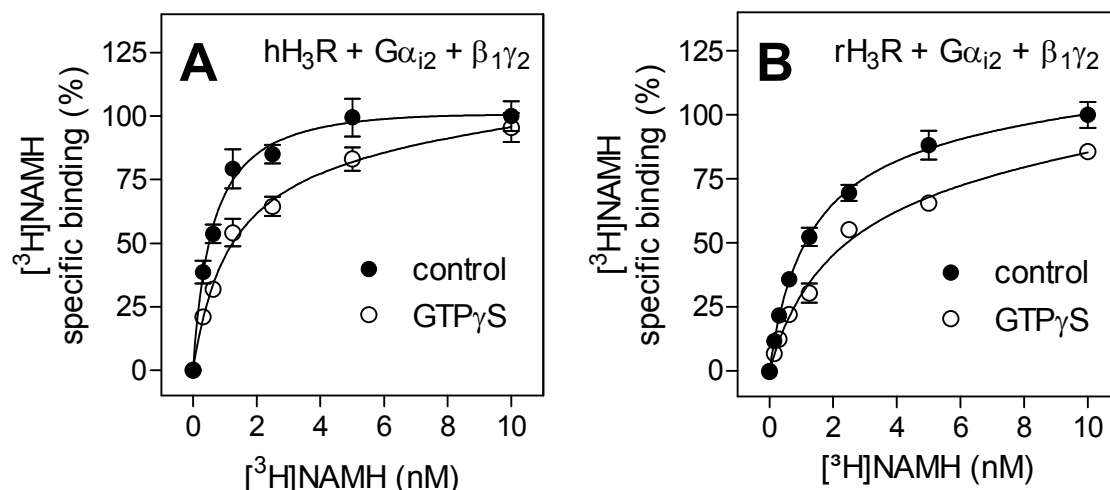


Fig. 3.6. [³H]NAMH saturation bindings in Sf9 cell membranes expressing hH₃R or rH₃R in combination with Gα_{i2} and β₁γ₂. Experiments were performed as described under *Methods*. Data were analyzed by nonlinear regression and were best fitted to hyperbolic one-site saturation isotherms. The closed circles (●) show the data for the specific [³H]NAMH binding in the absence of GTPγS (10 μM), the open circles (○) in the presence of GTPγS (10 μM). In **A**, hH₃R was analyzed and in **B**, rH₃R was analyzed. Data points shown are the means ± S. E. M. of 3 independent experiments performed in triplicate, using three different membrane preparations.

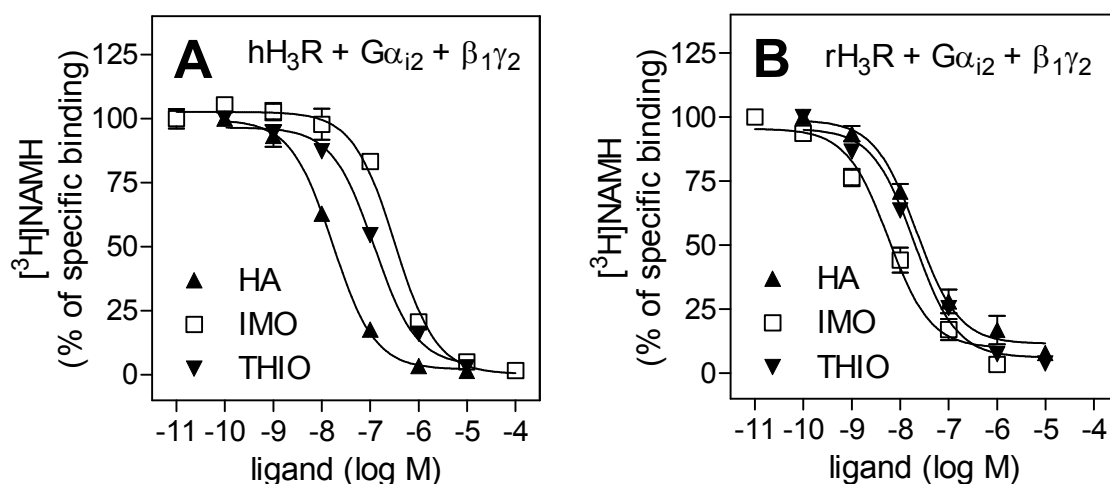


Fig. 3.7. Competition of [³H]NAMH binding by histamine, imoproxifan and thioperamide in Sf9 membranes expressing hH₃R and rH₃R in combination with Gα_{i2} and β₁γ₂. [³H]NAMH binding was determined as described under *Methods*. Reaction mixtures contained Sf9 membranes (10 - 50 μg of protein per tube) expressing the recombinant proteins, 1 nM [³H]NAMH, and ligands at the concentrations indicated on the abscissa. **A**, competition binding at hH₃R and **B**, competition binding at rH₃R. Data were analyzed for best fit to monophasic competition curves (*F* test). Data points shown are the means ± S. E. M. of 3 - 5 independent experiments performed in duplicate. A summary of all results is shown in Table 3.7.

Table 3.4: [³H]NAMH competition bindings in Sf9 membranes expressing hH₃R or rH₃R in combination with G α_{i2} and $\beta_1\gamma_2$.

	pK _i \pm S. E. M.	
	hH ₃ R + G α_{i2} + $\beta_1\gamma_2$	rH ₃ R + G α_{i2} + $\beta_1\gamma_2$
HA	8.20 \pm 0.04	7.89 \pm 0.07
NAMH	9.22 \pm 0.03	8.70 \pm 0.09
RAMH	8.91 \pm 0.07	8.62 \pm 0.07
IME	9.20 \pm 0.05	9.38 \pm 0.08
PRO	7.87 \pm 0.07	8.08 \pm 0.10
IMP	8.84 \pm 0.06	10.11 \pm 0.05
IMO	6.92 \pm 0.06	8.47 \pm 0.09
CIP	7.03 \pm 0.12	8.87 \pm 0.08
CLOB	9.34 \pm 0.06	9.11 \pm 0.06
THIO	7.34 \pm 0.04	7.94 \pm 0.04
r^2 (pK _i /pEC ₅₀)	0.83	0.50
<i>slope</i> (pK _i /pEC ₅₀)	0.94 \pm 0.15	0.83 \pm 0.29

Experiments were performed as described under *Methods*. Reaction mixtures contained Sf9 membranes (10 – 50 μ g of protein), 1 nM [³H]NAMH, and unlabeled ligands at concentrations of 0.1 nM to 10 μ M as appropriate to generate saturated competition curves. Data were analyzed by nonlinear regression and were best fit to one-site (monophasic) competition curves. Data shown are the means \pm S. E. M. of three to five independent experiments performed in duplicate at 3 different membrane preparations. Additionally, data shown were correlated and analyzed by linear regression. The affinities and potencies of ligands at membranes co-expressing the hH₃R or rH₃R plus G α_{i2} plus $\beta_1\gamma_2$ dimers, respectively, were correlated. The correlation coefficients (r^2) and the *slopes* of all tested ligands are presented at the bottom of the table.

The pK_i and pEC_{50} values determined at hH₃R correlated well, suggesting a direct signal transfer in the Sf9 cell system (Fig. 3.8). However, at rH₃R, the correlation coefficient was rather low, due to an extraordinary high affinity of impentamine (**6**). Interestingly, the pK_i values of imoproxifan (**7**) were significantly lower than the corresponding pEC_{50} values determined in the GTPase assay (t test, $p < 0.05$).

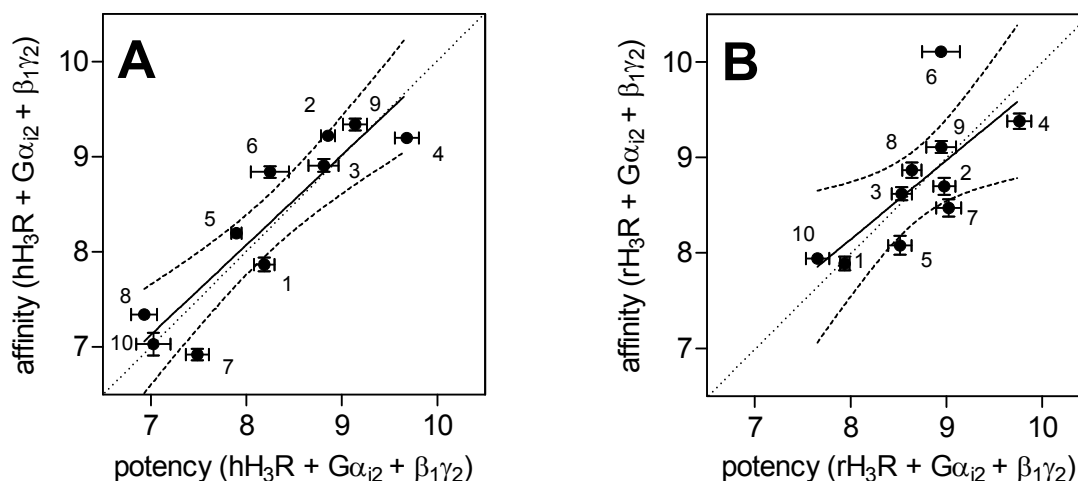


Fig. 3.8. Correlation of affinity and potency of ligands at the hH₃R and rH₃R. Data shown were analyzed by linear regression. Numbers designate individual ligands decoded in Fig. 3.2. In **A**, the affinities and potencies of ligands at membranes co-expressing the hH₃R, Gα_{i2} and β₁γ₂ dimers were correlated. **A**, $r^2 = 0.83$; $slope = 0.94 \pm 0.15$. In **B**, the affinities and potencies of ligands at membranes co-expressing the rH₃R, Gα_{i2} and β₁γ₂ dimers were correlated. **B**, $r^2 = 0.50$; $slope = 0.83 \pm 0.29$. The dotted lines indicate the 95% confidence intervals of the regression lines. The diagonal dashed line has a slope of 1 and represents a theoretical curve for identical values.

3.4.6 Binding mode of imoproxifan at hH₃R and rH₃R

To understand the molecular basis for the unique behaviour of imoproxifan, we performed molecular modelling studies with hH₃R and rH₃R. The binding modes of imoproxifan at active hH₃R and inactive rH₃R, representing the most favoured ligand-receptor-complexes, are presented in Fig. 3.9.

Imoproxifan is bound to hH₃R and rH₃R in *E*-configuration, representing the *trans*-isomer of the oxime-moiety. The *E*-configuration was also determined to be the favoured one by crystallographic studies (Sasse et al., 2000). The electrostatic surface potential of the amino acids with the ligand in the binding pocket is shown (Fig. 3.9, A and B). At hH₃R and rH₃R, the positively charged terminal imidazole moiety of imoproxifan interacts with the highly conserved Asp^{3.32} (Fig. 3.9, A and B, black arrow). However, there are large differences in electrostatic surface between TM V and TM III (Fig. 3.9, A and B, yellow, dotted line). In this region, the electrostatic surface potential is rather neutral at hH₃R, but negatively charged at rH₃R. The consequence is a different orientation of the oxime moiety of imoproxifan. At hH₃R, the methyl moiety points upward, whereas at rH₃R, the methyl moiety points downward.

The reason for the differences in electrostatic surface potential between hH₃R and rH₃R are explained by the amino acid difference at position 3.37 between hH₃R and rH₃R. At hH₃R, Glu^{5.46} can electrostatically interact with Thr^{3.37} (Fig. 3.9, C, yellow, dotted line). Thus, Glu^{5.46} points towards Thr^{3.37} and away from the binding pocket. Consequently, the electrostatic potential surface in this region is neutral. In contrast, at rH₃R, Thr^{3.37} is exchanged into Ala^{3.37}. Thus, an electrostatic interaction between Glu^{5.46} and the amino acid side chain in position 3.37 is no longer possible. Instead, the modelling studies revealed an electrostatic interaction of Glu^{5.46} and Tyr^{3.33} at rH₃R (Fig. 3.9, D, yellow, dotted line). Consequently, the negatively charged side chain of Glu^{5.46} points partially toward the binding pocket, resulting in a negative electrostatic potential surface in this region.

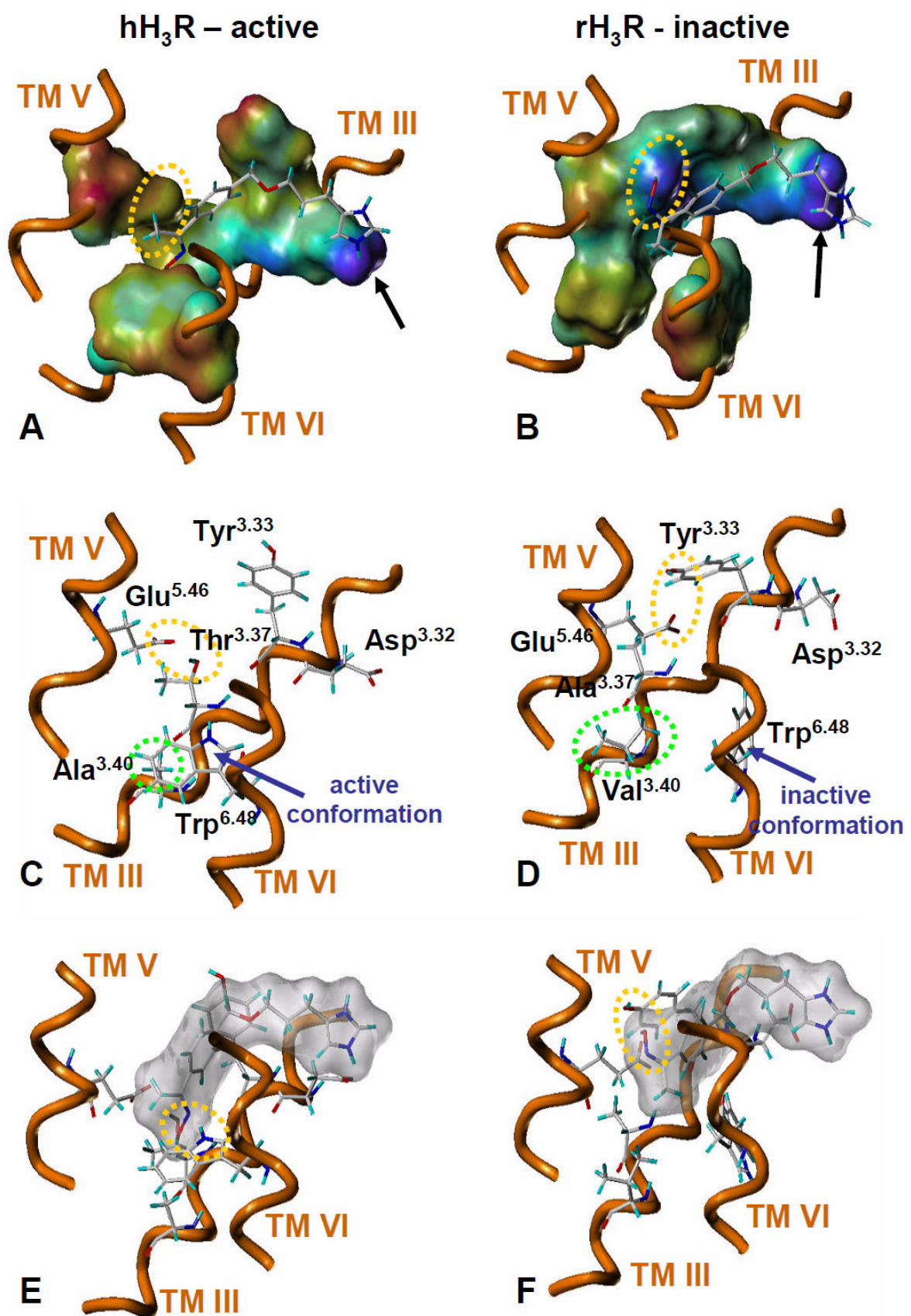


Fig. 3.9. Binding mode of imoproxifan at the active hH₃R and inactive rH₃R.

A, electrostatic potential surface in the binding pocket of active hH₃R with imoproxifan in its binding conformation. **B**, electrostatic potential surface in the binding pocket of the inactive rH₃R with imoproxifan in its binding conformation. **A** and **B**, yellow dotted circle: the electrostatic potential is rather neutral at hH₃R, but negatively charged at rH₃R. The consequence is a different orientation of the ligands oxime moiety. **C**, conformation of amino acids in the imoproxifan bound state of active hH₃R. **D**, conformation of amino acids in the imoproxifan bound state of inactive rH₃R. **C** and **D**, yellow dotted circle: important differences in side chain conformation of Glu^{5.46} between hH₃R and rH₃R. At hH₃R, Glu^{5.46} interacts with Thr^{3.37} and points away from the binding pocket. At rH₃R, Thr^{3.37} is exchanged to Ala^{3.37}. Thus, the interaction between Glu^{5.46} and the amino acid in position 3.37 is no longer possible and Glu^{5.46} interacts with Tyr^{3.33}. Green dotted circle: in position 3.40, there is a small Ala at hH₃R, but the more bulky Val at rH₃R. It is suggested that this species difference is also be important for the different orientations of the oxime moiety between hH₃R and rH₃R. **E**, interaction between imoproxifan and hH₃R; **F**, interaction between imoproxifan and rH₃R. **E** and **F**, yellow dotted circle: at hH₃R, the oxime moiety of imoproxifan points downwards and stabilizes the highly conserved Trp^{6.48} by a hydrogen bond; at rH₃R, the oxime moiety of imoproxifan points upwards interacts electrostatically with a negatively charged surface established by Glu^{5.46} and Tyr^{3.33}.

A second species-difference between hH₃R and rH₃R near to the binding pocket is located at position 3.40. There is an alanine at hH₃R, but a bulkier valine at rH₃R (Fig. 3.9, C and D, green, dotted line). It is likely that this amino acid difference also directs the oxime moiety of imoproxifan into a distinct orientation. Since Ala^{3.40} is not as bulky as Val^{3.40}, there is more space for the oxime moiety to point downward in direction to 3.40 at hH₃R, than at rH₃R.

Additionally, Trp^{6.48} is shown in its active conformation at hH₃R (Fig. 3.9, C, blue arrow) and in its inactive conformation at rH₃R (Fig. 3.9, D, blue arrow). Trp^{6.48} is part of a highly conserved motif among GPCRs, thought to function as a toggle-switch during receptor activation, as is evident due to structural and biophysical studies (Ahuja and Smith, 2009). Trp^{6.48} horizontal to the membrane surface stabilizes the active state of a GPCR. Trp^{6.48} vertical to the membrane surface stabilizes the inactive state of a GPCR. As consequence of the different amino acids at position 3.37 and 3.40 between hH₃R and rH₃R, the oxime moiety of imoproxifan can establish a hydrogen bond interaction to Trp^{6.48} in its active conformation, thus stabilizing the active conformation of hH₃R (Fig. 3.9, E, yellow, dotted line). This interaction was not found at rH₃R. Here, the hydrogen of the oxime moiety interacts electrostatically with a negatively charged surface established by Glu^{5.46} and Tyr^{3.33} (Fig. 3.9, F, yellow, dotted line). At rH₃R, the methyl group of imoproxifan is located in a small pocket established by Val^{3.40} and Trp^{6.48} in its inactive conformation.

Collectively, the different binding modes of imoproxifan at hH₃R and rH₃R presumably lead to differences in efficacies due to a different orientation of the oxime moiety and thus, stabilization of Trp^{6.48} either horizontal or vertical to the membrane surface.

3.5 Discussion

Ligand pharmacology at hH₃R and rH₃R is species-dependent. Unexpectedly, the species-differences can even span from agonism to inverse agonism in the case of imoproxifan. In this study, we unraveled the underlying molecular mechanism of this reversal in efficacy. In steady-state GTPase assays, imoproxifan was an inverse agonist at rH₃R, but almost full agonist at hH₃R. Competition binding studies with [³H]NAMH confirmed that the effect was receptor-mediated. Both hH₃R and rH₃R were expressed at similar levels and defined receptor-to-G protein stoichiometries. The basal activity in the two systems was comparable, as indicated by the similar inhibitory effects of the standard inverse agonist thioperamide. Thus, the unexpected behaviour of imoproxifan can only be due to species-specific differences in ligand recognition and receptor activation. Previous modelling studies described the binding mode of FUB181, a compound, similar to imoproxifan (Schlegel et al., 2007). The orientation of imoproxifan in the binding pocket of H₃R, determined in the present study, is similar to these previous findings. In another study, it was suggested, that the Ala^{3.40}Val amino acid difference between hH₃R and rH₃R is responsible for the observed species-differences in antagonist pharmacology (Yao et al., 2003). It was pointed out that thioperamide or compound A-304121 are in closer contact to Val^{3.40} at rH₃R, than to Ala^{3.40} at hH₃R. We could reproduce this finding because the affinity and potency of thioperamide was higher at rH₃R than hH₃R in our experimental system, too. Our molecular modelling studies further revealed that both amino acid differences in TM III, at position 3.37 and 3.40, are responsible for the differences in pharmacology of imoproxifan between hH₃R and rH₃R. Because of the lacking negative surface potential between TM V and TM III, the oxime moiety points downward in direction of Ala^{3.40} at hH₃R. Thus, the polar oxime moiety is able to establish a hydrogen bond interaction to Trp^{6.48} in its active conformation. In contrast, at rH₃R, the negatively charged surface of the binding pocket between TM V and TM III allows the oxime moiety to point upward. Additionally, the methyl moiety of imoproxifan fits optimally into a small pocket between the bulky Val^{3.40} and Trp^{6.48} in its inactive conformation. The highly conserved Trp^{6.48} is suggested to act as a switch for receptor activation within biogenic amine receptors. Trp^{6.48} horizontal to the membrane surface is thought to stabilize the active state of a receptor, while Trp^{6.48} vertical to the membrane surface stabilizes the inactive state of a receptor. Since the hydrogen bond interaction between the oxime moiety and Trp^{6.48} stabilizes Trp^{6.48} in its active conformation at hH₃R, the partial agonism of imoproxifan is explained on a molecular level. This hydrogen bond-supported stabilization of Trp^{6.48} in its active conformation is not possible at rH₃R. Here, in contrast to hH₃R, the methyl group near Val^{3.40} and Trp^{6.48} stabilizes Trp^{6.48} in its inactive conformation due to a hydrophobic

interaction. Thus, the modelling studies provide an explanation for the inverse agonism of imoproxifan at rH₃R on a molecular level, too.

Interestingly, the pK_i values imoproxifan (**7**) at hH₃R and rH₃R were significantly higher than their pEC_{50} values (t test, $p < 0.05$). These results suggest that hH₃R and rH₃R can exist in a state of low partial agonist/inverse agonist affinity that interacts efficiently with G proteins. Another study, analyzing the hH₃R expressed in SK-N-MC cells by [³H]NAMH competition binding and CRE- β -galactosidase reporter gene assays, revealed similar disparities (Lim et al., 2005). Similar results were also obtained when the human formyl peptide receptor, coupled to various G_i-proteins, was studied in Sf9 cell membranes (Wenzel-Seifert et al., 1999). In this study, the K_d of the agonist radioligand [³H]fMLP is ~100-fold lower than the EC_{50} determined in GTPase experiments. Interestingly, at hH₃R expressed in Sf9 cells the low affinity state stabilized by imoproxifan (**7**) leads to an activation of G proteins, whereas at rH₃R the low affinity state inhibits the activation of G proteins.

The G protein coupling profile hH₃R and rH₃R was similar, too (Table 3.2; Schnell et al., 2009). An important fact is that like for hH₃R (Schnell et al., 2009), at rH₃R no evidence for functional selectivity was observed (Table 3.3). Both hH₃R and rH₃R coupled effectively with G_i/G_o-proteins in Sf9 cell membranes, as was shown by GTP γ S-sensitive ternary complex formation, using [³H]NAMH as radioligand, and steady-state [γ -³²P]GTP hydrolysis. The similarly small shifts of the [³H]NAMH saturation binding curves at hH₃R and rH₃R by GTP γ S indicate a similarly strong interaction of both receptors with the G protein and are in line with the high constitutive activity of the H₃Rs. Thus, the results confirm the data of the GTPase experiments. Similar constitutive activity renders the system well suited for the analysis of species-specific ligand effects, since differences in constitutive activity between GPCRs can alter their pharmacological profiles and lead to a further complication of data interpretation (Preuss et al., 2007a, b).

The pharmacology of all histamine receptors (H_xRs) is species-dependent. This is especially true for H_xR agonists. At the H₁R, several classes of bulky ligands exhibit species differences (Seifert et al., 2003). Some of them show unique behaviours, like epimeric members of the ergoline family or chiral histaprodifens, switching from silent antagonism to partial agonism depending on the species studied (Pertz et al., 2006; Strasser et al., 2008a). Detailed molecular studies dissected some of the underlying mechanisms (Strasser et al., 2008b; Strasser et al., 2009). At the H₂R, bulky agonists like the long-chained impromidine- and arpromidine-derived guanidines or *N*⁶-acylated imidazolypropylguanidines (AIPGs), are more potent and efficacious at the gpH₂R than at the hH₂R (Kelley et al., 2001; Preuss et al., 2007b). Metiamide was identified to be an inverse agonist at the hH₂R, gpH₂R and rH₂R, but a weak partial agonist at the cH₂R (Preuss et al., 2007a). At the H₄R, which has the lowest sequence similarity between species, studies focusing on ligand-receptor interactions of

agonists are beginning to emerge (Lim et al., 2008; Igel et al., 2009). However, the species-differences of imoproxifan at hH₃R and rH₃R described in this study represent the most substantial differences in pharmacology among H_xRs identified so far. This is particularly compelling in view of the fact that hH₃R and rH₃R sequences display a high degree of homology and only two amino acid residues cause the disparities.

In conclusion, we have shown that hH₃R and rH₃R expressed in Sf9 cells both similarly couple to defined G_i/G_o-protein heterotrimers and display similar constitutive activities. We show species-differences in pharmacological properties of imoproxifan and offer an explanation on the molecular basis for these differences. Most importantly, we introduce novel active state models of hH₃R and rH₃R that are suitable to explain the efficacy of H₃R ligands.

3.6 References

- Ahuja S and Smith SO (2009) Multiple switches in G protein-coupled receptor activation. *Trends Pharmacol Sci* **30**:494-502.
- Arrang JM, Morisset S and Gbahou F (2007) Constitutive activity of the histamine H₃ receptor. *Trends Pharmacol Sci* **28**:350-357.
- Ballesteros JH and Weinstein H (1995) Integrated methods for the construction of three dimensional models and computational probing of structure-function relations in G-protein coupled receptors. *Methods Neurosci* **25**:366-428.
- Bongers G, Bakker RA and Leurs R (2007a) Molecular aspects of the histamine H₃ receptor. *Biochem Pharmacol* **73**:1195-1204.
- Bongers G, Krueger KM, Miller TR, Baranowski JL, Estvander BR, Witte DG, Strakhova MI, van Meer P, Bakker RA, Cowart MD, Hancock AA, Esbenshade TA and Leurs R (2007b) An 80-amino acid deletion in the third intracellular loop of a naturally occurring human histamine H₃ isoform confers pharmacological differences and constitutive activity. *J Pharmacol Exp Ther* **323**:888-898.
- Cherezov V, Rosenbaum DM, Hanson MA, Rasmussen SG, Thian FS, Kobilka TS, Choi HJ, Kuhn P, Weis WI, Kobilka BK and Stevens RC (2007) High-resolution crystal structure of an engineered human β_2 -adrenergic G protein-coupled receptor. *Science* **318**:1258-1265.
- Hancock AA, Esbenshade TA, Krueger KM and Yao BB (2003) Genetic and pharmacological aspects of histamine H₃ receptor heterogeneity. *Life Sci* **73**:3043-3072.
- Hill SJ, Ganellin CR, Timmerman H, Schwartz JC, Shankley NP, Young JM, Schunack W, Levi R and Haas HL (1997) International Union of Pharmacology. XIII. Classification of histamine receptors. *Pharmacol Rev* **49**:253-278.
- Igel P, Geyer R, Strasser A, Dove S, Seifert R and Buschauer A (2009) Synthesis and structure-activity relationships of cyanoguanidine-type and structurally related histamine H₄ receptor agonists. *J Med Chem* **52**:6297-6313.
- Ireland-Denny L, Parihar AS, Miller TR, Kang CH, Krueger KM, Esbenshade TA and Hancock AA (2001) Species-related pharmacological heterogeneity of histamine H₃ receptors. *Eur J Pharmacol* **433**:141-150.
- Jaakola VP, Griffith MT, Hanson MA, Cherezov V, Chien EY, Lane JR, Ijzerman AP and Stevens RC (2008) The 2.6 Å crystal structure of a human A_{2A} adenosine receptor bound to an antagonist. *Science* **322**:1211-1217.
- Kelley MT, Bürckstümmer T, Wenzel-Seifert K, Dove S, Buschauer A and Seifert R (2001) Distinct interaction of human and guinea pig histamine H₂-receptor with guanidine-type agonists. *Mol Pharmacol* **60**:1210-1225.
- Kobilka B and Schertler GF (2008) New G-protein-coupled receptor crystal structures: insights and limitations. *Trends Pharmacol Sci* **29**:79-83.
- Leurs R, Bakker RA, Timmerman H and de Esch IJ (2005) The histamine H₃ receptor: from gene cloning to H₃ receptor drugs. *Nat Rev Drug Discov* **4**:107-120.

- Leurs R, Chazot PL, Shenton FC, Lim HD and de Esch IJ (2009) Molecular and biochemical pharmacology of the histamine H₄ receptor. *Br J Pharmacol* **157**:14-23.
- Ligneau X, Morisset S, Tardivel-Lacombe J, Gbahou F, Ganellin CR, Stark H, Schunack W, Schwartz JC and Arrang JM (2000) Distinct pharmacology of rat and human histamine H₃ receptors: role of two amino acids in the third transmembrane domain. *Br J Pharmacol* **131**:1247-1250.
- Lim HD, Jongejan A, Bakker RA, Haaksma E, de Esch IJ and Leurs R (2008) Phenylalanine 169 in the second extracellular loop of the human histamine H₄ receptor is responsible for the difference in agonist binding between human and mouse H₄ receptors. *J Pharmacol Exp Ther* **327**:88-96.
- Lim HD, van Rijn RM, Ling P, Bakker RA, Thurmond RL and Leurs R (2005) Evaluation of histamine H₁-, H₂-, and H₃-receptor ligands at the human histamine H₄ receptor: identification of 4-methylhistamine as the first potent and selective H₄ receptor agonist. *J Pharmacol Exp Ther* **314**:1310-1321.
- Morisset S, Rouleau A, Ligneau X, Gbahou F, Tardivel-Lacombe J, Stark H, Schunack W, Ganellin CR, Schwartz JC and Arrang JM (2000) High constitutive activity of native H₃ receptors regulates histamine neurons in brain. *Nature* **408**:860-864.
- Park JH, Scheerer P, Hofmann KP, Choe HW and Ernst OP (2008) Crystal structure of the ligand-free G-protein-coupled receptor opsin. *Nature* **454**:183-187.
- Pertz HH, Gornemann T, Schurad B, Seifert R and Strasser A (2006) Striking differences of action of lisuride stereoisomers at histamine H₁ receptors. *Naunyn Schmiedeberg's Arch Pharmacol* **374**:215-222.
- Preuss H, Ghorai P, Kraus A, Dove S, Buschauer A and Seifert R (2007a) Constitutive activity and ligand selectivity of human, guinea pig, rat, and canine histamine H₂ receptors. *J Pharmacol Exp Ther* **321**:983-995.
- Preuss H, Ghorai P, Kraus A, Dove S, Buschauer A and Seifert R (2007b) Mutations of Cys-17 and Ala-271 in the human histamine H₂ receptor determine the species selectivity of guanidine-type agonists and increase constitutive activity. *J Pharmacol Exp Ther* **321**:975-982.
- Rasmussen SG, Choi HJ, Rosenbaum DM, Kobilka TS, Thian FS, Edwards PC, Burghammer M, Ratnala VR, Sanishvili R, Fischetti RF, Schertler GF, Weis WI and Kobilka BK (2007) Crystal structure of the human β_2 -adrenergic G-protein-coupled receptor. *Nature* **450**:383-387.
- Sasse A, Sadek B, Ligneau X, Elz S, Pertz HH, Luger P, Ganellin CR, Arrang JM, Schwartz JC, Schunack W and Stark H (2000) New histamine H₃-receptor ligands of the proxifan series: imoproxifan and other selective antagonists with high oral *in vivo* potency. *J Med Chem* **43**:3335-3343.
- Schlegel B, Laggner C, Meier R, Langer T, Schnell D, Seifert R, Stark H, Holtje HD and Sippl W (2007) Generation of a homology model of the human histamine H₃-receptor for ligand docking and pharmacophore-based screening. *J Comput Aided Mol Des* **21**:437-453.
- Schneider EH, Schnell D, Papa D and Seifert R (2009) High constitutive activity and a G-protein-independent high-affinity state of the human histamine H₄-receptor. *Biochemistry* **48**:1424-1438.

- Schnell D, Burleigh K, Trick J and Seifert R (2009) No evidence for functional selectivity of proxyfan at the human histamine H₃-receptor coupled to defined G_i/G_o protein heterotrimers. *J Pharmacol Exp Ther* (in press).
- Seifert R, Wenzel-Seifert K, Bürckstümmer T, Pertz HH, Schunack W, Dove S, Buschauer A and Elz S (2003) Multiple differences in agonist and antagonist pharmacology between human and guinea pig histamine H₁-receptor. *J Pharmacol Exp Ther* **305**:1104-1115.
- Strasser A, Striegl B, Wittmann HJ and Seifert R (2008a) Pharmacological profile of histaprodifens at four recombinant histamine H₁-receptor species isoforms. *J Pharmacol Exp Ther* **324**:60-71.
- Strasser A and Wittmann HJ (2007) Analysis of the activation mechanism of the guinea-pig Histamine H₁-receptor. *J Comput Aided Mol Des* **21**:499-509.
- Strasser A, Wittmann HJ, Kunze M, Elz S and Seifert R (2009) Molecular basis for the selective interaction of synthetic agonists with the human histamine H₁-receptor compared with the guinea pig H₁-receptor. *Mol Pharmacol* **75**:454-465.
- Strasser A, Wittmann HJ and Seifert R (2008b) Ligand-specific contribution of the N terminus and E2-loop to pharmacological properties of the histamine H₁-receptor. *J Pharmacol Exp Ther* **326**:783-791.
- Tiligada E, Zampeli E, Sander K and Stark H (2009) Histamine H₃ and H₄ receptors as novel drug targets. *Expert Opin Investig Drugs* **18**:1519-1531.
- Uveges AJ, Kowal D, Zhang J, Spangler TB, Dunlop J, Semus S and Jones PG (2002) The role of transmembrane helix 5 in agonist binding to the human histamine H₃ receptor. *J Pharmacol Exp Ther* **301**:451-458.
- van der Spoel D, Lindahl E, Hess B, van Buuren AR, Apol E, Meulenhoff PF, Tieleman DP, Sijbers ALTM, Feenstra KA, van Drunen R and Berendsen HJC (2004) Department of Biophysical Chemistry, University of Groningen, The Netherlands, in.
- Wenzel-Seifert K, Arthur JM, Liu HY and Seifert R (1999) Quantitative analysis of formyl peptide receptor coupling to G α_{i1} , G α_{i2} , and G α_{i3} . *J Biol Chem* **274**:33259-33266.
- Wulff BS, Hastrup S and Rimvall K (2002) Characteristics of recombinantly expressed rat and human histamine H₃ receptors. *Eur J Pharmacol* **453**:33-41.
- Yao BB, Hutchins CW, Carr TL, Cassar S, Masters JN, Bennani YL, Esbenshade TA and Hancock AA (2003) Molecular modeling and pharmacological analysis of species-related histamine H₃ receptor heterogeneity. *Neuropharmacology* **44**:773-786.
- Zampeli E and Tiligada E (2009) The role of histamine H₄ receptor in immune and inflammatory disorders. *Br J Pharmacol* **157**:24-33.

Chapter 4

Modulation of histamine H₃-receptor function by monovalent ions

This chapter is adapted from:

Schnell D and Seifert R (2009) Modulation of histamine H₃-receptor function by monovalent ions. *Neurosci Lett* (submitted).

4.1 Abstract

Monovalent ions differently affect ligand binding to G protein-coupled receptors (GPCRs) by as yet poorly defined mechanisms. In particular, NaCl often decreases the affinity of agonists but increases it for antagonists. We examined the effect of various monovalent ions on human histamine H₃ receptor (hH₃R), co-expressed with mammalian G proteins (G α_{i1} , G α_{i2} , G α_{i3} or G α_{o1} , and $\beta_1\gamma_2$ dimers, respectively) in Sf9 insect cell membranes, with respect to agonist binding and G protein activation. NaCl (100 mM) had no effect on affinity of the agonist [³H]*N*^L-methylhistamine ([³H]NAMH). In steady-state GTPase assays, the endogenous agonist histamine had a lower potency and the inverse agonist thioperamide had a higher potency, when NaCl (100 mM) was present. Monovalent ions reduced H₃R-regulated signalling in the order of efficacy Li⁺ ~ Na⁺ ~ K⁺ < Cl⁻ < Br⁻ < I⁻. NaCl had a stronger effect on basal hH₃R signalling when G α_{i3} was co-expressed. Asp80^{2.50}, a putative interaction site for Na⁺, was mutated to Asn80^{2.50} (D2.50N-hH₃R). Strikingly, the mutation was unable to activate G α_{i3} at all. The effects can be explained by a model, where (i) monovalent ions as well as a charge-neutralizing mutation of Asp80^{2.50} generally reduce the interaction of hH₃R with G proteins, (ii) monovalent anions increase the affinity of G proteins for GDP and thus, indirectly affect their interaction with hH₃R and, (iii) Asp80^{2.50} is a key residue for hH₃R/G α_{i3} protein-activation. The latter result suggests that hH₃R/G protein-coupling interfaces may differ even between closely related subunits.

4.2 Introduction

Histamine (HA) is an important local mediator and neurotransmitter (Haas et al., 2008). All four histamine receptor subtypes (H₁₋₄Rs) are expressed on neuronal cells. The histamine H₃ receptor (H₃R) is a G_i/G_o-coupled presynaptic auto- and heteroreceptor, regulating the release of histamine and various other neurotransmitters via negative feedback mechanisms. The H₃R is a promising drug target, because it participates in important physiological processes like the sleep-wake cycle, eating behaviour and cognition (Leurs et al., 2005). The H₃R displays ligand-independent activity in many experimental systems (Arrang et al., 2007). It is also one of the few GPCRs for which constitutive activity has been demonstrated *in vivo* (Morisset et al., 2000). The concept of constitutive GPCR activity can be described by a two-state model, assuming that GPCRs isomerize between an inactive state (R) and an active state (R*), with agonists stabilizing the R* state and inverse agonists stabilizing the R state (Seifert and Wenzel-Seifert, 2002; 2003).

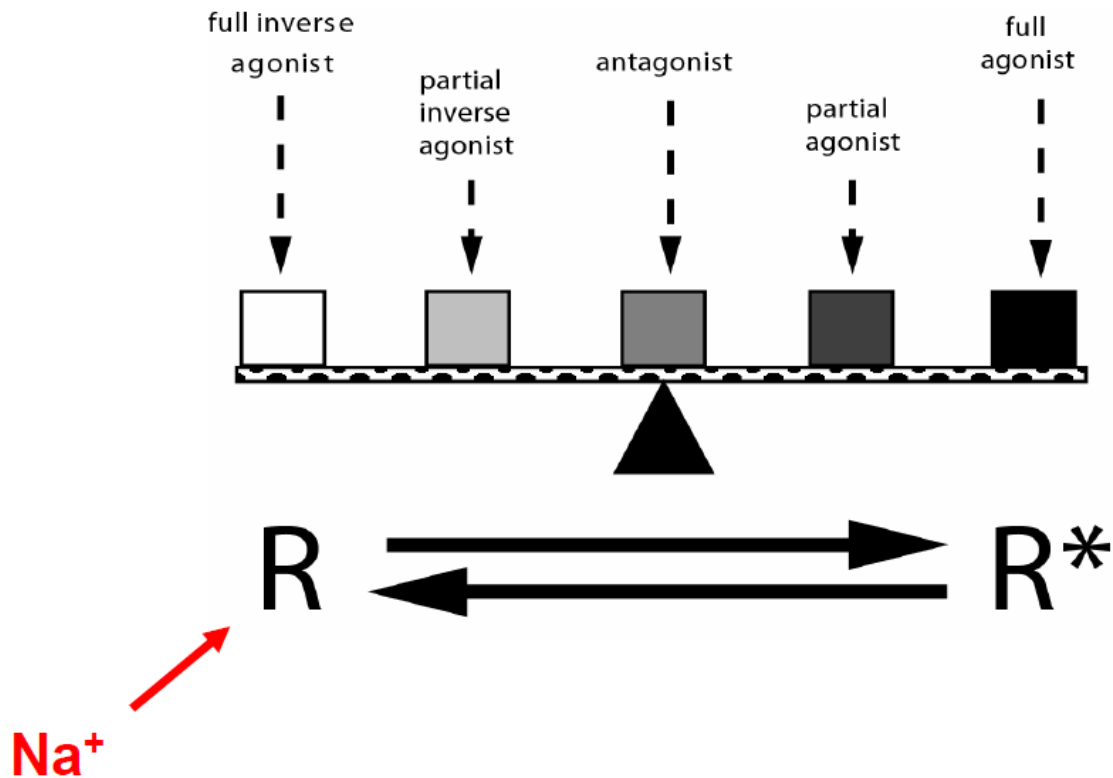


Fig. 4.1. The two state model of GPCR activation. GPCRs are able to isomerize from an inactive state (R) to an active state (R*). Ligands are classified according to their capability of shifting the equilibrium to either side of both states. Na⁺ - ions act as universal allosteric modulators at many GPCRs, stabilizing the inactive state (R).

Na⁺ - ions act as allosteric stabilizers of the R state of many GPCRs (Seifert and Wenzel-Seifert, 2001; 2003) (Fig. 4.1). Recently, we have shown that the hH₃R displays high constitutive activity when expressed in Sf9 insect cells (Schnell et al., 2009), like the structurally related hH₄R (Schneider et al., 2009). This basal receptor activity can be suppressed by increasing NaCl concentrations. However, it is not clear if this effect is mediated by the cation or anion. Additionally, it is not clear if monovalent ions bind to the receptor or the coupling G protein. In this study, we investigated the effect of different monovalent ions on hH₃R coupled to G_i/G_o proteins. Moreover, we mutated Asp80^{2.50}, a highly conserved amino acid among GPCRs, thought to be a binding site for Na⁺ - ions (Horstman et al., 1990) (Fig. 4.2).

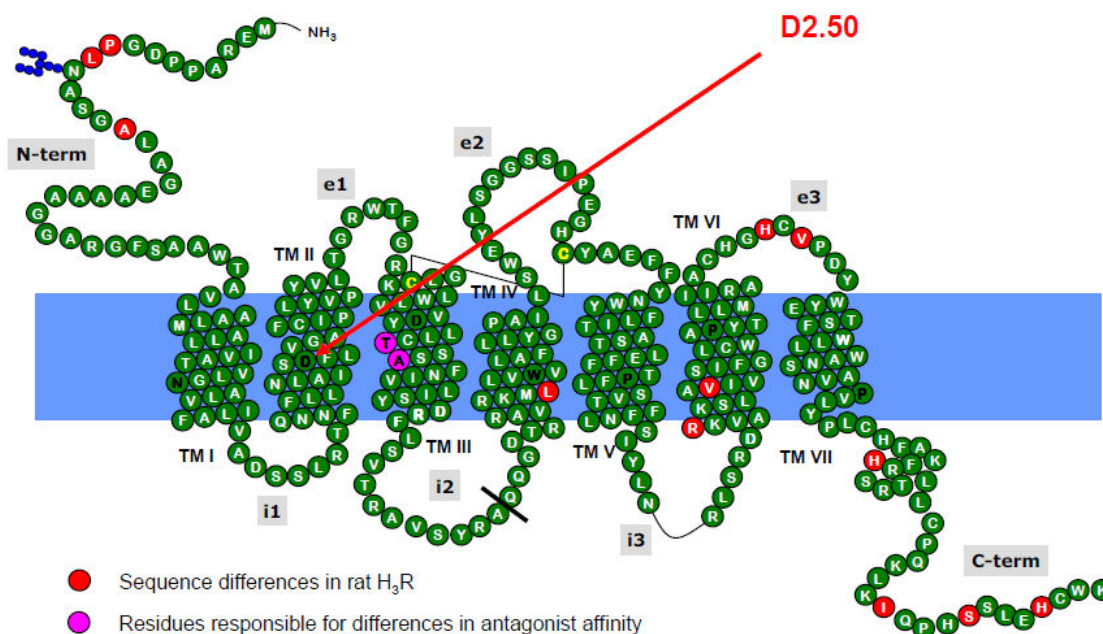


Fig. 4.2. Snake representation of the human H₃R. The red arrow points towards the highly conserved Asp80^{2.50}, which was mutated to Asn80^{2.50}. Residues within TM domains are named according to the Ballesteros/Weinstein nomenclature. The most conserved residue in each TM is numbered as X.50, where X is the number of the respective TM domain (Ballesteros and Weinstein, 1995).

4.3 Materials and Methods

The cDNA of the hH₃R was kindly provided by Dr. T. Lovenberg (Johnson & Johnson Pharmaceutical R&D, San Diego, CA, USA). Reagents for molecular biology, recombinant baculoviruses encoding mammalian G protein subunits, and the sources of ligands were described before (Schnell et al., 2009). *Pfu* Ultra II Fusion HS DNA polymerase was obtained from Stratagene (La Jolla, CA, USA). Stock solutions (10 mM) of all H₃R ligands described in this paper were prepared in distilled water and stored at -20°C. [³H]NAMH (74-85 Ci/mmol) was obtained from Perkin Elmer (Boston, MA, USA). [γ -³²P]GTP was synthesized as described (Schnell et al., 2009). Unlabeled nucleotides were from Roche (Indianapolis, IN, USA) and inorganic salts as well as all other reagents were of the highest purity available and from standard suppliers.

The cDNA for the mutated construct was generated using the QuickChange Site-Directed Mutagenesis Kit (Stratagene), with pVL1392-3Z-SF-hH₃R-His₆ as template (Schnell et al., 2009). As primers, D2.50N-fwd (5'-CTG CTC AAC CTC GCC ATC TCC AAC TTC CTC GTC GGA GCC TTC TGC-3') and D2.50N-rev (5'-GCA GAA GGC TCC GAC GAG GAA GTT GGA GAT GGC GAG GTTG AGC AG-3') were used, including a *codon introducing the mutation* and a silent mutation for a diagnostic restriction site (*Mme* I). The

product was verified by restriction digestion and sequencing. The procedures for the generation of recombinant baculoviruses, Sf9 insect cell culture and membrane preparation, SDS-PAGE and immunoblot analysis were described before (Schnell et al., 2009).

Essentially, [³H]NAMH binding experiments were performed as described in (Schnell et al., 2009). Each reaction tube contained 40 µg of protein. Non-specific binding was determined in the presence of [³H]NAMH at various concentrations plus 10 µM thioperamide and amounted to <10% of total binding at saturating concentrations. Incubations were conducted for 60 min at RT and shaking at 250 rpm. Experiments were carried out using 0.3 to 5 (10) nM final [³H]NAMH. Bound [³H]NAMH was separated from free [³H]NAMH by filtration through 0.3% (m/v) polyethyleneimine-pretreated GF/C filters, followed by three washes with 2 ml of binding buffer (4°C). Filter-bound radioactivity was determined by liquid scintillation counting. The experimental conditions chosen ensured that not more than 10 % of the total amount of radioactivity added to binding tubes was bound to filters.

Steady-state GTPase activity experiments were also performed in analogy to the assays described in (Schnell et al., 2009). Briefly, assay tubes contained Sf9 membranes (20 µg of protein/tube), 5.0 mM MgCl₂, 0.1 mM EDTA, 0.1 mM ATP, 100 nM GTP, 0.1 mM adenylyl imidodiphosphate, 1.2 mM creatine phosphate, 1 µg of creatine kinase, and 0.2% (w/v) bovine serum albumin in 50 mM Tris/HCl, pH 7.4, and H₃R ligands at various concentrations. Reaction mixtures (80 µl) were incubated for 2 min at 25°C before the addition of 20 µl of [γ -³²P]GTP (0.1 µCi/tube). All stock and work dilutions of [γ -³²P]GTP were prepared in 20 mM Tris/HCl, pH 7.4. Reactions were conducted for 20 min at 25°C. Reactions were terminated by the addition of 900 µl of slurry consisting of 5% (m/v) activated charcoal and 50 mM NaH₂PO₄, pH 2.0. Charcoal absorbs nucleotides but not P_i. Charcoal-quenched reaction mixtures were centrifuged for 7 min at room temperature at 15,000g. Six hundred microliters of the supernatant fluid of reaction mixtures were removed, and ³²P_i was determined by liquid scintillation counting. Enzyme activities were corrected for spontaneous degradation of [γ -³²P]GTP. Spontaneous [γ -³²P]GTP degradation was determined in tubes containing all of the above described components plus a very high concentration of unlabeled GTP (1 mM) that, by competition with [γ -³²P]GTP, prevents [γ -³²P]GTP hydrolysis by enzymatic activities present in Sf9 membranes. Spontaneous [γ -³²P]GTP degradation was <1% of the total amount of radioactivity added using 20 mM Tris/HCl, pH 7.4, as solvent for [γ -³²P]GTP. The experimental conditions chosen ensured that not more than 10% of the total amount of [γ -³²P]GTP added was converted to ³²P_i.

Molecular biology was planned with GCK 2.5 (Textco BioSoftware, West Lebanon, NH, USA), protein was determined using the DC protein assay kit (Bio-Rad, Hercules, CA, USA) and all analyses of experimental data were performed with the Prism 5 program (GraphPad Software, San Diego, CA, USA).

4.4 Results

We determined binding parameters of the agonist radioligand [³H]NAMH in Sf9 cell membranes co-expressing hH₃R, G α_{i2} and $\beta_1\gamma_2$ dimers in parallel in the absence and presence of NaCl (100 mM) (Fig. 4.3A). Unexpectedly, NaCl did not affect the affinity of [³H]NAMH at hH₃R, but increased the number of binding sites. In the absence of NaCl, the K_d -value was 0.60 ± 0.07 nM (S. E. M., $n = 3$) and the B_{max} -value was 0.62 ± 0.02 pmol/mg (S. E. M., $n = 3$). In the presence of NaCl (100 mM), [³H]NAMH bound to the hH₃R with a K_d of 0.74 ± 0.06 nM (S. E. M., $n = 3$) and a B_{max} of 0.85 ± 0.02 pmol/mg (S. E. M., $n = 3$). This is surprising, because classically NaCl decreases the affinity of agonists at GPCRs (Limbird et al., 1982; Neve et al., 1990).

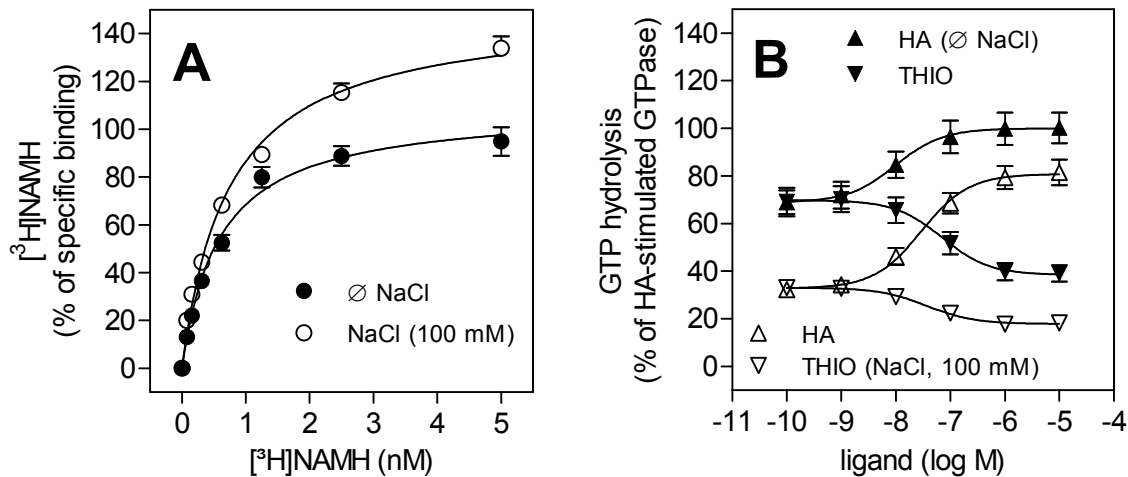


Fig. 4.3. The effect of NaCl on high-affinity agonist binding and steady-state GTP hydrolysis in Sf9 cell membranes expressing hH₃R in combination with G α_{i2} and $\beta_1\gamma_2$. Experiments were performed as described under *Materials and Methods*. In **A**, reaction tubes contained membranes and [³H]NAMH in concentrations indicated on the abscissa. Nonspecific binding was determined in the presence of THIO (10 μ M). Data were analyzed by nonlinear regression and were best fitted to hyperbolic one-site saturation isotherms. The closed circles (●) show the data for specific [³H]NAMH binding in the absence of NaCl, the open circles (○) in the presence of NaCl (100 mM). Data points shown are the means \pm S. E. M. of 3 independent experiments performed in duplicate. Data are expressed as percentage change of specific [³H]NAMH binding in the presence of NaCl (100 mM) compared to the binding in the absence of NaCl, which was defined to be 100%. In **B**, reaction mixtures contained HA or THIO at the concentrations indicated on the abscissa to achieve saturation. Data were analyzed by nonlinear regression and were best fitted to sigmoidal concentration/response curves. Data are expressed as percentage change in GTPase activity induced by the ligands compared to the GTPase activity stimulated by HA (10 μ M) in the absence of NaCl, which was defined to be 100%. The closed symbols show data in the absence of NaCl, the open symbols data in the presence of NaCl (100 mM). Data points shown are the means \pm S. E. M. of 3 independent experiments performed in duplicate.

However, in steady-state GTPase assays the pEC_{50} -value of the endogenous agonist histamine (HA) (8.01 ± 0.39 , S. E. M., $n = 3$) was decreased to 7.53 ± 0.18 (S. E. M., $n = 3$) in the presence of NaCl (100 mM) (Fig. 4.3B). In contrast, the pEC_{50} of the inverse agonist thioperamide (THIO) (7.15 ± 0.31 , S. E. M., $n = 3$) was increased to 7.43 ± 0.28 (S. E. M., $n = 3$) in the presence of NaCl (100 mM) (Fig. 4.3B), indicating a reduced constitutive activity of the system. This result is in line with a lower basal hH₃R-activity and efficacy of THIO in the presence of NaCl. Additionally, NaCl also enhanced the efficacy of HA at hH₃R. Collectively, these functional data are in accordance with the two-state model of GPCR-activation (Seifert and Wenzel-Seifert, 2002; Seifert and Wenzel-Seifert, 2003). Thus, NaCl stabilizes the R-state of hH₃R. The NaCl-insensitivity of [³H]NAMH-binding could be due to the very high constitutive activity of hH₃R. At the structurally related hH₄R, which shows even higher constitutive activity, NaCl has no effect on basal activity at all (Schneider et al., 2009).

Still, at the hH₃R, it was not clear whether Na⁺ or Cl⁻ caused the effect on constitutive activity. Therefore, we examined the effect of different salts of monovalent ions with varying radii on hH₃R-activity in the steady-state GTPase assay (Fig. 4.4). Monovalent ions reduced hH₃R-regulated signalling in the order of efficacy Li⁺ ~ Na⁺ ~ K⁺ < Cl⁻ < Br⁻ < I⁻. Especially, basal hH₃R-signalling was more effectively reduced by salts of monovalent anions with greater radii.

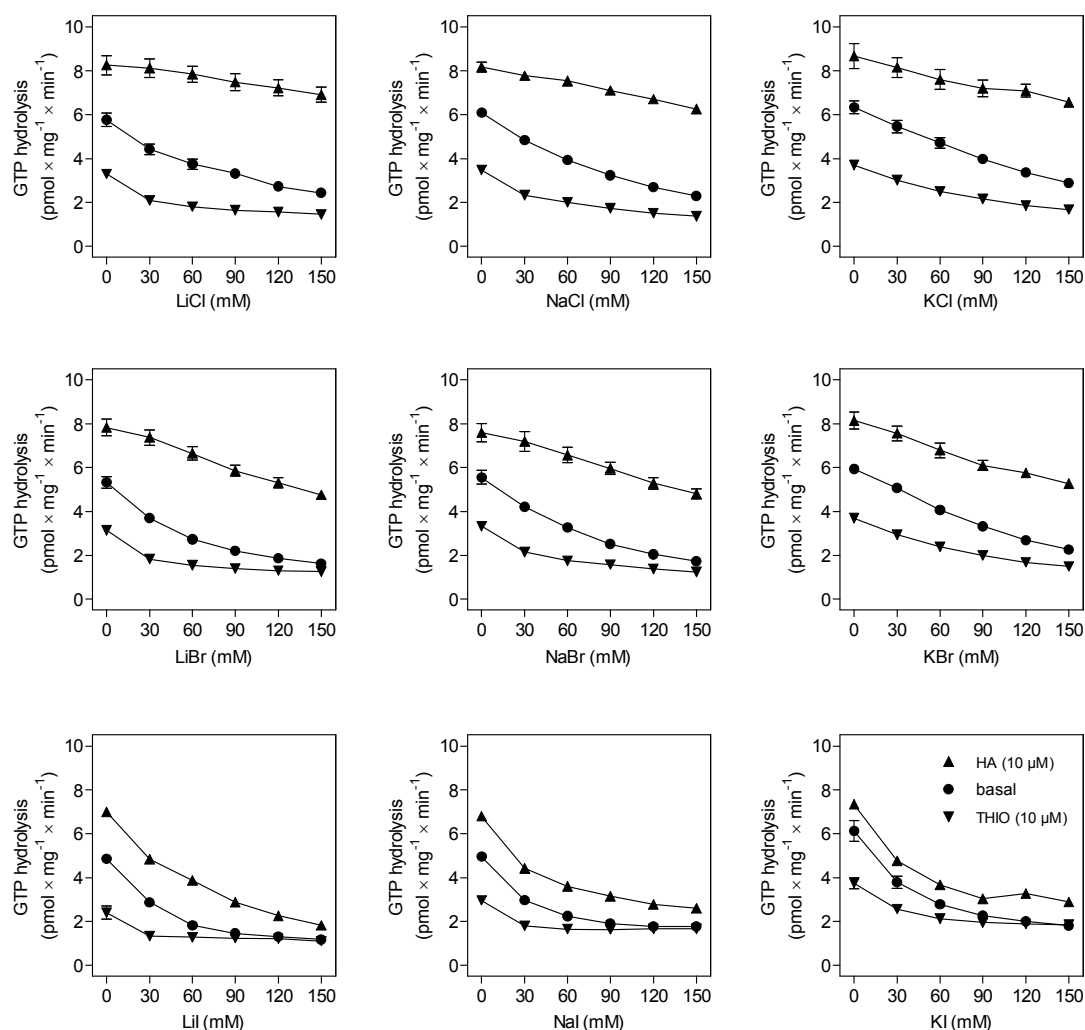


Fig. 4.4. Regulation of HA-, basal and THIO-regulated GTPase activity by different salts of monovalent ions. GTPase experiments were performed as described under *Materials and Methods*. Reaction mixtures contained Sf9 cell membranes expressing hH₃R plus G α_{i2} plus $\beta_1\gamma_2$, HA (10 μ M), ddH₂O (basal) or THIO (10 μ M) and salts in concentrations indicated on the abscissa. Data points shown are the means \pm S. E. M. of 3 – 4 independent experiments performed in duplicate.

To find out which protein is modulated, we also tested the effect of NaCl on hH₃R coupled to different G_i/G_o-proteins. Interestingly, NaCl had a stronger effect on basal hH₃R-signalling when G α_{i3} was co-expressed (Fig. 4.5).

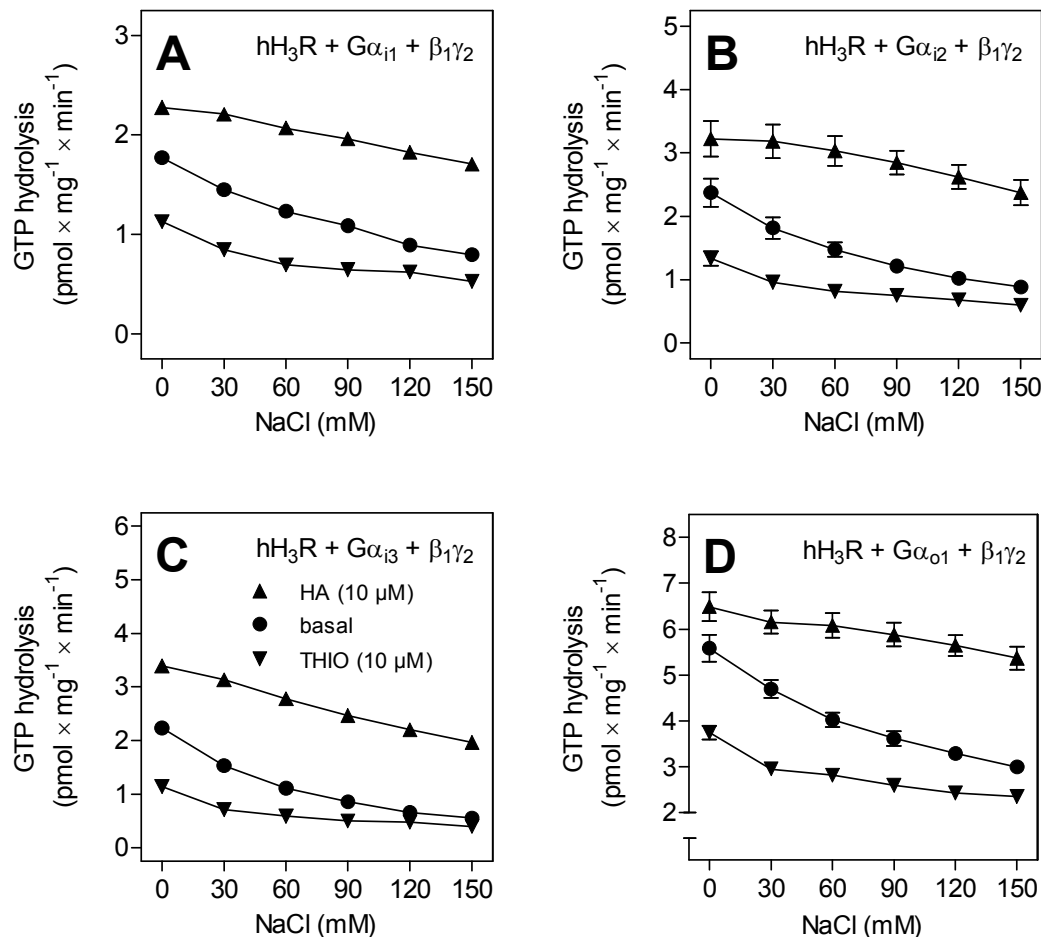


Fig. 4.5. Regulation of HA-, basal and THIO-regulated GTPase activity by NaCl in the presence of different G_i/G_o-proteins. GTPase experiments were performed as described under *Materials and Methods*. Reaction mixtures contained Sf9 cell membranes expressing hH₃R plus mammalian G proteins (G α_{i1} , G α_{i2} , G α_{i3} or G α_{o1} , and $\beta_1\gamma_2$ dimers, respectively), HA (10 μ M), ddH₂O (basal) or THIO (10 μ M) and NaCl in concentrations indicated on the abscissa. Data points shown are the means \pm S. E. M. of 3 independent experiments performed in duplicate.

In addition, we mutated Asp80^{2.50}, a highly conserved amino acid residue among GPCRs thought to act as a binding site for Na⁺ [4] (Horstman et al., 1990), to Asn80^{2.50} (D2.50N-hH₃R). This charge-neutralizing point-mutation decreased the affinity of [³H]NAMH at hH₃R about 10-fold ($K_d = 5.09 \pm 1.11$ nM, S. E. M., $n = 3$) (Fig. 4.6A).

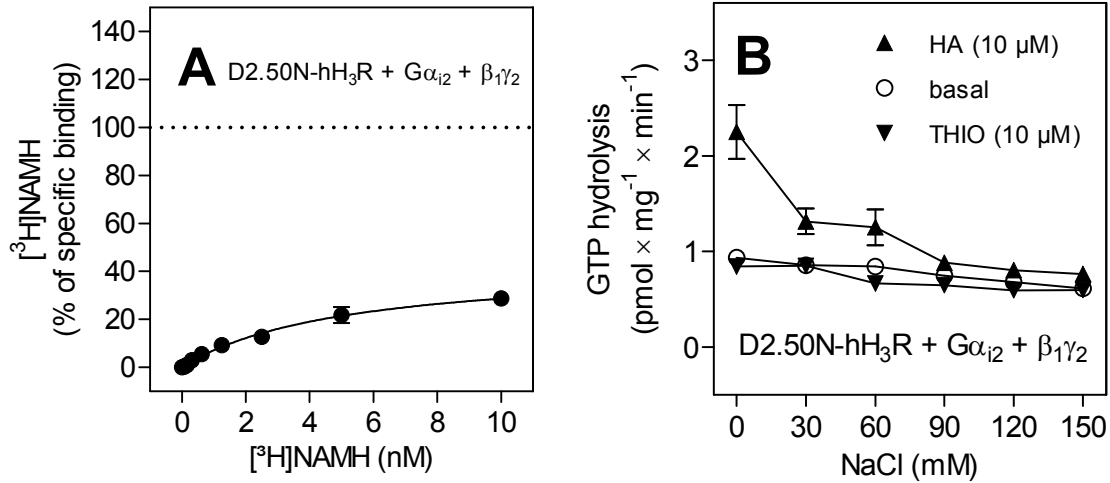


Fig. 4.6. The effect of Asp80^{2.50}→Asn80^{2.50} mutation (D2.50N-hH₃R) on high-affinity agonist binding and steady-state GTP hydrolysis in Sf9 cell membranes expressing the mutant in combination with G α_{i2} and $\beta_1\gamma_2$. Experiments were performed as described under *Materials and Methods*. In **A**, reaction tubes contained membranes and [³H]NAMH in concentrations indicated on the abscissa. Nonspecific binding was determined in the presence of THIO (10 μ M). Data were analyzed by nonlinear regression and were best fitted to a hyperbolic one-site saturation isotherm. Data points shown are the means \pm S. E. M. of 3 independent experiments performed in duplicate. The dotted line indicates the B_{max} value of [³H]NAMH binding at the wild-type hH₃R, co-expressed with G α_{i2} and $\beta_1\gamma_2$, which was defined to be 100%. In **B**, reaction mixtures contained membranes, HA (10 μ M), ddH₂O (basal) or THIO (10 μ M) and NaCl at concentrations indicated on the abscissa. Data points shown are the means \pm S. E. M. of 3 independent experiments performed in duplicate.

The experiments were performed in parallel with wild-type hH₃R in the absence of NaCl (Fig. 4.3A). Compared to the wild-type hH₃R ($B_{\max} = 100\%$, per definition), D2.50N-hH₃R displayed a substantially lower number of binding sites for [³H]NAMH ($B_{\max} = 43.2 \pm 4.6\%$) (Fig. 4.6A). In the steady-state GTPase assay, D2.50N-hH₃R was not constitutively active, as indicated by the absent inhibitory effect of NaCl and the inverse agonist THIO (Fig. 4.6B).

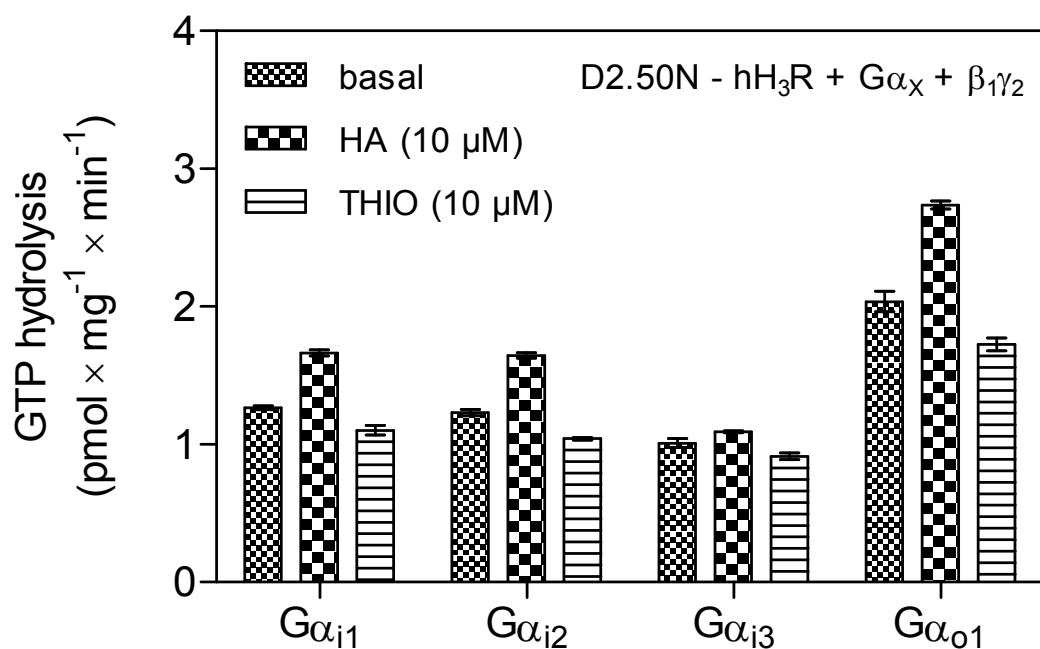


Fig. 4.7. The G-protein coupling profile of D2.50N-hH₃R. Experiments were performed as described under *Materials and Methods*. Reaction mixtures contained membranes co-expressing D2.50N-hH₃R and mammalian G proteins (Gα_{i1}, Gα_{i2}, Gα_{i3} or Gα_{o1}, and β₁γ₂ dimers, respectively), HA (10 μM), ddH₂O (basal) or THIO (10 μM). Data points shown are the means ± S. E. M. of 3 independent experiments performed in duplicate.

However, NaCl had a strong inhibitory effect on HA-regulated GTPase. At concentrations above 90 mM, D2.50N-hH₃R was completely inactive. Most strikingly, the mutation was unable to activate G α_{i3} at all (Fig. 4.7), suggesting a key role of Asp80^{2.50} and Na⁺ in hH₃R/G α_{i3} -interaction.

4.5 Discussion

We systematically studied the effect of NaCl on hH₃R coupled to various G_i/G_o-proteins. Surprisingly, NaCl preferentially abolished constitutive signalling through G α_{i3} . Most interestingly, a charge-neutralizing mutation of Asp80^{2.50}, thought to be an interaction site of Na⁺ - ions (Horstman et al., 1990), rendered hH₃R unable to couple to G α_{i3} at all. First of all, these findings indicate that Asp80^{2.50} is crucial for G α_{i3} -coupling, but not for activation of other G-proteins. Although constitutive signalling of D2.50N-hH₃R was abolished, the mutation was still able to activate the other G-proteins co-expressed. The data also point to a role of Asp80^{2.50} as an interaction site for Na⁺ - ions, since the mutation partially mimicked the effects of high NaCl concentrations with respect to a suppression of constitutive signalling. However, the effects of high NaCl concentrations and mutation of Asp80^{2.50} were not exactly the same and depended on the type of G-protein co-expressed. Additionally, high NaCl concentrations in combination with a charge-neutralizing mutation of Asp80^{2.50} completely abolished the activity of hH₃R in every case, indicating a more complex interaction of ions with hH₃R and/or G_i/G_o-proteins. If only an Asp80^{2.50}/Na⁺-interaction had played a role, the mutation would have been NaCl-insensitive. Thus, there is no definitive evidence of an Asp80^{2.50}/Na⁺-interaction. Nevertheless, the results indicate that the hH₃R/G α_{i3} -protein coupling interface is unique and different compared to the other ones.

It must be noticed that a mutation of Asp80^{2.50} may also substantially influence the expression or proper folding of hH₃R, since it causes a marked reduction of [³H]NAMH binding sites. This could have lead to a general reduction in G-protein interaction. Similar results were obtained, when the α_{2A} -adrenoceptor (α_{2A} AR), another prototypical G_i/G_o-coupled receptor, was mutated at Asp79^{2.50}. It was shown that the point-mutated α_{2A} AR (Asp79^{2.50}→Asn79^{2.50}) could signal through adenylyl cyclase and Ca²⁺-channels, but not K⁺-channels, suggesting a differential G-protein coupling profile of the mutant (Surprenant et al., 1992). Transgenic mice carrying this mutation showed characteristics very similar to α_{2A} AR knock-out mice, because the mutation markedly reduced the expression of the receptor (MacMillan et al., 1998). These mice could not be used to study biased K⁺-channel signalling of α_{2A} AR *in vivo*. A following study using receptor-G α_i fusion proteins then clearly showed that

the mutation leads to a general reduction of GTP turnover and not to G protein selectivity (Ward and Milligan, 1999).

We also systematically tested the effect of different monovalent ions on hH₃R activity. Here, interestingly halides of increasing radii showed more prominent effects on constitutive and agonist-mediated hH₃R activity, suggesting that it is not the cation, but the anion, causing a decrease in hH₃R signalling. Similar effects were shown when the hβ₂AR fused to the long splice-variant of Gα_s (Gα_{sL}) was studied (Seifert, 2001). The effects were explained by a model, where anions increase the affinity of GDP for the G-protein and thereby decrease the efficiency of the agonist-free and agonist-occupied hβ₂AR at promoting GDP dissociation from Gα_{sL}. Similar effects were also observed when the human chemokine receptor CXCR4 was studied in Sf9 cell membranes (Kleemann et al., 2008). In accordance with the model, Cl⁻ anions decrease GDP dissociation from purified Gα_o (Higashijima et al., 1987). By analogy, halides could increase the GDP-affinity of other G_i/G_o-proteins, thereby rendering GDP/GTP-exchange less efficient. Moreover, halides could differentially alter the GDP-affinity of specific G_i/G_o-proteins, which would be an alternative explanation for G-protein specificity found for hH₃R. Additionally, salts could interfere with the ligand binding process.

Collectively, we have shown that salts differently modulate hH₃R G_i/G_o-protein interaction. However, the underlying mechanisms are complex. Regardless of the specific mechanisms involved, from a practical perspective, the substantial impact of monovalent ions on hH₃R-mediated G_i/G_o-protein activation should be considered in future experiments. It is unknown, if there is any *in vivo*-relevance of the regulation of hH₃R G_i/G_o-protein interaction by monovalent anions and cations, but it is possible that (patho)physiological changes in intracellular Na⁺, K⁺ or Cl⁻ concentrations could affect hH₃R-signalling. Li⁺, Br⁻ and I⁻ are of no physiological relevance and constitute only pharmacological tools.

4.6 References

- Arrang JM, Morisset S and Gbahou F (2007) Constitutive activity of the histamine H₃ receptor. *Trends Pharmacol Sci* **28**:350-357.
- Ballesteros JH and Weinstein H (1995) Integrated methods for the construction of three dimensional models and computational probing of structure-function relations in G-protein coupled receptors. *Methods Neurosci* **25**:366-428.
- Haas HL, Sergeeva OA and Selbach O (2008) Histamine in the nervous system. *Physiol Rev* **88**:1183-1241.
- Higashijima T, Ferguson KM and Sternweis PC (1987) Regulation of hormone-sensitive GTP-dependent regulatory proteins by chloride. *J Biol Chem* **262**:3597-3602.
- Horstman DA, Brandon S, Wilson AL, Guyer CA, Cragoe EJ, Jr. and Limbird LE (1990) An aspartate conserved among G-protein receptors confers allosteric regulation of α_2 -adrenergic receptors by sodium. *J Biol Chem* **265**:21590-21595.
- Kleemann P, Papa D, Vigil-Cruz S and Seifert R (2008) Functional reconstitution of the human chemokine receptor CXCR4 with G_i/G_o-proteins in Sf9 insect cells. *Naunyn Schmiedebergs Arch Pharmacol* **378**:261-274.
- Leurs R, Bakker RA, Timmerman H and de Esch IJ (2005) The histamine H₃ receptor: from gene cloning to H₃ receptor drugs. *Nat Rev Drug Discov* **4**:107-120.
- Limbird LE, Speck JL and Smith SK (1982) Sodium ion modulates agonist and antagonist interactions with the human platelet α_2 -adrenergic receptor in membrane and solubilized preparations. *Mol Pharmacol* **21**:609-617.
- MacMillan LB, Lakhani P, Lovinger D and Limbird LE (1998) α_2 -adrenergic receptor subtypes: subtle mutation of the α_2 -adrenergic receptor in vivo by gene targeting strategies reveals the role of this subtype in multiple physiological settings. *Recent Prog Horm Res* **53**:25-42.
- Morisset S, Rouleau A, Ligneau X, Gbahou F, Tardivel-Lacombe J, Stark H, Schunack W, Ganellin CR, Schwartz JC and Arrang JM (2000) High constitutive activity of native H₃ receptors regulates histamine neurons in brain. *Nature* **408**:860-864.
- Neve KA, Henningsen RA, Kinzie JM, De Paulis T, Schmidt DE, Kessler RM and Janowsky A (1990) Sodium-dependent isomerization of dopamine D₂ receptors characterized using [¹²⁵I]epidepride, a high-affinity substituted benzamide ligand. *J Pharmacol Exp Ther* **252**:1108-1116.
- Schneider EH, Schnell D, Papa D and Seifert R (2009) High constitutive activity and a G-protein-independent high-affinity state of the human histamine H₄-receptor. *Biochemistry* **48**:1424-1438.
- Schnell D, Burleigh K, Trick J and Seifert R (2009) No evidence for functional selectivity of proxyfan at the human histamine H₃-receptor coupled to defined G_i/G_o protein heterotrimers. *J Pharmacol Exp Ther.* (in press)
- Seifert R (2001) Monovalent anions differentially modulate coupling of the β_2 -adrenoceptor to G_s alpha splice variants. *J Pharmacol Exp Ther* **298**:840-847.

- Seifert R and Wenzel-Seifert K (2001) Unmasking different constitutive activity of four chemoattractant receptors using Na⁺ as universal stabilizer of the inactive (R) state. *Receptors Channels* **7**:357-369.
- Seifert R and Wenzel-Seifert K (2002) Constitutive activity of G-protein-coupled receptors: cause of disease and common property of wild-type receptors. *Naunyn Schmiedebergs Arch Pharmacol* **366**:381-416.
- Seifert R and Wenzel-Seifert K (2003) The human formyl peptide receptor as model system for constitutively active G-protein-coupled receptors. *Life Sci* **73**:2263-2280.
- Surprenant A, Horstman DA, Akbarali H and Limbird LE (1992) A point mutation of the α_2 -adrenoceptor that blocks coupling to potassium but not calcium currents. *Science* **257**:977-980.
- Ward RJ and Milligan G (1999) An Asp79Asn mutation of the α_{2A} -adrenoceptor interferes equally with agonist activation of individual G α_i -family G protein subtypes. *FEBS Lett* **462**:459-463.

Chapter 5

Summary/Zusammenfassung

5.1 Summary

The histamine H₃ receptor (H₃R) is a biogenic amine receptor that belongs to family I of G protein-coupled receptors (GPCRs). During the past two decades, the H₃R has gained much interest in academia and industry. The H₃R is predominantly localized in the brain and regulates the release of histamine as well as other neurotransmitters into the synaptic cleft via negative feedback mechanisms. Thus, H₃R serves as presynaptic auto- or heteroreceptors. H₃R plays an important role in processes like cognition and the sleep-wake-cycle. Numerous ligands targeting H₃R have been developed as pharmacological tools or potential therapeutics. Some of them show unexpected and pleiotropic effects. The currently available data are not sufficient to explain this uncommon behaviour.

The aim of this thesis was to investigate the detailed molecular mechanisms of some yet unexplained H₃R-ligand effects. Therefore, sensitive baculovirus/Sf9 cell-based assay systems to analyze human H₃R (hH₃R) and rat H₃R (rH₃R) on a molecular level, were established.

It is known that certain imidazole-containing H₃R-ligands like proxyfan are functionally selective, i. e. activate only specific pathways mediated by H₃R. In this work, the detailed G protein coupling-profile of H₃R was investigated and various imidazole-based ligands were examined. We did not obtain evidence for differences in the G protein coupling profile of the H₃R or functional selectivity of any of the compounds assayed. Possible reasons for the discrepancies between the results and data obtained from the literature are discussed. These “negative” results cannot be attributed to unsuitability of our expression system for exclusion of ligand functional selectivity. However, our system is not suitable to definitely exclude protean agonism, a special case of functional selectivity, at H₃R, since that would require a systematic and precise variation of receptor-to-G protein stoichiometries. Extensive systematic studies under clearly defined experimental conditions are required to reconcile the discrepancies. Thus, presently, a specific and generally applicable mechanistic explanation for the previously observed pleiotropic effects of proxyfan cannot yet be provided.

Additionally, despite a very high sequence homology of hH₃R and rH₃R, there are substantial pharmacological species differences. Imoproxifan is an inverse agonist at rH₃R, but almost full agonist at hH₃R. We have shown that hH₃R and rH₃R expressed in Sf9 cells both couple similarly to defined G_i/G_o-protein heterotrimers and display similar constitutive activities. We show species-differences in pharmacological properties of imoproxifan and offer an explanation on the molecular basis for these differences. Most importantly, we introduce novel active state models of hH₃R and rH₃R that are suitable to explain the efficacy of H₃R ligands. Two amino acid residues between hH₃R and rH₃R cause the reversal in

efficacy of imoproxifan due to substantial differences in the electrostatic potential surfaces of the binding pockets.

Monovalent ions differentially affect GPCR signalling by as yet poorly understood mechanisms. In particular, Na^+ is known as universal allosteric GPCR modulator. However, it is unknown how Na^+ - ions exert the effects and whether it is not the counter-ion, which is responsible for the salt effects. Therefore, the H_3R was used as a model system to study the effect of various monovalent ions. Moreover, a highly conserved aspartate in TM II, thought to be an interaction site of Na^+ - ions in GPCRs, was mutated to asparagine. It turned out that most probably both, cation and anion, exert a modulatory effect on GPCR/G protein-coupling. Monovalent cations may stabilize an inactive H_3R -state *via* interaction with the conserved aspartate in TM II, while anions may increase the affinity of G proteins for GDP and thus, indirectly affect their interaction with H_3R . Interestingly, NaCl differentially affects the G protein coupling-profile of H_3R . NaCl selectively abolished constitutive signalling of H_3R only in the presence of $\text{G}\alpha_{i3}$. Obviously, the conserved aspartate in TM II is a key residue for $\text{H}_3\text{R}/\text{G}\alpha_{i3}$ protein-activation. The latter result suggests that $\text{H}_3\text{R}/\text{G}$ protein-coupling interfaces may differ even between closely related subunits.

In conclusion, this thesis provides new insight into the molecular mechanisms of H_3R function, G protein-coupling and species-differences. The availability of a sensitive H_3R test system will improve the development of new histamine receptor ligands, especially with respect to selectivity over the structurally related H_4R , and contribute to a better understanding of ligand effects. Most importantly, a gap was filled regarding the interaction of H_3R with specific G protein α -subunits, an until now insufficiently investigated area.

5.2 Zusammenfassung

Der Histamin H_3 -Rezeptor (H_3R) gehört zur Superfamilie der G-Protein-gekoppelten Rezeptoren (GPCRs). Die Klonierung des H_3R hat bei Wissenschaftlern im akademischen Bereich und in der Industrie großes Interesse geweckt. Der H_3R wird hauptsächlich im Gehirn exprimiert und reguliert die Ausschüttung von Histamin und anderen Neurotransmittern in den synaptischen Spalt über negative Rückkopplungsmechanismen. H_3R s werden deshalb als präsynaptische Auto- oder auch Heterorezeptoren bezeichnet. H_3R s spielen eine wichtige Rolle bei kognitiven Prozessen und der Regulation des Schlaf-Wach-Rhythmus. Viele H_3R -Liganden wurden bereits entwickelt, entweder als pharmakologische Werkzeuge oder mögliche Therapeutika. Einige von diesen Substanzen zeigen unerwartete Effekte in verschiedenen pharmakologischen Testsystemen. Anhand

bisheriger Daten kann die ungewöhnliche Pharmakologie dieser Verbindungen aber nicht eindeutig erklärt werden.

Ziel dieser Arbeit war es, den detaillierten molekularen Aktivierungsmechanismus des H_3R näher zu beschreiben. Zu diesem Zweck wurde ein sensibles, auf Bakuloviren und Sf9-Zellen basierendes, Testsystem zur Analyse des humanen H_3R (h H_3R) und Ratten H_3R (r H_3R) auf molekularer Ebene, etabliert.

Es ist bekannt, dass bestimmte imidazol-haltige H_3R -Liganden, wie Proxyfan, funktionell selektiv sind, d. h. nur bestimmte H_3R -vermittelte Signalwege aktivieren. Deshalb wurde in dieser Arbeit die Kopplung des H_3R an verschiedene G-Proteine untersucht und eine Reihe von imidazol-haltigen Liganden getestet. Keine der Verbindungen war funktionell selektiv. Mögliche Ursachen für die Diskrepanzen zwischen diesen Ergebnissen und Daten aus der Literatur werden diskutiert. Diese „negativen“ Daten, welche gegen eine funktionelle Selektivität der untersuchten Substanzen sprechen, sind nicht auf das von uns entwickelte Testsystem zurückzuführen. Jedoch kann auf Grundlage dieser Daten „protean agonism“, eine spezielle Form von funktioneller Selektivität, nicht ausgeschlossen werden. Dazu müsste die Rezeptor/G-Protein-Stöchiometrie gezielt und systematisch verändert werden. Aufwändige Studien unter klar definierten experimentellen Bedingungen werden dafür in Zukunft notwendig sein. Zum jetzigen Zeitpunkt gibt es also noch keine zufriedenstellende Erklärung für die ungewöhnliche Pharmakologie von Proxyfan.

Trotz einer hohen Sequenzhomologie zwischen h H_3R und r H_3R gibt es erhebliche pharmakologische Speziesunterschiede. Imoproxifan, ein inverser Agonist am r H_3R , ist fast ein voller Agonist am h H_3R . Wir konnten zeigen, dass h H_3R und r H_3R in Sf9-Zellen ähnlich gut an heterotrimere G_i/G_o -Proteine koppeln und eine ähnlich hohe konstitutive Aktivität besitzen. Die molekulare Ursache für das Spezies-spezifische Verhalten von Imoproxifan wurde aufgeklärt. Dafür wurden neue und bisher nicht verfügbare Computermodelle des aktiven Zustandes von h H_3R und r H_3R generiert. Unterschiede in nur zwei Aminosäuren zwischen h H_3R und r H_3R führen zu den pharmakologischen Unterschieden aufgrund unterschiedlicher elektrostatischer Oberflächenpotentiale der Bindetaschen.

Monovalente Ionen beeinflussen die GPCR-Signaltransduktion auf verschiedene Art und Weise. Die zugrunde liegenden Mechanismen werden aber nur wenig verstanden. Natriumionen sind universelle allosterische GPCR-Modulatoren. Wie Natriumionen aber diese Effekte verursachen, und ob nicht das Gegenion auch eine Rolle spielt, ist bisher allerdings nur unzureichend untersucht. Um sich dem Problem anzunähern, wurde der H_3R als Modellsystem verwendet und die Effekte verschiedener Salze monovalenter Ionen studiert. Zusätzlich wurde ein hochkonserviertes Aspartat in TM II, welches eine potentielle Interaktionsstelle für Natriumionen in GPCRs darstellt, zu Asparagin mutiert. Aufgrund der vorliegenden Daten wird geschlussfolgert, dass wahrscheinlich sowohl Kationen als auch

Anionen die GPCR/G-Proteinkopplung modulieren. Monovalente Kationen stabilisieren einen inaktiven H₃R-Zustand über eine Interaktion mit dem konservierten Aspartat in TM II, während Anionen die Affinität von G-Proteinen zu GDP erhöhen und daher indirekt deren Interaktion mit dem H₃R beeinflussen. Interessanterweise beeinflusst NaCl die Kopplung des H₃R an verschiedene G-Proteine auf unterschiedliche Art und Weise. NaCl unterdrückt selektiv die konstitutive Aktivität des H₃R nur in Anwesenheit von G α_{i3} . Das konservierte Aspartat in TM II spielt bei der H₃R/G α_{i3} -Interaktion eine Schlüsselrolle. Diese Daten suggerieren, dass die H₃R/G-Proteininteraktionsflächen unterschiedlich sein müssen, sogar bei sehr nah verwandten Untereinheiten.

Zusammenfassend erbrachte diese Dissertation neue Einblicke in den molekularen Aktivierungsmechanismus des H₃R und dessen G-Proteinkopplung. Außerdem wurden wichtige Speziesunterschiede auf molekularer Ebene geklärt. Die Verfügbarkeit eines sensitiven und robusten H₃R-Testsystems ist eine wichtige Voraussetzung für die Entwicklung neuer selektiver Histamin-Rezeptorliganden, speziell gegenüber dem strukturell verwandten H₄R, und zur Erlangung eines besseren Verständnisses von ungewöhnlichen Ligandeneffekten.

Appendix

A.1 Abstracts and Publications

Prior to submission of this thesis, results (or related studies) were published in part or were presented as short lectures or posters.

A.1.1 Original Publications:

2009

Schnell D, Schneider EH, Igel P, Buschauer A and Seifert R (2009) Multiple functional differences of histamine H₄-receptor species homologs. (*in preparation*)

Schnell D and Seifert R (2009) Modulation of histamine H₃-receptor function by monovalent ions. *Neurosci Lett* (submitted).

Schnell D, Strasser A and Seifert R (2009) Comparison of the pharmacological properties of human and rat histamine H₃-receptors. *J Pharmacol Exp Ther* (submitted).

Schneider EH, **Schnell D**, Strasser A, Dove S and Seifert R (2009) Impact of the DRY motif and the missing "ionic lock" on constitutive activity and G-protein-coupling of the human histamine H₄-receptor. *J Pharmacol Exp Ther* (in revision).

Schnell D, Burleigh K, Trick J and Seifert R (2009) No evidence for functional selectivity of proxyfan at the human histamine H₃-receptor coupled to defined G_i/G_o protein heterotrimers. *J Pharmacol Exp Ther* (published online: <http://jpet.aspetjournals.org/content/early/2009/12/03/jpet.109.162339.long>).

Igel P, Schneider E, **Schnell D**, Elz S, Seifert R and Buschauer A (2009) N^G-acylated imidazolylpropylguanidines as potent histamine H₄ receptor agonists: selectivity by variation of the N^G-substituent. *J Med Chem* 52:2623-2627.

Schneider EH, **Schnell D**, Papa D and Seifert R (2009) High constitutive activity and a G-protein-independent high-affinity state of the human histamine H₄-receptor. *Biochemistry* 48:1424-1438.

Igel P, **Schnell D**, Bernhardt G, Seifert R and Buschauer A (2009) Tritium-labeled N¹-[3-(1H-imidazol-4-yl)propyl]-N²-propionylguanidine ([³H]UR-PI294), a high-affinity histamine H₃ and H₄ receptor radioligand. *ChemMedChem* 4:225-231.

Kraus A, Ghorai P, Birnkammer T, **Schnell D**, Elz S, Seifert R, Dove S, Bernhardt G and Buschauer A (2009) N^G-acylated aminothiazolylpropylguanidines as potent and selective histamine H₂ receptor agonists. *ChemMedChem* 4:232-240.

2008

Ghorai P, Kraus A, Keller M, Götte C, Igel P, Schneider E, **Schnell D**, Bernhardt G, Dove S, Zabel M, Elz S, Seifert R and Buschauer A (2008) Acylguanidines as bioisosteres of guanidines: N^G-acylated imidazolylpropylguanidines, a new class of histamine H₂ receptor agonists. *J Med Chem* 51:7193-7204.

2007

Schlegel B, Laggner C, Meier R, Langer T, **Schnell D**, Seifert R, Stark H, Höltje HD and Sippl W (2007) Generation of a homology model of the human histamine H₃ receptor for ligand docking and pharmacophore-based screening. *J Comput Aided Mol Des* 21:437-453.

A.1.2 Short Lectures:**2009**

Schnell D, Schneider EH and Seifert R: Species homologs for the molecular analysis of constitutive H₄ receptor activity. 50. Jahrestagung der Deutschen Gesellschaft für experimentelle und klinische Pharmakologie (DGPT), Mainz.

2008

Schnell D and Seifert R: Analysis of putative ligand-specific conformations of histamine H₃ receptor species isoforms. 49. Jahrestagung der Deutschen Gesellschaft für experimentelle und klinische Pharmakologie (DGPT), Mainz.

2007

Schnell D, Trick J and Seifert R: Molecular analysis of histamine H₃ receptor coupling to G_{i/o}-proteins. Workshop of the graduate colleges GRK 760 and GRK 677 of the German Research Foundation (DFG), Nuremberg.

A.1.3 Poster Presentations:**2008**

Schnell D, Schneider EH and Seifert R: Species homologs for the molecular analysis of constitutive H₄ receptor activity. Symposium "Signal transduction – innovative fount for pharmacology", Medizinische Hochschule Hannover and Jahrestagung der Deutschen Pharmazeutischen Gesellschaft (DPhG), Bonn. Posterpreis der DPhG und Lesmüller-Stiftung.

Schnell D and Seifert R: Probing putative ligand-specific histamine H₃ receptor conformations. 4th Summer School "Medicinal Chemistry", Regensburg and Fachgruppentagung der Gesellschaft Deutscher Chemiker (GDCh) und Deutschen Pharmazeutischen Gesellschaft (DPhG) Pharmazeutische/Medizinische Chemie („Frontiers in Medicinal Chemistry“), Regensburg.

2007

Schnell D, Trick J and Seifert R: Quantitative analysis of human histamine H₃ receptor coupling to G proteins of the G_{i/o} family. Jahrestagung der Deutschen Pharmazeutischen Gesellschaft (DPhG), Erlangen and Workshop of the graduate colleges GRK 760 and GRK 677 of the German Research Foundation (DFG), Nuremberg.

Schnell D, Burleigh K and Seifert R: Molecular analysis of human histamine H₃ receptor using the baculovirus/Sf9 cell system. 48. Jahrestagung der Deutschen Gesellschaft für experimentelle und klinische Pharmakologie (DGPT), Mainz.

2006

Schnell D, Burleigh K and Seifert R: Functional reconstitution of the histamine H₃ receptor in Sf9 cells. 3rd Summer School "Medicinal Chemistry", Regensburg.

Schnell D, Schneider EH, Dove S and Seifert R: Molecular and cellular analysis of the histamine H₃- and H₄-receptor – project description. Poster contribution at the occasion of the evaluation of the Research Training Group (Graduiertenkolleg GRK 760) by the German Research Foundation, University of Regensburg.

A.2 Lebenslauf

Persönliche Daten

Name: David Schnell
Geburtsdatum: 15. Januar 1979
Geburtsort: Neuburg a. d. Donau

Beruflicher Werdegang

Seit 08/2005 Arbeitskreis Prof. Dr. med. Roland Seifert
Universität Regensburg/Medizinische Hochschule Hannover
(Lehrstuhl für Pharmakologie)

Doktorandenstipendium des DFG-Graduiertenkollegs
"Medizinische Chemie: Molekulare Erkennung - Ligand-Rezeptor-
Wechselwirkungen" (GRK 760)

07/2005 Approbation als Apotheker

06/2005 Abschluss der Pharmazeutischen Prüfung (3. Abschnitt)

11/2004 – 05/2005 Apotheke der Barmherzigen Brüder, Nicolaus Weigl e. K.

05/2004 – 10/2004 HEXAL Pharmaforschung GmbH

Universitärer Werdegang

04/2004 Abschluss: 2. Abschnitt der Pharmazeutischen Prüfung

01/2001 – 04/2003 Studentischer Mitarbeiter, Chromeon GmbH

11/1999 – 04/2004 Studium der Pharmazie, Universität Regensburg

Wehrdienst

07/1998 – 04/1999 Sanitätssoldat der Bundeswehr

Schule

06/1998 Abitur

09/1989 – 05/1998 Descartes-Gymnasium Neuburg

09/1985 – 07/1989 Grundschule Neuburg-Ost

A.3 Ausgewählte Zusatzqualifikationen/Fortbildung

03/2009	Advanced Courses in Pharmacology Teil 1: Tiermodelle in der Pharmakologischen Forschung Teil 2: Arzneimittelinteraktionen, -metabolismus und -transport
04/2006 – 03/2007	Weiterbildung „Versuchstierkunde und Tierschutz“ Bestandteil des Nachweises der Sachkunde für den Umgang mit Versuchstieren (FELASA Kategorie B) innerhalb der EU
04/2006	Fortbildungsveranstaltung für Projektleiter und Beauftragte für Biologische Sicherheit (BBS) Nach §15 und 17 der Gentechnik-sicherheitsverordnung

A.4 Teilnahme an Austauschprogrammen

2007

RISE - Research Internships in Science and Engineering
Deutscher Akademischer Austauschdienst (DAAD)
Juni – August 2007

2006

RISE - Research Internships in Science and Engineering
Deutscher Akademischer Austauschdienst (DAAD)
Juni - August 2006

A.5 Eidesstattliche Erklärung

Ich erkläre hiermit an Eides statt, dass ich die vorliegende Arbeit ohne unzulässige Hilfe Dritter und ohne Benutzung anderer als der angegebenen Hilfsmittel angefertigt habe; die aus anderen Quellen direkt oder indirekt übernommenen Daten und Konzepte sind unter Angabe des Literaturzitats gekennzeichnet. Weitere Personen waren an der inhaltlich-materiellen Herstellung der vorliegenden Arbeit nicht beteiligt. Insbesondere habe ich hierfür nicht die entgeltliche Hilfe eines Promotionsberaters oder anderer Personen in Anspruch genommen. Niemand hat von mir weder unmittelbar noch mittelbar geldwerte Leistungen für Arbeiten erhalten, die im Zusammenhang mit dem Inhalt der vorgelegten Dissertation stehen. Die Arbeit wurde bisher weder im In- noch im Ausland in gleicher oder ähnlicher Form einer anderen Prüfungsbehörde vorgelegt.

Regensburg, den _____

David Schnell